



THE UNIVERSITY OF
WAIKATO
Te Whare Wānanga o Waikato

Research Commons

<http://researchcommons.waikato.ac.nz/>

Research Commons at the University of Waikato

Copyright Statement:

The digital copy of this thesis is protected by the Copyright Act 1994 (New Zealand).

The thesis may be consulted by you, provided you comply with the provisions of the Act and the following conditions of use:

- Any use you make of these documents or images must be for research or private study purposes only, and you may not make them available to any other person.
- Authors control the copyright of their thesis. You will recognise the author's right to be identified as the author of the thesis, and due acknowledgement will be made to the author where appropriate.
- You will obtain the author's permission before publishing any material from the thesis.

**Stream Sediment Sources:
A Comparison Between a Native Forest Catchment and a
Mixed-Use Pine and Pasture Catchment in the
Waikato Region of New Zealand**

A thesis
submitted in partial fulfilment
of the requirements for the degree
of
Master of Science (Research)
in
Environmental Science
at
The University of Waikato
by
MANAWA KOKIRI HUIRAMA



THE UNIVERSITY OF
WAIKATO
Te Whare Wānanga o Waikato

2019

Abstract

Sediment entering streams and rivers is a global concern for water quality. Suspended sediment can reduce visual clarity, light penetration, and amenity values of water. Transported sediment can also smother benthic fauna and flora and increase the infilling of receiving environments such as lakes and estuaries. In New Zealand catchments, there are three primary sources of erosion i) hillslopes through sheetwash and rill erosion ii) stream bank erosion and iii) mass wasting of hillslopes. There has been little research conducted on the relative contribution of sediment sources to fine sediment within New Zealand. However, some limited research in New Zealand, and research from other countries has identified stream bank erosion as a major source of fine sediment.

The aim of this thesis was to identify the contribution of various erosion sources to sediment in streams. This study tested the hypothesis that stream bank erosion would be dominant in a pasture catchment, and hillslope erosion would be dominant in a native catchment. This study used paired, adjacent headwater catchments with similar sizes, slopes, soils, and underlying geology but contrasting land uses. The Mangaotama catchment was predominantly pastoral land use, with some areas of pine plantation, while the Whakakai catchment had regenerated and pristine indigenous forest.

Qualitative field surveys were conducted in the Mangaotama catchment (total length 1.3 km with 0.9 km under pastoral land use and 0.4 km under pine plantation) and Whakakai catchment (0.9 km) to assess stream and riparian conditions including stream bank erosion. Stream banks in the Mangaotama catchment were primarily stable (pasture section (left: 64%, right: 65%); pine section (left: 91%, right: 85%)) and the Whakakai catchment was generally stable (left: 84%, right: 86%). Stock damage dominated stream bank erosion in the pastoral section of the Mangaotama catchment (left: 23%, right: 19%), while stream bank undercutting dominated the pine section of the Mangaotama (left: 9%, right: 13%) and the Whakakai catchment (left: 15% and right: 13%).

Sediment fingerprinting used radionuclides (^{137}Cs , $^{210}\text{Pb}_{\text{ex}}$, ^{226}Ra and ^{228}Ra), to determine the relative contribution of stream bank erosion and hillslope erosion in suspended sediment samples collected during high flow events. The concentrations of all radionuclides were higher in the hillslopes ($P < 0.001$) ((mean ^{137}Cs : 5.8 Bq

kg⁻¹, std: 2.4 Bq kg⁻¹); (mean ²¹⁰Pb_{ex}: 32.5 Bq kg⁻¹, std: 16.0 Bq kg⁻¹); (mean ²²⁶Ra: 24.9 Bq kg⁻¹, std: 2.1 Bq kg⁻¹); (mean ²²⁸Ra: 35.3 Bq kg⁻¹, std: 4.0 Bq kg⁻¹)) of both the Mangaotama and Whakakai catchments than in the streambanks ((mean ¹³⁷Cs: 0.9 Bq kg⁻¹, std: 0.3 Bq kg⁻¹); (mean ²¹⁰Pb_{ex}: 8.4 Bq kg⁻¹, std: 4.6 Bq kg⁻¹); (mean ²²⁶Ra: 28.8 Bq kg⁻¹, std: 1.7 Bq kg⁻¹); (mean ²²⁸Ra: 47.2 Bq kg⁻¹, std: 2.2 Bq kg⁻¹)), clearly distinguishing the sources of sediment. A numerical mixing model determined that stream bank erosion was the dominant source of sediment (90%) within both catchments, with the remaining 10% originating from hillslope erosion.

Simultaneously recorded continuous turbidity and discharge (Q) data were analysed for the previous year (2017). Six flood events were analysed in the Mangaotama and Whakakai catchments (three large events $Q > 1,000 \text{ l s}^{-1}$ and three smaller events (Mangaotama: Q between 127 l s^{-1} to 606 l s^{-1} , Whakakai: Q between 219 l s^{-1} and 1398 l s^{-1}). Turbidity was greater in the Mangaotama catchment for four events (ranging from 237 NTU to 3,402 NTU) and greater in the Whakakai catchment for two events (1,293 NTU and 1,435 NTU). Strong clockwise hysteresis dominated (5 out of 6) of the flood events in the Mangaotama catchment, suggesting that stream bank erosion was the dominant source of sediment. Weak anti-clockwise hysteresis dominated the Whakakai catchment (5 out of 6) flood events, indicating sources further away from the sample point. Anti-clockwise hysteresis is primarily associated with hillslope erosion, however, in this study, it was most likely attributed to stream bank erosion sources in the upper reaches of the Whakakai catchment.

Terrestrial photogrammetry was tested, as it is potentially an effective, simple and cost-effective tool to monitor stream bank erosion over time. Further, a baseline was established which could be re-surveyed though it is recommended that further baseline sites be established to provide improved rigour.

Stream bank erosion was the greatest contributor (90%) to stream sediment loads in both the Mangaotama and Whakakai catchments, with the remaining 10% the stream sediment in both catchments being derived from hillslope erosion. Thus, the hypothesis for this study was **rejected**. This study demonstrates that stream bank erosion is a natural process and can dominate the supply of sediment to river systems even in relatively unimpacted catchments. Catchment managers need to take this into account when considering catchment rehabilitation projects aimed at reducing the delivery of sediment to streams.



*He puna aroha teenei ki tooku koroua a Erueti Te Houpapa Huirama.
Naau i takahi i teenei huarahi o te maatauranga ki te whare waananga.
Moe mai raa.*

He mihi

Tuatahi ake, me wehi ki te atua, te timatanga o te whakaaro nui. E mihi ana ki a Kiingi Tuheitia e noho mai nei i runga i te ahurewa tapu, otiraa ki te whare kaahui ariki, pai maarire ki a raatou. Ki ngaa tini mate kua whetuurangitia, moe mai ra, takoto mai ra.

Kei aku rangatira mo teenei mahi rangahau, nei raa te mihi, nei raa te mihi. Ngaa mihi nui ki a koe Megan, te kauhautu o teenei tuhinga roa, naau i arahi i au ki roto i teenei ao tuhituhi, teenei ao rangahau hoki. Ka nui te mihi ki a koe Andrew, i arahi i au ki roto i teenei mahi rangahau, i koowhirihia hoki i ngaa awa o Whatawhata hei kaupapa rangahau mooku. Teenei te mihi atu ki a koe Vicki mo te arahi me te tautoko hooki i au i roto i teenei mahi rangahau. Nooku te maringanui, ki te noho hei tauira i raro i a koutou.

Nei raa te mihi kia Waikato-Tainui raaua ko NIWA i tautoko a-putea mai, a-rauemi mai, a-whakaaro mai ki teenei kaupapa rangahau kia whakaora ai i o taatou awa me too taatou whenua. E mihi ana ki a Sarah-Jane Tiakiwai, raatou ko Nicholas Manukau, Taipu Paki, Kui Paki no Waikato-Tainui, ki a Cindy Baker raaua ko Dave Roper no NIWA, i whakarite ai i teenei karahipi mooku. Ka mutu, ka nui te mihi ki aku hoa mahi o NIWA i manaakitia mai i au ki roto i teenei tuhinga roa.

Nei raa te mihi kia Kerry Costley me Marina Hape i takahi haere i ngaa awa o Whatawhata ki tooku taha, ki a Ron Ovenden i aarahi i au ki roto i ngaa mahi o te taiwhanga puutaiao, kia Glen Balks i whakarite i ngaa mahi rorohiko 3D me Cheryl Ward i whakatika ai i teenei tuhinga roa. Ka nui te mihi ki a koutou.

Ka tika me mihi atu ki te kohanga reo o Turangawaewae me Te Wharekura o Raakaumangamanga i whakatoo ki roto i au i ngaa aahuatanga o te kiingitanga me ngaa kawa o Waikato. He piko he taniwha, he piko he taniwha. Waikato Taniwharau!

Me mihi hoki ki ooku hapuu me ngaa puna katoa i taakoha putea mai ki au e whai nei i tooku tohu paetahi o te maatauranga. Kia Waikato-Tainui, Ngaati Maniapoto,

Ngaapuhi, Ngaati Ruanui, Paritata Ahuwhenua Trust, Genesis Energy, otiraa ki Te Whare Waananga o Waikato, ka nui te mihi.

Ki taku hoa tane, e mihi ana ki a koe i tautoko i au, aa-tiinana mai, aa-wairua mai hoki, i au e whakaoti ana i teenei tuhinga roa. Aroha nui.

E taku maamaa, naau i poipoi i au mai i taku pipi paopaotanga, ki taku pakeketanga. Mei kore ko koe, ka kore ko au. Aroha nui.

Ki ooku kaumaatua o teenaa marae, o teenaa marae i manaakitia mai i au e tupu ana, teenei ka mihi. Ka mutu, nei ra te mihi atu ki tooku whaanau whaanui, ki ooku hoa hoki i tautoko mai i au, kia ea ai teenei mahi.

Ehara taku toa i te toa takitahi, engari he toa takitini.

Naaku iti noa nei,

Naa Manawa

Table of Contents

Abstract	i
He mihi.....	v
Table of Contents	vii
List of Figures	xi
List of Tables.....	xix
Chapter 1: Introduction	1
1.1 Background.....	1
1.2 Study site.....	2
1.3 Research objectives.....	4
Chapter 2: Literature Review	5
2.1 Introduction.....	5
2.1.1 Land-use and erosion	5
2.2 Environmental and social concerns	6
2.2.1 Impacts on freshwater ecology.....	6
2.2.2 Impacts on recreation and amenity values	6
2.2.3 Impacts on cultural connection to freshwater	7
2.3 Streambank erosion.....	7
2.3.1 Bank erosion processes	7
2.3.2 Bank erosion zonation.....	9
2.3.3 Drivers of bank erosion	11
2.3.4 Bank erosion and stream sediment yields	12
2.4 Sediment fingerprinting	12
2.4.1 Caesium-137.....	13
2.4.2 Excess Lead-210	19
2.4.3 Suspended sediment sampling (Phillips sampler).....	21
2.5 Suspended sediment concentrations and discharge	23
2.6 Field survey methods	25
2.6.1 Riparian Management Classification (RMC).....	26

2.6.2	Three-dimensional (3D) models for surveys	27
2.7	Discussion and synthesis	30
2.8	Conclusions	30
Chapter 3:	Catchment Surveys of Stream Bank Erosion.....	33
3.1	Introduction	33
3.2	Methods.....	33
3.2.1	Riparian Management Classification.....	33
3.2.2	Establishment of a photo-based 3D baseline	38
3.3	Results	40
3.3.1	Riparian Management Classification.....	40
3.3.2	Establishment of a photo based 3D baseline	63
3.4	Discussion	68
3.4.1	Riparian Management Classification.....	68
3.4.2	Establishment of a baseline for 3D monitoring	72
3.5	Summary and conclusion	73
3.5.1	Catchment surveys.....	73
3.5.2	Baseline for 3D monitoring	74
Chapter 4:	Using Sediment Fingerprinting to Determine the Relative Contribution of Main Erosion Sources	75
4.1	Introduction	75
4.2	Methods.....	76
4.2.1	Soil samples	76
4.2.2	Suspended sediment samples.....	83
4.2.3	Laboratory work	85
4.2.4	Laboratory analysis.....	88
4.2.5	Numerical mixing model	89
4.2.6	Statistical analysis and calculations.....	90
4.3	Results	90
4.3.1	Soil descriptions.....	90
4.3.2	Caesium-137 and Excess lead-210	91
4.3.3	Radium-226	93

4.3.4 Radium-228.....	94
4.3.5 Numerical mixing model.....	95
4.4 Discussion.....	95
4.4.1 Radionuclide concentrations	95
4.4.2 Statistical results.....	96
4.4.3 Outlier.....	96
4.4.4 Source of suspended sediment	97
4.4.5 Limitations of sediment fingerprinting	100
4.5 Summary and conclusions	100
Chapter 5: Using Turbidity and Stream Flow Data to Identify Sources of Sediment.....	103
5.1 Introduction.....	103
5.2 Methods	103
5.2.1 Analysis of flood events.....	105
5.3 Results.....	107
5.3.1 Large flood events analysed.....	108
5.3.2 Small flood events analysed.....	122
5.4 Discussion.....	136
5.4.1 Discharge.....	136
5.4.2 Hysteresis	137
5.4.3 Turbidity.....	138
5.5 Summary and conclusions	138
Chapter 6: Summary, Discussion and Conclusions	141
6.1 Introduction.....	141
6.2 Summary of the research and main findings	141
6.2.1 Objective 1: Catchment surveys (Chapter 3)	141
6.2.2 Objective 2: Terrestrial photogrammetry (Chapter 3).....	143
6.3 Objective 3: Sources of sediment (Chapter 3, 4 & 5).....	144
6.3.1 Sediment fingerprinting (Chapter 4)	144
6.3.2 Turbidity and discharge data (Chapter 5).....	145
6.4 Discussion.....	148

6.4.1 Main findings.....	148
6.4.2 Hypothesis	149
6.4.3 Implications of this study.....	150
6.5 Limitations of this study.....	151
6.6 Recommendations for future work.....	151
6.7 Conclusions	151
References	155
Appendices	165

List of Figures

Figure 1.1. Whatawhata Research Station and adjacent headwater catchments, Whakakai (predominantly indigenous forest) and Mangaotama (predominantly pastoral land use).	3
Figure 2.1. Hydraulic (a) and gravity (mass failure) (b) driven bank erosion processes (Reproduced from Brierley and Fryirs (2013)).....	8
Figure 2.2. The relationship between hydraulic action and mass failure bank erosion processes. Detachment occurs firstly by hydraulic action then mass failure process, eventually leading to the suspended sediment being carried downstream (entrainment) (Reproduced from Brierley and Fryirs (2013)).....	9
Figure 2.3. Dominant bank erosion processes change between the headwaters, middle reaches and lower reaches. Overlap of dominant processes occurs in certain areas of the stream (Lawler, 1995).	11
Figure 2.4. The distribution of ^{137}Cs is shown to decrease with depth in soils that are undisturbed. The graph shows soil profiles from a range of soil textures in the UK (A to E) and soil profiles from three countries with different climatic conditions (Reproduced from Cawse and Horrill (1986)).	14
Figure 2.5. A) Soil profiles with aerial activities of ^{137}Cs in the upper terraces (a to c) (DeRose 1998) and a standard ridge profile (d) (De Rose. In prep as cited in De Rose 1998) at Whatawhata Research Station (De Rose 1998). B) Soil profile concentrations of ^{137}Cs in the lower terraces (a to c) N.B. The star represents peak deposition (Reproduced from DeRose 1998).	17
Figure 2.6. Soil profiles aerial activities of ^{137}Cs in the upper stream plot (A) and lower stream plot (B). N.B. The star represents peak deposition, no star means there was no peak deposition (De Rose, 1998).....	18
Figure 2.7. The origin of ‘supported’ lead-210 (^{210}Pb) and ‘excess’ lead-210 ($^{210}\text{Pb}_{\text{ex}}$) from the subsequent decay process of uranium (^{238}U) in geological and soil material (Reproduced from Mabit <i>et al.</i> , 2004).....	19
Figure 2.8. Concentrations of $^{210}\text{Pb}_{\text{ex}}$ through undisturbed (A) and cultivated (B) soil profiles in Morocco (Reproduced from Mabit <i>et al.</i> , 2014).....	20
Figure 2.9. Conceptual diagram representing the concentration of lead-210 (^{210}Pb) and caesium-137 (^{137}Cs) in various erosion processes (Adapted from Olley <i>et al.</i> (2001)).....	21
Figure 2.10. Cross-section diagram of the time-integrated sampler created by Phillips <i>et al</i> (2011).	22

Figure 2.11. Peak discharge (Q), suspended sediment concentrations (SSC) and rainfall in the Mangaotama (A) and Whakakai (B) streams during a flood event in August 2010. Hysteresis patterns are also shown for the same flood event (Reproduced from Hughes <i>et al.</i> (2012)).	24
Figure 2.12. Peak discharge (Q), suspended sediment concentrations (SSC) and rainfall in the Mangaotama (A) and Whakakai (B) streams during a flood event in May 2010. Hysteresis patterns are also shown for the same flood event (Reproduced from Hughes <i>et al.</i> (2012)).	24
Figure 2.13. Comparison of the annual specific yields in the Mangaotama and Whakakai catchments from 1999 to 2010 (Reproduced from Hughes <i>et al.</i> (2012)).	25
Figure 3.1. GPS points showing the top and bottom of the reaches assessed using the Riparian Management Classification in the Mangaotama and Whakakai Catchments. Note: WQ = water quality	34
Figure 3.2. Example diagram of how reaches were chosen, where one reach has a wider water width, multiple pools and was sinuous, while the other reach was narrower and semi-straight. The perforated red line represents the separation between two reaches, and the blue line represents a waterfall.	36
Figure 3.3. Recording stream and riparian characteristics within the pine section of the Mangaotama catchment (Photo: F. Khan, 2019).	37
Figure 3.4. Example of on 3D modelling bank sites (left). Close up of marked garden stakes used for scale during the creation of the 3D models (right).	38
Figure 3.5. Conceptual schematic of the orientation of the photographs (arrows) for 3D modelling of streambanks (rectangle). Birds eye view showing simplified changes in angles and distances used while photographing the banks (a) and a simplified side view of the banks showing (adapted from Agisoft LLC (2018)).	39
Figure 3.6. Chart showing the processing steps used by the Pix4D software to create 3D models from terrestrial based imagery (Pix4D, 2017).	40
Figure 3.7. Mangaotama catchment (top) pastoral land use (Photo M. Balks, 2018) and (bottom) pine forest.	41
Figure 3.8. Stock damage on the stream bank in the Mangaotama catchment pastoral section (top) and broken bridge in the Mangaotama catchment pastoral section (bottom).	42
Figure 3.9. Fallen pine trees (top) and broken fencing (bottom) in the pastoral section of the Mangaotama catchment.	43

Figure 3.10. Whakakai stream (top) (Photo: M. Balks, 2018).....	44
Figure 3.11. Conservation management showing twin planted poplars (top) and planting on steep hills (bottom) in the pastoral section of the Mangaotama catchment.....	45
Figure 3.12. Evidence of past sediment accumulation in the Mangaotama catchment (top) Buried posts batons in the stream bank in the pastoral section (indicated by yellow arrows) and (bottom) buried fence post in the pine section (Photos: M. Balks, 2018).....	46
Figure 3.13. Woody debris from fallen trees (a) and mass wasting on hillslope (b) in the Whakakai catchment (Photo: F.Khan, 2018).....	48
Figure 3.14. Mean water (a) and mean channel (b) widths for the Mangaotama pastoral and pine catchment sections, and the Whakakai catchment. NB. Pine section reaches were changed from reach 15 to 26, to reach 1 to 12 on the graph for comparison with the pastoral section of the Mangaotama catchment and the Whakakai catchment. Mean values were the mean of the smallest to largest width in each reach.	49
Figure 3.15. Mean bankfull (a) and mean valley (b) widths for the Mangaotama pastoral and pine catchment sections, and the Whakakai catchment. NB. Pine section reaches were changed from reach 15 to 26, to reach 1 to 12 on the graph for comparison with the pastoral section of the Mangaotama catchment and the Whakakai catchment. Mean values were used were widths were recorded as ranges (smallest to largest width in the reach). Gaps in graph represent unrecorded data.	50
Figure 3.16. Summary of riffle/run/pool in Mangaotama catchment (a = pasture section, b = pine section) and the Whakakai catchment.....	51
Figure 3.17. Small waterfall and pool in the Whakakai catchment.	52
Figure 3.18. Slope lengths in the pastoral and pine sections of the Mangaotama catchment and the Whakakai catchment; left bank (a) and right bank (b). Slope lengths (m) include the number and greater than numbers (e.g. 20m and values greater than 20m). For readability purposes values that were between the selected slope lengths in the graphs were placed in the group with the closest value (e.g. 15 m slope length was placed in the >10m slope length category).	53
Figure 3.19. Left (a) and right (b) slope classes in the pastoral and pine sections of the Mangaotama catchment and the Whakakai catchment. Some classes have been grouped into the nearest category where values were greater than a particular slope class (e.g. values that were >10-15°, were grouped in the 10-15° category). Where there was more than one slope class recorded (due to the changing topography) the highest slope class value was used (e.g. 10-15°, 15-25°: the 15-25° value was used).	54

Figure 3.20. Bank heights in the pastoral and pine section of the Mangaotama catchment and the Whakakai catchment; left bank (a) and right bank (b).N.B. Mean values were graphed were lower and upper bank height values were recorded in the Riparian Management Classification field form.....	55
Figure 3.21. Stability (%) in the pastoral section on the left (a) and right (b) banks of the Mangaotama catchment.	56
Figure 3.22. Stability (%) in the pine section on the left (a) and right (b) banks of the Mangaotama catchment.	57
Figure 3.23. Stability (%) of the left (a) and right (b) banks in the Whakakai catchment.....	58
Figure 3.24. Summary percentage (%) of erosion in the Mangaotama (a = pasture section, b = pine section) and Whakakai catchments.....	59
Figure 3.25. Stream bank in the pastoral section of the Mangaotama catchment. Stock damage (top) and a small area of slumping (bottom).	60
Figure 3.26. Stream bank undercutting in the pine section of the Mangaotama catchment (both pictures).....	61
Figure 3.27. Streambank undercutting in the Whakakai catchment (both pictures) (both photographs taken by M. Balks, 2018).	62
Figure 3.28. Hillslope erosion observed in the Mangaotama pastoral section (left) and small mass movement event observed in the Whakakai catchment (right).....	63
Figure 3.29. The top and bottom images are of the Native 1 3D model. Image top image shows the point cloud 3D model and the photographs used to create the model. Image bottom image shows the final 3D model. Note: There are significant holes in the 3D model.....	64
Figure 3.30. Close up images of the point cloud created for the Pine 1 3D model. The top image shows the orientation of the photographs used and the bottom image is a closer image of the model.	65
Figure 3.31. 3D model of the Pine 1 site in the Mangaotama catchment.....	66
Figure 3.32. 3D model of the Pine 2 site in the Mangaotama catchment.....	66
Figure 3.33. 3D model of the Pine 3 site in the Mangaotama catchment.....	67
Figure 3.34. 3D model of the Pasture 1 site in the Mangaotama catchment.	67
Figure 3.35. 3D model of the Native 2 site in the Whakakai catchment.....	67

Figure 4.1. Location of stream bank and hillslope sites selected in the Mangaotama and Whakakai catchments for soil sampling and radionuclide analysis	77
Figure 4.2. Example of streambank sites sampled in the Mangaotama (top) and Whakakai (bottom) catchments.....	79
Figure 4.3. Soil sample collection from a hillslope site under pine plantation in the Mangaotama catchment. Soil samples were collected in a semi-straight transect from the bottom of the hill to the top of the hill, and more samples were taken at the apex of the hill (Photo: K. Huirama, 2018).....	81
Figure 4.4. Soil sample collection at one the colluvial toe slope sites in the Mangaotama catchment. The site was located in the pine section.....	81
Figure 4.5. Soil sample collection from one of the hillslope sites in the Whakakai catchment. N.B. The circle shows one of the field volunteers (F. Khan) helping to collect the hillslope samples, indicated here to show scale.....	82
Figure 4.6. Phillips samples in the Mangaotama (top) and Whakakai catchment (Photo: M. Balks, 2018) (bottom) installed 15cm above base flow. N.B. The photograph was taken after the samplers were re-installed ~40m from the NIWA monitoring station on July 13.....	84
Figure 4.7. Sub-merged Phillips samplers during the same flood event in the Mangaotama (left photo) and Whakakai (right photo) catchments. (Both photographs taken by K. Costley, 2018).....	84
Figure 4.8. Some stream bank and hillslope samples collected in the Mangaotama catchment and returned to the laboratory.....	85
Figure 4.9. Wet sieving area in the laboratory, showing sieves ranging from 4mm to <63 μm	86
Figure 4.10. Wet sieving a suspended sediment sample (sampler near the left bank) in the Mangaotama catchment.....	86
Figure 4.11. Example of a wet sieved stream bank soil sample (<63 μm), 20 minutes after sieving and shows the sediment beginning to settle in the bottom of the beaker.....	87
Figure 4.12. Example of dried soil sample being crushed by mortar and pastel (left) and final stream bank and hillslope soil samples from the Whakakai catchment, post drying and sieved to <500 μm before being sent to ESR for radionuclide analysis (right).....	88
Figure 4.13. A hillslope soil sample from the Whakakai catchment (WHILL1 Appendices Table A.1) that developed a dark black colour post drying in the 60°C oven, compared to other steam	

bank and hillslope samples from the Whakakai catchment, which had a light brown colour post drying.	91
Figure 4.14. Radionuclide concentrations of ^{137}Cs and $^{210}\text{Pb}_{\text{ex}}$ in the stream bank and hillslope samples collected in the Mangaotama (M) and Whakakai catchments (W). N.B. SB = stream bank samples, H = Hillslope samples and SS = Suspended sediment samples. The error bars were results from the gamma analysis.	93
Figure 4.15. Radionuclide concentrations of ^{137}Cs and ^{226}Ra in the stream bank and hillslope samples collected in the Mangaotama (M) and Whakakai (W) catchments. N.B. SB = stream bank samples, H = Hillslope samples and SS = Suspended sediment samples. The error bars were results from the gamma analysis.	94
Figure 4.16. Radionuclide concentrations of ^{137}Cs and ^{228}Ra in the stream bank and hillslope samples collected in the Mangaotama (M) and Whakakai (W) catchments. N.B. SB = stream bank samples, H = Hillslope samples and SS = Suspended sediment samples. The error bars were results from the gamma analysis.	95
Figure 5.1. Comparison of flow (Q) and turbidity (NTU) data between the Mangaotama catchment and Whakakai catchment from 1 January to 31 December 2017. N.B. The circles on the Q graphs highlight the six flood events analysed in both the Mangaotama and Whakakai catchments.	106
Figure 5.2. Flow (Q) and turbidity data from the storm event on 5 April 2017 in the Mangaotama (a) and Whakakai (b) catchments.	109
Figure 5.3. Close up view of the first peak of the storm event on 5 April 2017 in the Mangaotama (a) and Whakakai (b) catchments. N.B. The graphs are not plotted on the same y-axis scale (Q and turbidity) and have instead been exaggerated to showcase the Q and turbidity peaks in both catchments.	110
Figure 5.4. Hysteresis graphs for the first peak of the storm event 5 April 2017 in the Mangaotama (a) and Whakakai (b) catchments. N.B. The hysteresis graph scales are not equal and have instead been exaggerated to showcase the hysteresis in each catchment.	111
Figure 5.5. Close up view of the second peak of the storm event on 5 April 2017 in the Mangaotama (a) and Whakakai (b) catchments. N.B. The graphs are not plotted on the same y-axis scale (Q and turbidity) and have instead been exaggerated to showcase the Q and turbidity peaks in both catchments.	112
Figure 5.6. Hysteresis graphs for the second peak of the storm event on 5 April 2017 in the Mangaotama (a) and Whakakai (b) catchments. N.B. The hysteresis graph scales are not equal and have instead been exaggerated to showcase the hysteresis in each catchment. No arrows indicates no hysteresis, as Q and turbidity peaked at the same time.	113

Figure 5.7. Flow (Q) and turbidity graphs for the storm event on 22 July 2017 in Mangaotama (a) and Whakakai (b).....	115
Figure 5.8. Close up view of the storm event on 22 July 2017 in Mangaotama (a) and Whakakai (b). N.B. The graphs are not plotted on the same y-axis scale (Q and turbidity) and have instead been exaggerated to showcase the Q and turbidity peaks in both catchments.....	116
Figure 5.9. Hysteresis graphs for the storm event on 22 July 2017 in the Mangaotama (a) and Whakakai (b). N.B. The hysteresis graph scales are not equal and have instead been exaggerated to showcase the hysteresis in each catchment.	117
Figure 5.10. Flow (Q) and turbidity data for the storm event on 9 August 2017 in the Mangaotama (a) and Whakakai(b).....	119
Figure 5.11. Close up view of the storm event 9 August 2017 in the Mangaotama (a) and Whakakai (b). N.B. The graphs are not plotted on the same y-axis scale (Q and turbidity) and have instead been exaggerated to showcase the Q and turbidity peaks in both catchments.....	120
Figure 5.12. Hysteresis graphs for the storm event on 9 August 2017 in the Mangaotama (a) and Whakakai (b). N.B. The hysteresis graph scales are not equal and have instead been exaggerated to showcase the hysteresis in each catchment.	121
Figure 5.13. Flow (Q) and turbidity data from the storm event on 3 February 2017 in the Mangaotama and Whakakai catchments	123
Figure 5.14. Close up view of the storm event on 3 February 2017 in the Mangaotama (a) and Whakakai (b). N.B. The graphs are not plotted on the same y-axis scale (Q and turbidity) and have instead been exaggerated to showcase the Q and turbidity peaks in both catchments.....	124
Figure 5.15. Hysteresis graphs for the storm event on 3 February 2017 in the Mangaotama (a) and Whakakai (b) catchments. N.B. The hysteresis graph scales are not equal and have instead been exaggerated to showcase the hysteresis in each catchment.....	125
Figure 5.16. Flow (Q) and turbidity data for the storm event on 12 May 2017 in the Mangaotama (a) and Whakakai (b) catchments.	127
Figure 5.17. Close up view of the first peak of the storm event on 12 May 2017 in Mangaotama (a) and Whakakai (b). N.B. The graphs are not plotted on the same y-axis scale (Q and turbidity) and have instead been exaggerated to showcase the Q and turbidity peaks in both catchments.....	128
Figure 5.18. Hysteresis graphs for the first peak of the storm event on 12 May 2017 in the Mangaotama (a) and Whakakai (b) catchments.	

N.B. The hysteresis graph scales are not equal and have instead been exaggerated to showcase the hysteresis in each catchment.	129
Figure 5.19. Close up view of the second peak of the storm event on 12 May 2017 in Mangaotama (a) and Whakakai (b). N.B. The graphs are not plotted on the same y-axis scale (Q and turbidity) and have instead been exaggerated to showcase the Q and turbidity peaks in both catchments.	130
Figure 5.20. Hysteresis graphs for the second peak of the storm event on 12 May 2017 in the Mangaotama (a) and Whakakai (b) catchments. N.B. The hysteresis graph scales are not equal and have instead been exaggerated to showcase the hysteresis in each catchment.	131
Figure 5.21. Flow (Q) and turbidity data from the storm event on 23 June 2017 in the Mangaotama (a) and Whakakai (b) catchments.	133
Figure 5.22. Close-up view of the storm event on 23 June 2017 in Mangaotama (a) and Whakakai (b). N.B. The graphs are not plotted on the same y-axis scale (Q and turbidity) and have instead been exaggerated to showcase the Q and turbidity peaks in both catchments.	134
Figure 5.23. Hysteresis graphs for the storm event on 23 June 2017 in the Mangaotama (a) and Whakakai (b) catchments. N.B. The hysteresis graph scales are not equal and have instead been exaggerated to showcase the hysteresis in each catchment.	135

List of Tables

Table 3.1. Reaches in the Mangaotama and Whakakai Streams with GPS locations for the top and bottom of each reach.	35
Table 3.2. Results of the initial processing stage of the 3D modelling software.	64
Table 4.1. GPS locations of the stream bank and hillslope sites sampled for radionuclide analysis	78
Table 4.2. Summary of the mean, minimum, maximum and standard deviation of radionuclide concentrations (^{137}Cs , $^{210}\text{Pb}_{\text{ex}}$, ^{226}Ra & ^{228}Ra) in stream bank and hillslope samples collected from the Mangaotama (M) and Whakakai (Wh) catchments. N.B. Data is the mean of 5 samples.	92
Table 4.3. Course calculations of stream bank erosion rates to test the reasonability of the numerical mixing model results from this study that both the Mangaotama and Whakakai catchments are dominated by stream bank erosion.....	99
Table 5.1. Max Q (1 s^{-1}) and turbidity (NTU) values for the six flood events analysed in the Mangaotama and Whakakai catchments	107

Chapter 1

Introduction

1.1 Background

The elevated delivery of fine sediment into streams and rivers is a major concern for water quality (Walling, 2006), and has been described as the ‘universal pollutant’ because it is invariably mobilised whenever land cover and/or soils are disturbed. Fine sediments affect fluvial systems in two ways (1) in suspension (2) upon deposition. Transported in suspension, fine sediments can reduce water clarity, reduce light penetration and reduce amenity values of streams. Upon deposition, fine sediments can smother benthic fauna and flora and infill receiving environments (lakes and estuaries) (Davies-Colley *et al.*, 2014).

To mitigate the adverse effects of sediment on freshwater ecosystems and estuaries it is important to identify the sources of sediment within a catchment (Collins *et al.*, 2011). In New Zealand catchments there are three primary sources to catchment sediment i) hillslopes through sheetwash and rill erosion, ii) stream bank erosion, and mass wasting (e.g. landslides and mudflows). There has been very little research undertaken on quantifying the relative contribution of sediment sources in New Zealand catchments (Basher, 2013). Some limited studies in New Zealand have identified stream bank erosion as a major contributor of sediment to fluvial systems (De Rose, 1998; Watson & Basher, 2006; Hicks *et al.*, 2011; Hughes & Hoyle, 2014). However, there has been very little quantitative research on both bank erosion processes and the contribution of bank erosion to sediment yields (Watson & Basher, 2006; Basher, 2013).

The hypothesis for this research is that stream banks would be the main source of sediment in pasture catchments, while hillslope erosion would be the main source of sediment in forested catchments. The basis for this hypothesis is that in pasture catchments, grass cover on stream banks may provide less protection against erosion (Stott, 1997), livestock trampling can damage stream banks, increasing the delivery of sediment to streams (Trimble & Mendel, 1995) and that the grass cover on stream banks is effective at buffering sediment from hillslope erosion (McKergow *et al.*,

2003). Contrastingly, in native catchments, the lack of grass cover, means hillslope erosion is more easily delivered to streams (i.e. no buffering effect) and that the trees in the native catchment may provide greater protection against stream bank erosion (Stott, 1997).

1.2 Study site

The Whatawhata Research Station (also known as Te Rauputiputi) is located within the Waikato Region of the North Island of New Zealand (Figure 1.1). The Whatawhata Research Station was established in the year 1949 as a scientific research site for the farming sector and has supported a long history of agricultural research including soil fertiliser research, farm management practices, animal health, pasture production, sheep and beef research, including wool production). The Whatawhata Research Station has also been a long-term research site for the National Institute of Water and Atmospheric Research (NIWA) for areas such as freshwater ecology and water quality. Ownership of the Whatawhata Research Station was returned to Waikato-Tainui through the Treaty settlements in the Waikato Region (Quinn *et al.*, 1998; Dodd *et al.*, 2008).

The Mangaotama (268 ha) and Kiripaka (266 ha) catchments are two headwater catchments that lie within the Whatawhata Research Station. The Mangaotama catchment is predominantly pasture, with smaller areas of pine plantation (*P. radiata*) and native plantation, while the Kiripaka catchment is a mixture of pasture, indigenous forest and pine forest. Directly adjacent to the Whatawhata Research Station, lies the Whakakai catchment (311 ha), also a headwater catchment. The Whakakai catchment is part of a forest reserve. The indigenous forest in the Whakakai catchment has been regenerating for over 80 years since logging occurred in the lower part of the catchment. The Mangaotama and Whakakai catchments discharge to the Waipa River, the main tributary of the Waikato River (Quinn *et al.*, 1998; Dodd *et al.*, 2008).

Due to their proximity, all three catchments (Mangaotama, Kiripaka and Whakakai) have similar topography, geology, soils, and climatic conditions. The topography is predominantly steep (mean slope ~23 degrees) and hilly. The underlying geology is Mesozoic sedimentary sandstones and siltstones (greywacke and argillite) with

Pleistocene tephra overlying the bedrock on the more gently sloping areas. The soils are strongly weathered yellow brown earths (Ultic Soils).

The catchments have a humid-temperate climate with a mean annual rainfall of 1,663 mm (1993-2010); NIWA unpublished data) and a mean average temperature of 13.7°C (Dodd *et al.*, 2008).

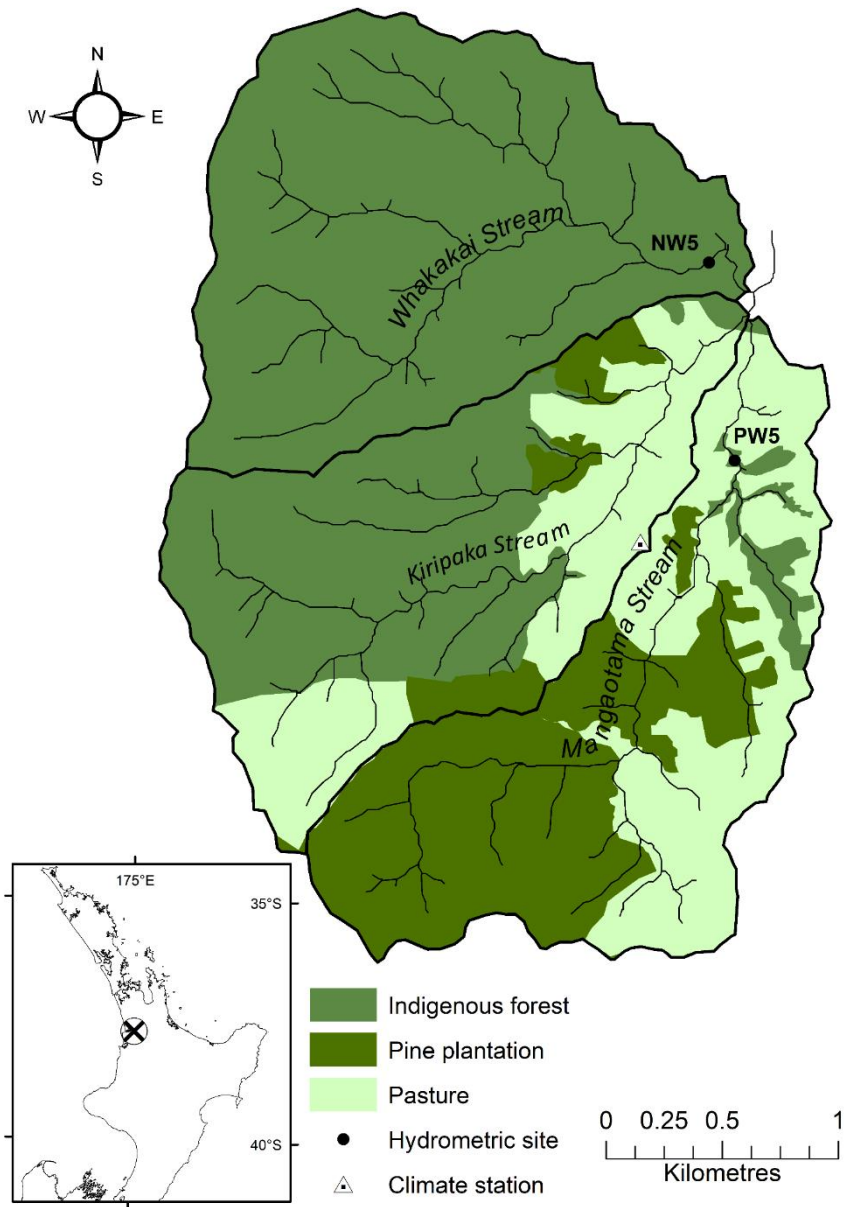


Figure 1.1. Whatawhata Research Station and adjacent headwater catchments, Whakakai (predominantly indigenous forest) and Mangaotama (predominantly pastoral land use).

1.3 Research objectives

The overall aim of my research was to identify the contribution of various sources of sediment in streams. The hypothesis for this study is that stream bank erosion is the dominant source of suspended sediment to pasture catchments (i.e. the Mangaotama catchment), while hillslope erosion is the dominant source of suspended sediment from indigenous forests (i.e. the Whakakai catchment).

The specific objectives of this research were to:

- Identify similarities and differences between the Mangaotama and Whakakai catchments, by conducting field surveys.
- Investigate the potential of using terrestrial photogrammetry to monitor stream bank erosion over time.
- Identify the dominant source of sediment within the Mangaotama and Whakakai catchments.

Chapter 2

Literature Review

2.1 Introduction

Soil erosion is the detachment and removal of soil particles predominantly by means of water or wind erosion (McLaren & Cameron, 1996) and gravity (Charman & Murphy, 2007). Broadly speaking there are three main types of erosion that occur in New Zealand catchments (Basher, 2013). The main types of erosion are hillslope erosion (surface erosion) such as sheet (uniform removal of soil), rill (small channelized erosion) (Charman & Murphy, 2007) or wind (McLaren & Cameron, 1996); stream bank erosion (see following paragraphs), and mass wasting (erosion induced by gravity) such as landslides (Charman & Murphy, 2007; Basher, 2013).

The soil materials that have been eroded from the land and transported into a receiving water body are termed ‘sediment’ (Stewart *et al.*, 2003). There are two categories of sediment within fluvial systems; deposited and suspended sediment. Deposited sediments are particles that have settled on the stream bed ($> 2\text{mm}$) (Davies-Colley *et al.*, 2015), while suspended sediment is typically clay and/or silt particles ($< 63\mu\text{m}$) that are floating in suspension in the water column (Davies-Colley *et al.*, 2014; Parsons *et al.*, 2015). Rivers and streams eventually transport sediment to estuaries and the ocean (Basher *et al.*, 2011).

2.1.1 Land-use and erosion

Although soil erosion is a natural process, human activities can accelerate soil erosion and subsequently increase the delivery of fine sediment to receiving environments (such as lakes and streams) (Ongley, 1996; Walling, 2006). Syvitski *et al.* (2005) noted that accelerated erosion has globally increased the delivery of soil to stream sediments (by 2.3 ± 0.6 billion metric tons per year).

Human-induced land-use changes such as deforestation and agriculture, are well known to cause increased erosion rates and subsequently increase sedimentation rates (Walling, 2013). For example, large areas of deforestation occurred in New Zealand for farming practices and timber after the arrival of the European settlers (early 19th century) (Roche, 1994).

Over the past 150 years, around half of New Zealand has been converted to land for animal grazing (Collier *et al.*, 1995). Consequently, erosion rates and subsequent delivery of sediment to New Zealand water bodies has increased, due to historical land clearance and farming (Glade, 2003). Intensification of stocking rates on farms and urban growth may have also increased sediment delivery to receiving water bodies (Trimble, 1997).

2.2 Environmental and social concerns

2.2.1 Impacts on freshwater ecology

Excess suspended sediment can detrimentally alter the physical, biological and chemical characteristics of a waterbody (Bilotta & Brazier, 2008). Physical impacts include the deposition of sediment on a river bed (e.g. causing mortality of salmonid eggs and larvae within gravel-reeds (Haygarth *et al.*, 2006); particles floating in the water column (e.g. damaging respiratory organs in fish (Kemp, 1949) and aquatic invertebrates; and reduced light penetration (e.g. limiting the photosynthesis of macrophytes and algae, eventually impacting primary consumers (Bilotta & Brazier, 2008). Biological impacts include increased invertebrate drift and reduced feeding efficiency (e.g. clogging feeding structures of filter feeding organisms (Bilotta & Brazier, 2008). Chemical impacts include changes in the abundance of macrophytes and periphyton (e.g. from nutrient (Kemp, 1949) and toxic compounds inputs (Bilotta & Brazier, 2008). The degree at which these changes are harmful to aquatic organisms depends on the concentration, particle size and geochemical properties of the suspended sediment (Bilotta & Brazier, 2008).

2.2.2 Impacts on recreation and amenity values

Suspended sediment concentrations can affect the ability of a river to be used for recreation purposes. The visual clarity of a river is impacted by suspended sediment concentrations and at certain levels are deemed unsuitable for recreational activities (Anzecc *et al.*, 2000). A report published by Davies-Colley and Bellantine (2010) analysed black disk (i.e. visual clarity) and faecal pollution data from 77 key river sites in New Zealand. Davies-Colley and Bellantine (2010) showed that 39% (30 out of 77) of rivers were unsuitable for recreational use, with a third of these, deemed unsuitable due to poor visual clarity. Some rivers had low clarity (i.e. high-

suspended sediment concentrations) due to natural geological and soil conditions and were not strongly influenced by land use. Additionally, the combination of both geological, soil and land use was found to be the cause of low clarity in rivers (Davies-Colley & Bellantine, 2010).

2.2.3 Impacts on cultural connection to freshwater

Streams and rivers are important to the cultural heritage of indigenous people (e.g. Jackson, 2006; Nakamura, 2008; Te Aho, 2010). For example, Maaori (the indigenous people of New Zealand) share a physical, spiritual and cultural connection to freshwater. These connections stem from whakapapa (genealogy) and relate to Maori stories of cosmology. In these stories, Maaori descend from Io (god) and his descendants Papatuanuku (earth mother) and Ranginui (sky father) and their children who are the personifications of the environment (e.g. water, forests). Thus, aspects of the environment are viewed as living ancestors (Best, 1922; Te Aho, 2010). Maaori maintain their connection with their ancestral waters through recreational activities such as waka taua and traditional customs that involve prayer and healing. Excess sediment can impact the ability of iwi to perform traditional customs (Waikato-Tainui Te Kauhanganui Incorporated, 2013).

2.3 Streambank erosion

2.3.1 Bank erosion processes

The process of bank erosion occurs in two phases (Lawler, 1993);

1. The detachment of soil particles from the bank and;
2. The input of soil particles into the stream (entrainment)

Most often, preparatory processes are responsible for partial or complete detachment of soil particles from the banks. The stream is then able to entrain and carry the particles with the flow. Other times, hydraulic power can drive both detachment and entrainment phases (Lawler, 1993).

Bank erosion can be grouped into two categories based on the main drivers of erosion (Figure 2.1).

- Hydraulic force, and
- Mass failure (Gravitational force).

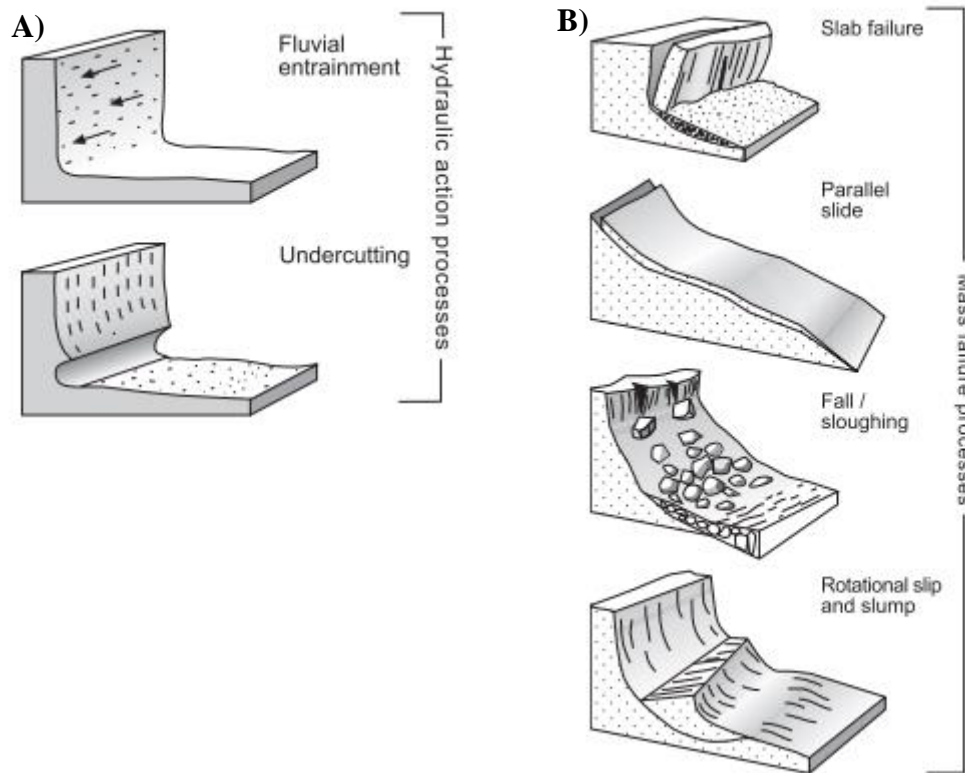


Figure 2.1. Hydraulic (a) and gravity (mass failure) (b) driven bank erosion processes (Reproduced from Brierley and Fryirs (2013)).

Water driven bank erosion detachment refers to fluid entrainment and undercutting processes (Figure 2.1). Fluid entrainment can remove individual soil particles or induce shallow slips over a flat surface. The peak flood of a stream can sometimes be evident after the flood event from an indentation or cut on the banks. Undercutting is the process of stream power eroding the lower half of the bank. The top half of the bank consequently overhangs, and eventually mass failure occurs (Figure 2.1). Both entrainment and undercutting are most commonly found on the outside of bends, due to high water velocities and large-scale eddies generated at stream bends (Thorne & Lewin, 1979; Thorne & Tovey, 1981).

Mass failure bank erosion occurs due to the force of gravity. Properties that make banks susceptible to mass failure are the banks geometry (height and slope) (Watson & Basher, 2006), soil, and structure. Mass failure processes refer to slab failures, parallel slides, fall/sloughing and rotational slumps (Watson & Basher, 2006). Slab failures are when a block of bank falls directly into the stream, while a rotational slump is when a block of the bank breaks and rotates before entering the

stream. Parallel slides occur when a thin layer of the bank slides into the stream, while sloughing is where smaller blocks of soil build up at the lower end of the bank (Watson & Basher, 2006).

Both hydraulic and mass failure processes are linked and create a cycle of bank erosion (Figure 2.2). For example, undercutting makes the bank unstable, which can eventually lead to slab failure (Figure 2.2)

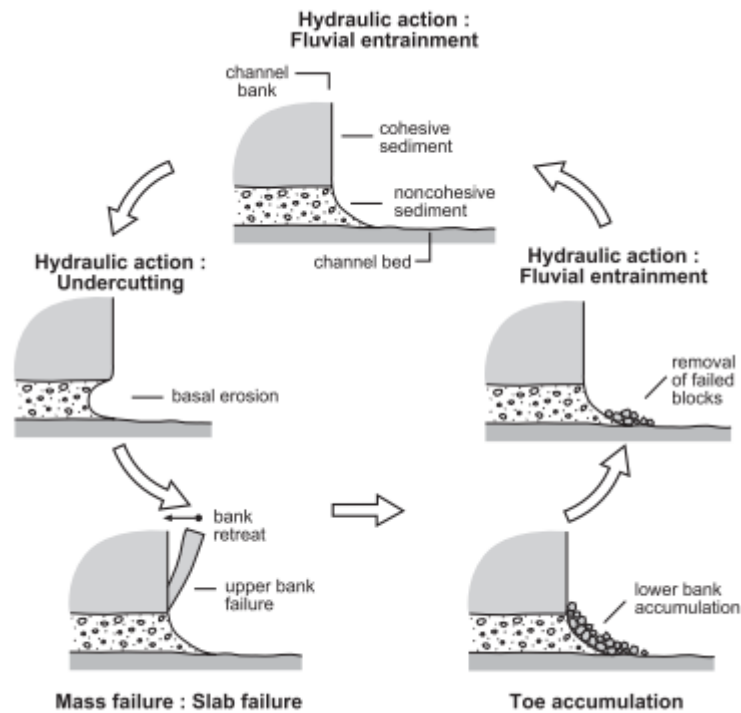


Figure 2.2. The relationship between hydraulic action and mass failure bank erosion processes. Detachment occurs firstly by hydraulic action then mass failure process, eventually leading to the suspended sediment being carried downstream (entrainment) (Reproduced from Brierley and Fryirs (2013)).

2.3.2 Bank erosion zonation

Lawler (1995) proposed that dominant bank erosion processes change downstream in a river system. In general, three areas can be considered for bank erosion processes, these are;

- Headwaters,
- Mid-reaches, and
- Lower reaches

The headwaters are dominated by sub-aerial weathering erosion processes. Sub-aerial processes (i.e. freezing-thawing or desiccation) are external micro-climatic conditions that are dominant because hydraulic energy in the stream is low and the banks are small. In humid and sub-arctic countries the banks in the headwaters go through a cycle of freezing and thawing (Lawler, 1993). However, these effects are less effective downstream and with decreasing altitude. Desiccation occurs when there is little to no rainfall but temperatures and evaporation rates are high causing the banks to become extremely dry.

These sub-aerial processes either loosen the bank material enough so that sediment is input into the stream or sediment is transported in the next flood event.

The middle reaches are dominated by direct fluid entrainment processes. Fluid entrainment processes are when stream power is strong enough to induce shear stress (friction) eventually eroding the banks. Soil materials in the middle reaches (fine sand and coarse silt) are also more easily susceptible to fluid entrainment than soil materials in the headwaters (course materials) and lower reaches (predominantly clay) (Lawler, 1995).

The lower reaches are dominated by mass failure/wasting processes. Mass failure processes are when whole blocks break and fall into the river. The broken bank blocks can either instantly break further apart or slowly “leak” sediment over a longer period of time. The lower reaches are more susceptible to mass failure because channel depth and bank heights tend to increase downstream, whereby at a particular critical height the bank is likely to collapse. The critical height of a stream is dependent on the bank material, where critical bank height increases with material cohesion and decreases with dense material (Lawler, 1995).

Despite the clear zonation of dominant processes in the fluvial system, there is an overlap between bank erosion processes (Figure 2.3). Thus, understanding bank erosion processes is complex (Lawler, 1995).

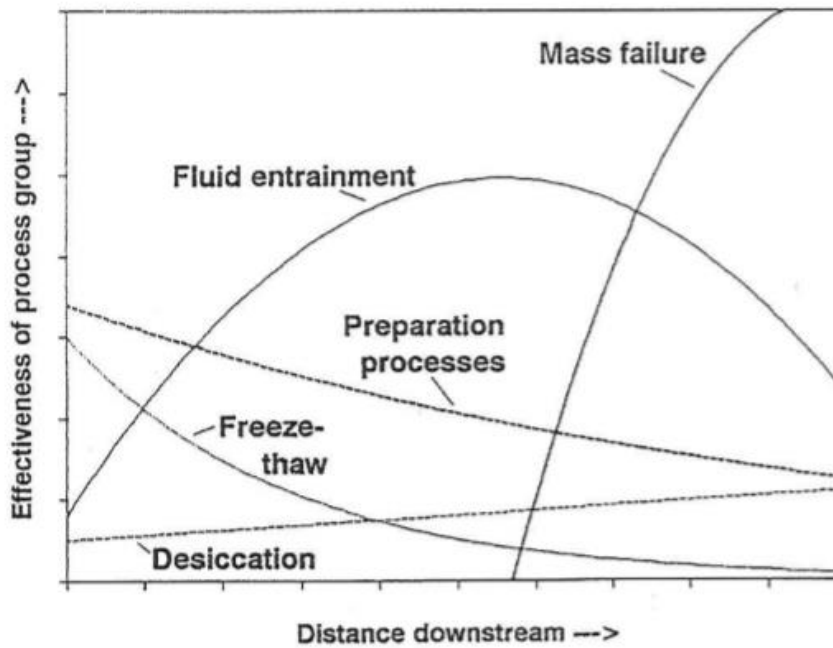


Figure 2.3. Dominant bank erosion processes change between the headwaters, middle reaches and lower reaches. Overlap of dominant processes occurs in certain areas of the stream (Lawler, 1995).

2.3.3 Drivers of bank erosion

Drivers of erosion are similar across all processes, including bank erosion. Although precipitation is an important driver of some erosion processes (e.g. sheet wash erosion) (Charman & Murphy, 2007), it has little direct effect on bank erosion (Watson & Basher, 2006). However, rainfall controls flood event magnitude and durations (influencing discharge) and saturates banks making them more susceptible to mass failures in the future. Discharge velocities (impacted by rainfall frequency & magnitude) are important in bank erosion processes (Knighton, 2014). Soil properties are important for determining the erodibility and susceptibility of the banks. For example, soils with a coarser texture (non-cohesive bank material) are well drained and are more likely to erode as soil particles. On the other hand, soils with fine texture (cohesive bank material) are poorly drained and tend to erode as mass movement processes (Thorne & Tovey, 1981).

Vegetation on the banks is crucial to strengthen the bank against erosion (Watson & Mardern, 2004), with previous studies showing that unvegetated stream banks

erode at a faster rate than unvegetated banks (e.g. Stott (1997) and Prosser *et al.* (2000)). Finally, human activities such as livestock grazing and vehicles can compact the soil minimizing infiltration rates and eventually leading to water erosion (e.g. runoff). Livestock trampling of river banks (especially by cattle) can also result in erosion and/or weakening of the river bank structure (Trimble & Mendel, 1995).

2.3.4 Bank erosion and stream sediment yields

Stream bank erosion has been identified as a major contributor to catchment sediment yields in many regions. Stream bank erosion has also been identified as important in some New Zealand catchments (De Rose, 1998; Watson & Basher, 2006; Hicks *et al.*, 2011; Hughes & Hoyle, 2014). However, there has been very little quantitative research on both bank erosion processes and the contribution of bank erosion to sediment yields (Watson & Basher, 2006; Basher, 2013). Hence, it is an area where more research is warranted. This research would be particularly useful for improving our general understanding of the sources of sediment in New Zealand catchments. In particular, this information could be used to inform catchment sediment yield models such as SedNetNZ (Smith *et al.*, 2018), as well as providing information to catchment managers on where to focus catchment rehabilitation efforts.

2.4 Sediment fingerprinting

Sediment fingerprinting is a method that can be used to identify the dominant sources of sediment within a catchment. Physical and geochemical properties are compared between suspended sediment and potential erosion sources within the same catchment. The sediment fingerprinting technique is useful to discern the dominant sources of sediment and therefore implement mitigation and catchment restoration activities (Walling, 2013).

Sources of sediment can be identified in two ways; spatial source (e.g. distinguish between land uses in sub-catchments) or dominant processes (e.g. sheet erosion, bank erosion) (Walling, 1999).

Many physical and geochemical properties can be used in sediment fingerprinting research such as fallout radionuclides (He & Owens, 1995), sediment colour

(Grimshaw & Lewin, 1980), stable isotopes (Douglas *et al.*, 1995), plant pollen (Brown & Landforms, 1985) and compound stable specific isotopes (CSSIs) with plant fatty acids (Gibbs & Coasts, 2008).

The use of fallout radionuclide sediment fingerprinting is an approach that has been widely used internationally to determine the contribution of subsurface (i.e. bank and/or gully derived) and surface (i.e. sheetwash and rill erosion derived) sediment (Walling, 2013). Two of the most widely used fallout radionuclides in sediment fingerprinting research are caesium-137 (^{137}Cs) and excess lead-210 (^{210}Pb) (Walling, 2013).

2.4.1 Caesium-137

Caesium-137 (half-life 30.2 years) (Longmore, 1982) was one of the radionuclides chosen for this research. Caesium-137 is a man-made radionuclide, created during atmospheric thermonuclear weapon testing between 1952 and the mid-1980s. During the atmospheric weapon testing, ^{137}Cs entered the stratosphere (Longmore, 1982) and was deposited back on the surface through rainfall (Ritchie & McHenry, 1990). The global distribution of ^{137}Cs is directly related to the latitude and mean annual rainfall of a given area (linear relationship within latitudinal zones) (Ritchie & McHenry, 1990). Maximum deposition of ^{137}Cs occurred between 1954 – 1968 (Walling & Quine, 1992) and smaller amounts of ^{137}Cs were deposited from accidents at nuclear power stations such as the Chernobyl (1986) and Fukushima (2011) disasters (Lomenick & Tamura, 1965). The southern hemisphere has lower concentrations of deposited ^{137}Cs as most of the bomb tests occurred in the northern hemisphere (Walling & Quine, 1992).

The distribution of ^{137}Cs in soil profiles is well researched, with findings showing that ^{137}Cs decreases exponentially with soil depth (Figure 2.4). The decrease of ^{137}Cs with depth is due to the rapid adsorption of ^{137}Cs by soil particles (as soon as deposition occurred) (Walling, 2013).

The highest concentrations of ^{137}Cs are in the topsoil (15 cm) suggesting that vertical migration is minimal after adsorption to the soil particles (Walling, 2013). However, in areas such as those in the vicinity of the Chernobyl disaster, soil particle adsorption has been found to be weak due to acid organic soils in upland

areas (Walling & Quine, 1992). Soil texture may play an important role in the adsorption of ^{137}Cs , with some studies suggesting that a greater proportion of clay minerals improves the rate of adsorption (Livens & Loveland, 1988) while other studies suggest that adsorption is the same for all minerals (Livens & Baxter, 1988).

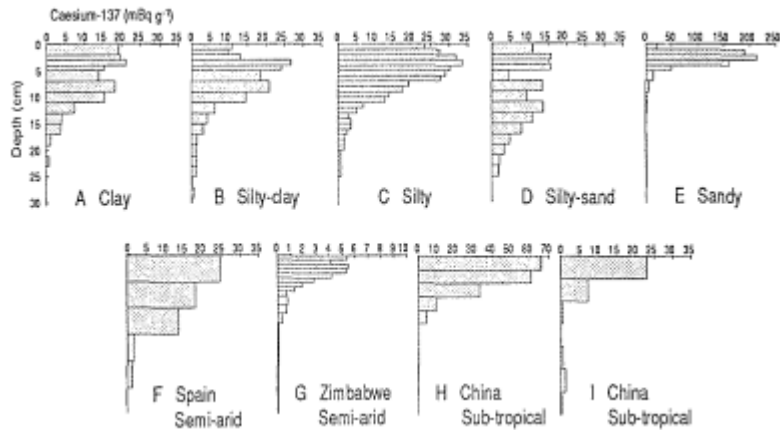


Figure 2.4. The distribution of ^{137}Cs is shown to decrease with depth in soils that are undisturbed. The graph shows soil profiles from a range of soil textures in the UK (A to E) and soil profiles from three countries with different climatic conditions (Reproduced from Cawse and Horrill (1986)).

When used as an environmental tracer, it is assumed that after deposition and subsequent adsorption in the upper horizons, ^{137}Cs can only be redistributed by soil erosion and transported sediment within a stream (Walling & Quine, 1992). The rapid fixing of ^{137}Cs by soil particles (shown by the decrease with soil depth) and studies from cultivated sites showing concentrations of ^{137}Cs to be higher in ploughed soil layers and eroded site concentrations to be contrastingly minimal, support the assumption that soil and sediment movement cause the redistribution of ^{137}Cs (Walling & Quine, 1992).

To estimate the total amount of soil erosion that has occurred in a catchment using ^{137}Cs an ‘input value’ must first be established. The ‘input value’ is an estimation of the amount of ^{137}Cs that was deposited in a given area during atmospheric nuclear testing. The ‘input value’ creates a baseline of ^{137}Cs and erosion rates are calculated by comparing current levels of ^{137}Cs within the soil of a particular area to the original ‘input value’ of ^{137}Cs . Thus, it is crucial to determine the correct ‘input value’ of ^{137}Cs for a particular study site (Ritchie & McHenry, 1990). Generally, the ‘input value’ is determined by collecting a large number soil samples (by depth

increments and coring) from an undisturbed site (forest or uncultivated land use, with no past erosion or deposition) and examining the distribution of ^{137}Cs with depth (Campbell *et al.*, 1988). Refer to Campbell *et al.* (1988) for information on the criteria for determining an ‘input value’ for ^{137}Cs .

Matthews (1989) developed an equation to determine the ‘input value’ of ^{137}Cs in New Zealand (Equation 1), from historical records (1955 to 1990) of strontium-90 (^{90}Sr) and its deposition by rainfall. Measured ratios of $^{137}\text{Cs}/^{90}\text{Sr}$ were then determined and a linear relationship between cumulative fallout deposition of ^{137}Cs and mean annual rainfall was determined. The input equation is as follows;

$$\text{fallout} - \text{Cs} = 53.4 + 0.6736R$$

- *fallout-Cs* = Cumulative deposition of ^{137}Cs (Bq m^{-2}) until 1990
- *R* = mean annual rainfall (mm)

Fallout deposition in New Zealand ceased in 1990, therefore corrections for the decay of ^{137}Cs need to be made to the ‘input’ equation in later years (Matthews, 1989). Basher and Matthews (1993) further validated the ‘input’ equation by collecting soil samples from 10 undisturbed sites in New Zealand and examining the relationship between ^{137}Cs in soils and rainfall distribution. Basher and Matthews (1993) found a strong correlation between ^{137}Cs in soils and rainfall ($r^2 = 73\%$), and a strong correlation between ^{137}Cs in soils and the deposition of ^{137}Cs from equation 1 ($r^2 = 73\%$) (Basher & Matthews, 1993).

An ‘input value’ was established at Whatawhata Research Station, within the Mangaotama catchment in 1994 (De Rose *et al.*, In prep as cited in De Rose, 1998), for ^{137}Cs of $1090 \pm 80 \text{ Bq m}^{-2}$ (equivalent to 1020 Bq m^{-2} after radioactive decay to the end of 1997).

De Rose *et al.*, In prep as cited in De Rose (1998), verified their ‘input value’ using the equation found in Basher & Matthews (1993) (equation 1), resulting in a similar ‘input value’ for ^{137}Cs of $1060 \pm 160 \text{ Bq m}^{-2}$ (= 990 Bq m^{-2} in 1997). The average annual rainfall that was used for equation (1) was 1650 mm yr^{-1} (De Rose *et al.*, In prep as cited in De Rose, 1998). Radionuclide concentrations of ^{137}Cs decreased with soil depth at Whatawhata Research Station. Peak concentrations of ^{137}Cs are

found in the top 15 – 20 cm of the soil at stable sites and there is little ^{137}Cs below 30 cm in the soil profile (Figure 2.5). At about 3 cm soil depth from the surface, concentrations of ^{137}Cs slightly decrease which was attributed to higher humus and decreased bulk density in the soil (De Rose et al., In prep as cited in De Rose, 1998).

De Rose (1998) further built on his earlier work De Rose et al., In prep as cited in De Rose (1998) by investigating 14 soil profiles; Two plots located at the top and bottom ends of the Mangaotama Stream. Seven sites were sampled at each plot and were located mostly on lower terraces near the stream, while some were located on the upper terraces. Six soil cores (0.05 m diameter, 0.75 m depth) were taken from 13 out of 14 sites, with most soil cores reaching the coarser textured bed material. One site was sampled manually, by collecting bank material at 5 cm increments. The six cores from each site were bulked, dried and sieved through a 1 mm sieve and were analysed for ^{137}Cs isotope analysis. Areal activities (Bq m^{-2}) of ^{137}Cs were calculated by dividing total sample activity by the total cross sectional area (0.0118 m^2), and minor corrections were made for soil loss during coring. Total areal activities (Bq m^{-2}) were determined by summing the areal activities of each individual soil depth (Figure 2.6).

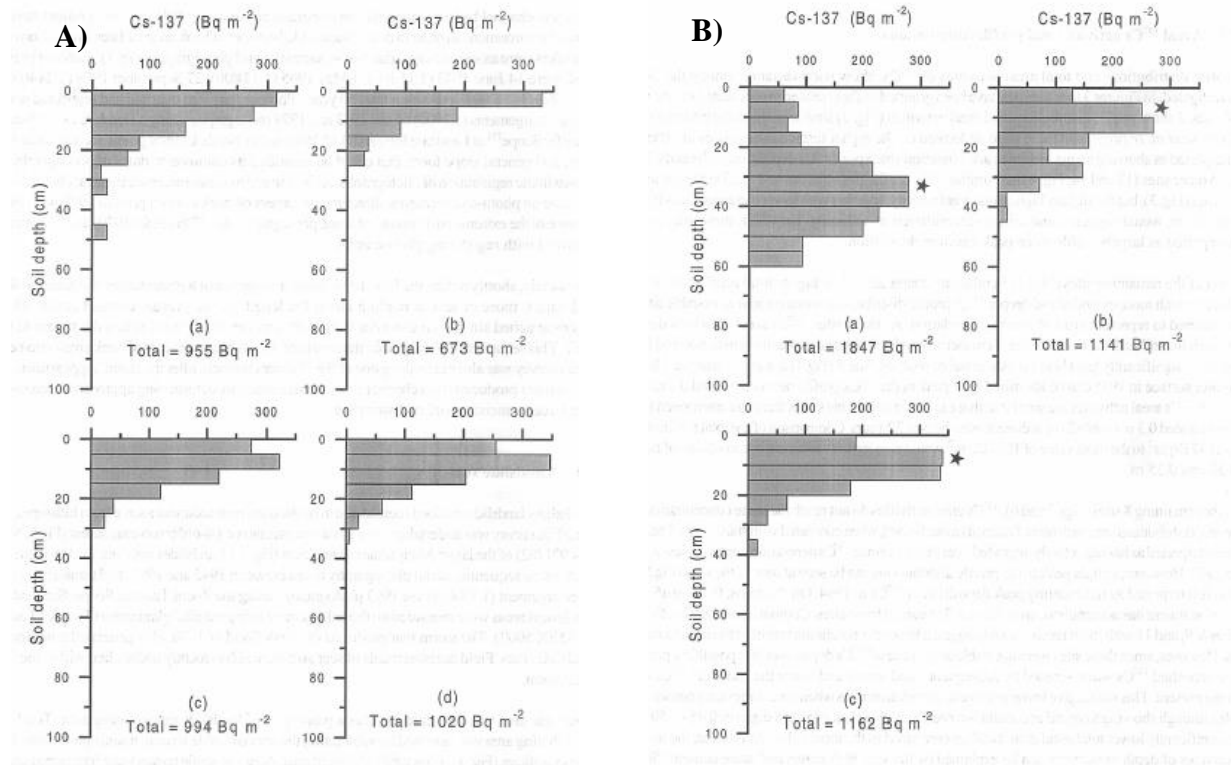


Figure 2.5. A) Soil profiles with aerial activities of ^{137}Cs in the upper terraces (a to c) (DeRose 1998) and a standard ridge profile (d) (De Rose. In prep as cited in De Rose 1998) at Whatawhata Research Station (De Rose 1998). B) Soil profile concentrations of ^{137}Cs in the lower terraces (a to c) N.B. The star represents peak deposition (Reproduced from DeRose 1998).

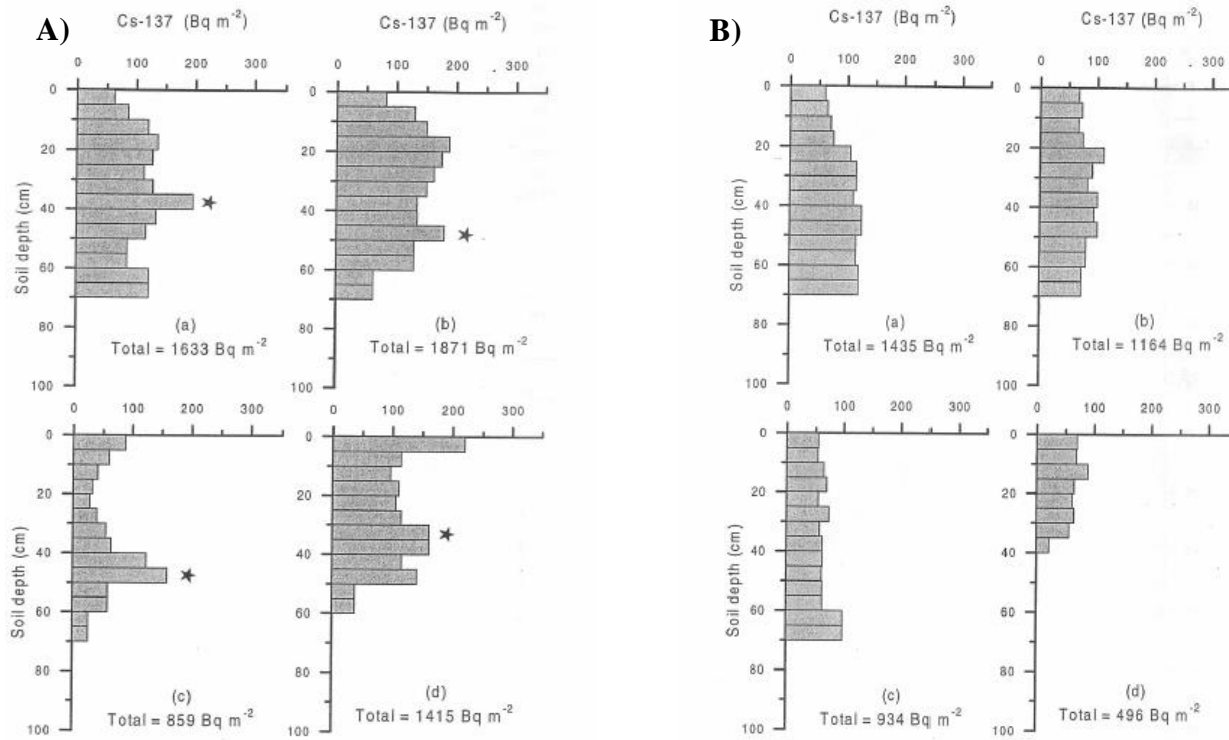


Figure 2.6. Soil profiles aerial activities of ^{137}Cs in the upper stream plot (A) and lower stream plot (B). N.B. The star represents peak deposition, no star means there was no peak deposition (De Rose, 1998).

Caesium-137 has the potential to be used as a tracer in this research because of its distribution through the soil profile (exponential decrease with depth) and because of the past research in ^{137}Cs by De Rose (1998) at Whatawhata Research Station (although DeRose, 1998 focused on total soil erosion and this research will focus on dominant erosion processes).

2.4.2 Excess Lead-210

Excess Lead-210 (half-life = 22.23 years) is the other radionuclide selected for this research. Excess Lead-210 is a natural radionuclide formed during the decay process of Uranium (^{238}U) in geological and soil materials (Figure 2.7). Uranium eventually decays into Radium (^{226}Ra), which in turn produces Radon (^{222}Rn). A fraction of ^{222}Rn diffuses into the atmosphere, while the remaining ^{222}Rn remains in the geological and soil materials. Diffusion of ^{222}Rn into the atmosphere occurs until equilibrium is reached between ^{226}Ra and ^{222}Rn in the rocks and soils. Lead-210 (^{210}Pb) is one of the daughter isotopes of ^{222}Rn and is produced in both the atmosphere and the earth (termed ‘supported’ ^{210}Pb because it is in equilibrium with ^{226}Ra). In the atmosphere, ^{210}Pb attaches to aerosol and dust particles, eventually falling back to the surface through wet and dry fallout and continuously falling over time (Mabit *et al.*, 2014).

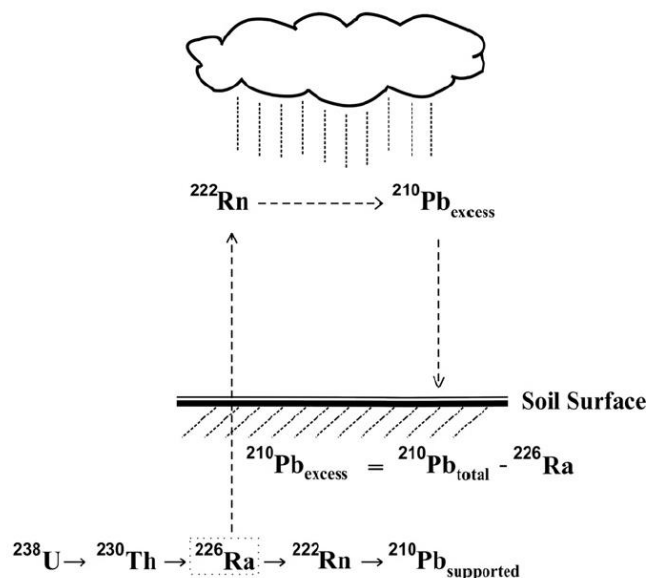


Figure 2.7. The origin of ‘supported’ lead-210 (^{210}Pb) and ‘excess’ lead-210 ($^{210}\text{Pb}_{\text{ex}}$) from the subsequent decay process of uranium (^{238}U) in geological and soil material (Reproduced from Mabit *et al.*, 2004).

Atmospheric fallout ^{210}Pb is termed ‘excess’ lead-210 ($^{210}\text{Pb}_{\text{ex}}$) and upon reaching the surface, $^{210}\text{Pb}_{\text{ex}}$ is rapidly adsorbed and strongly bound by clay particles and organic matter, quickly accumulating in the upper horizons (Figure 2.8). Migration of $^{210}\text{Pb}_{\text{ex}}$ through the soil profile is not very likely, with $^{210}\text{Pb}_{\text{ex}}$ being found to be highly immobile. The concentrations of $^{210}\text{Pb}_{\text{ex}}$, much like ^{137}Cs decrease exponentially through the soil profile (Mabit *et al.*, 2014) (Figure 2.9).

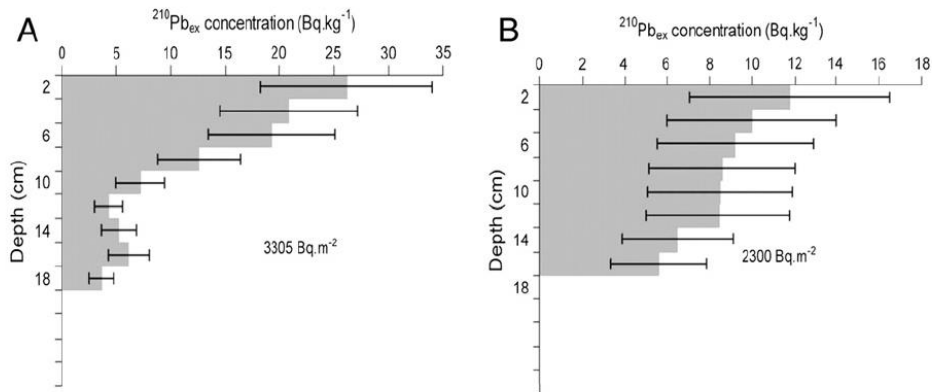


Figure 2.8. Concentrations of $^{210}\text{Pb}_{\text{ex}}$ through undisturbed (A) and cultivated (B) soil profiles in Morocco (Reproduced from Mabit *et al.*, 2014).

Previous research also indicates that plant and root absorption of $^{210}\text{Pb}_{\text{ex}}$ is limited (Klaminder *et al.*, 2006) however more research is needed investigating soil-plant transfers $^{210}\text{Pb}_{\text{ex}}$. Soil physical (e.g. texture) and chemical (e.g. cation exchange, pH) characteristics have been found to be primarily responsible for the bio-availability of $^{210}\text{Pb}_{\text{ex}}$ (Mabit *et al.*, 2014).

The measurement of $^{210}\text{Pb}_{\text{ex}}$ from a soil sample, cannot be tested directly, but rather indirectly through measuring and dividing concentrations of ^{226}Ra from total ^{210}Pb (supported ^{210}Pb) (i.e. $^{210}\text{Pb}_{\text{ex}} = ^{210}\text{Pb} - ^{226}\text{Ra}$). Concentrations of ^{226}Ra from total ^{210}Pb can be measured in numerous ways (e.g. beta counting, alpha spectrometry) however the gamma spectrometry method allows multiple radionuclides to be tested (e.g. ^{226}Ra , ^{210}Pb , ^{137}Cs) as the sample is not destroyed during analysis and costs are reduced compared to other methods (Mabit *et al.*, 2014).

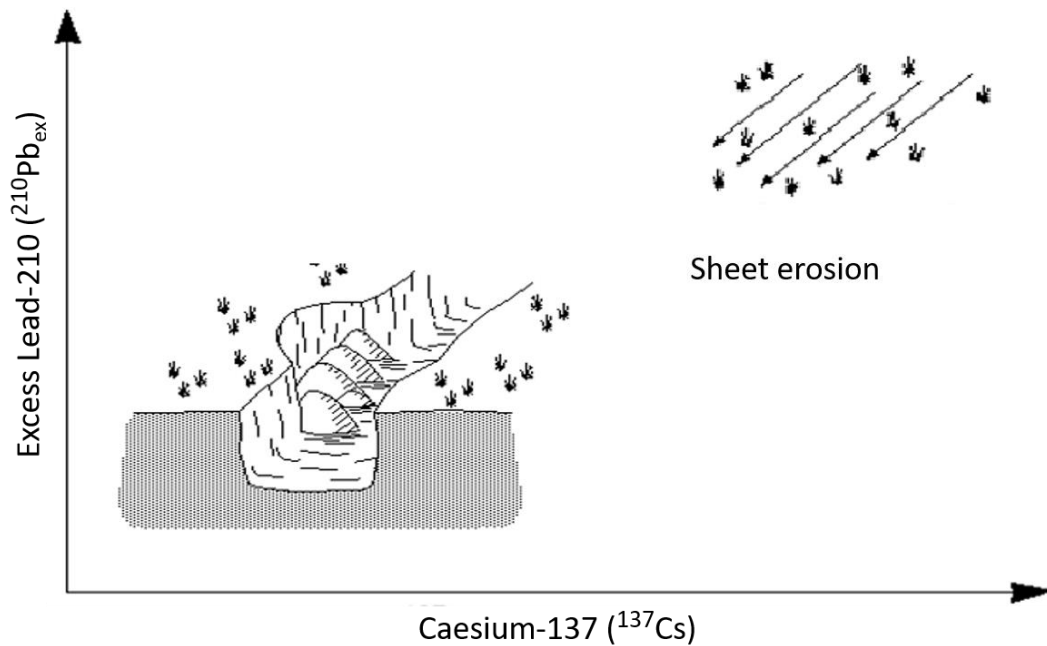


Figure 2.9. Conceptual diagram representing the concentration of lead-210 (^{210}Pb) and caesium-137 (^{137}Cs) in various erosion processes (Adapted from Olley *et al.* (2001)).

Excess lead-210 could be used as another tracer in this research. Much like ^{137}Cs , ^{210}Pb decreases with depth and could be used to determine dominant erosion processes.

2.4.3 Suspended sediment sampling (Phillips sampler)

There are various ways that source sediment samples are collected (Walling, 2013), however, suspended sediment samples in this research will be collected using a ‘Phillips sampler’ (Phillips *et al.*, 2000). The Phillips sampler is a time-integrated suspended sediment sampler designed to operate in small streams. Field research has shown that the sampler can collect a statistically representative grain distribution over time in a stream. However, sample collection is dependent on the particle size of the suspended sediment and the velocity of the ambient flow. The advantages of this sampler over other methods (e.g. automatic samplers) are that the Phillips samplers are affordable and easy to build (Phillips *et al.*, 2000).

The Phillips sampler (Figure 2.10) is composed of the following elements;

- Main body: Polyvinylchloride (PVC) pipe with an internal cross-sectional area of 7543 mm^2
- Sealed end caps: Located on both ends of the main body
- Inlet/Outlet tubes: Semi-rigid nylon pneumatic tubing with an internal cross-sectional area of 12.6 mm^2 ; Located in drilled holes through the centre of the end caps and later sealed in place
- Funnel: Located over the inlet tube, allowing for streamlined and uninterrupted flow into the inlet tube.
- Metal eyes: Located at the upper and lower end of the main body and used to secure the Phillips sampler to steel poles that have been placed in the channel bed (e.g. waratahs) (Phillips *et al.*, 2000).

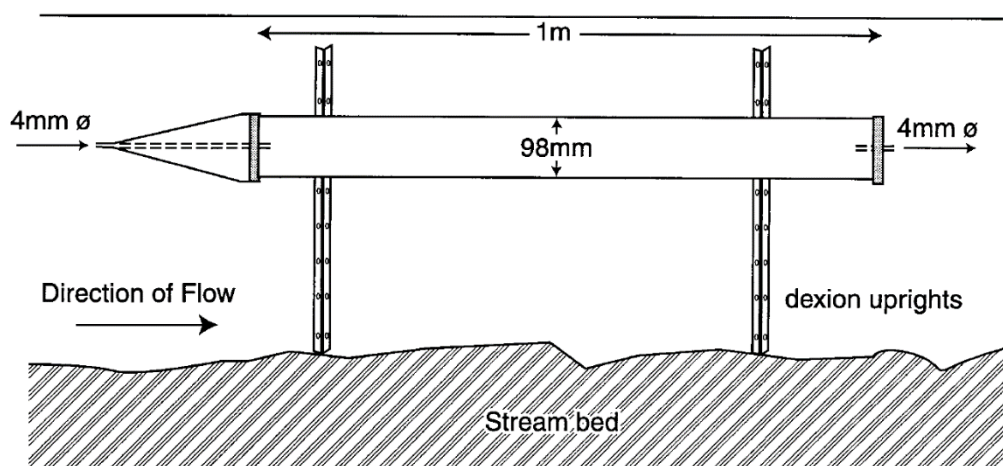


Figure 2.10. Cross-section diagram of the time-integrated sampler created by Phillips et al (2011).

Prior to installation, the Phillips sampler needs to be filled with native water. The sampler then must be fully submerged (60% of mean water depth), directed towards the stream flow and located within the middle of the channel (Phillips *et al.*, 2000). Once operating in the stream, water enters the sampler through the inlet tube at the same velocity as the ambient flow. Water within the sampler is then slowed within the main body (up to an excess of 600) due to its larger cross-sectional area. Sediment particles settle into the main body due to reduced velocities and water can exit through outlet tube.

Although velocities within the inlet tube are somewhat reduced due to friction, velocities remain strong enough so that no sedimentation occurs within the inlet tube (Phillips *et al.*, 2000).

The Phillips sampler is an ideal choice to collect suspended sediment samples for this research due to its low cost and efficiency at sampling fine sediment (Phillips *et al.* sampler).

2.5 Suspended sediment concentrations and discharge

Simultaneously recorded continuous stream flow (Q) and turbidity (acting as a proxy for suspended sediment concentration) can provide information about the main sources of sediment within a catchment, particularly during storm events. Identifying the main sources of sediment provides useful information for catchment management planning and mitigation efforts (Wasson *et al.*, 2002; Minella *et al.*, 2008).

Hughes *et al.* (2012) analysed the relationship between suspended sediment (converted from continuously collected turbidity data) and discharge in the Mangaotama and Whakakai catchment at Whatawhata Research Station (refer to Hughes *et al.*, 2012 and/or chapter 5 of this thesis for more detailed methods). Seventeen flood events (≥ 1.01 -year return period; 2209 l s^{-1} at Whakakai and 1217 l/s at Mangaotama) were recorded by NIWA between 1999 to 2010. Hughes *et al.* (2012) showed that 67% of the Whakakai catchment flood events had anti-clockwise hysteresis, while 100% of the Mangaotama flood events had clock-wise hysteresis. The dominance of anti-clockwise hysteresis in the Whakakai catchment, and clockwise hysteresis in the Mangaotama catchment indicate that there is a distinguishable difference between sources of sediment (Figure 2.11 & 2.12) between 1999 and 2010, with Whakakai appearing to be dominated by sources further from the stream and Mangaotama appearing to be dominated by sources near the stream. Clockwise hysteresis is identified when the turbidity peak is before the Q peak during a storm event. On the other hand, anti-clockwise hysteresis is identified when the Q peak is after the turbidity peak (Hughes *et al.*, 2012).

Between 1999 to 2010 the specific annual yield in the Mangaotama catchment (55 to 157 t/km²) was always greater than the specific annual yield in the Whakakai catchment (32 to 100 t/km²) (Figure 2.13). The mean yield over the same period of time in the Mangaotama catchment was 97 (\pm 39) t/km²/year and for the Whakakai catchment, the mean yield was 60 (\pm 22) t/km²/year (Hughes *et al.*, 2012).

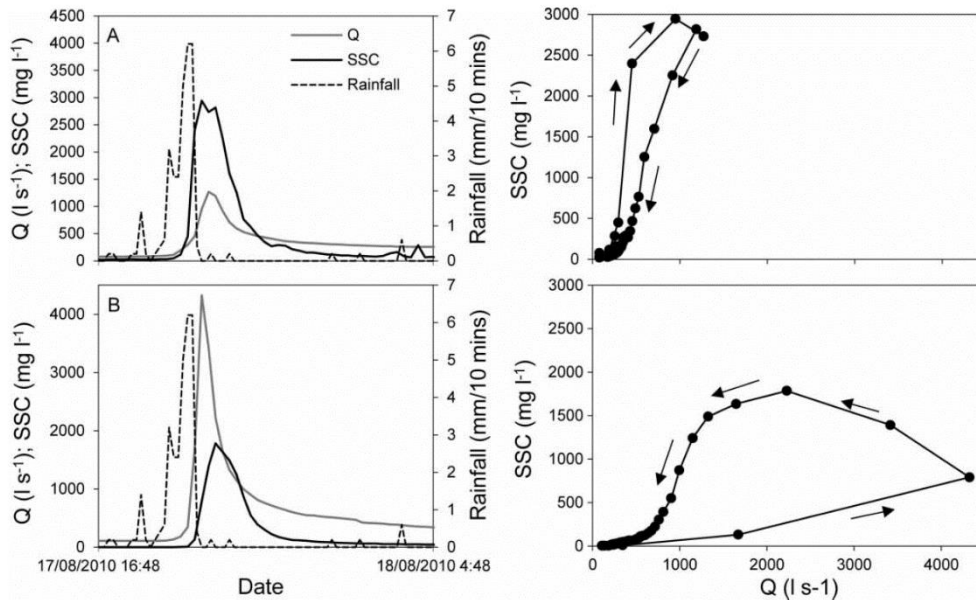


Figure 2.11. Peak discharge (Q), suspended sediment concentrations (SSC) and rainfall in the Mangaotama (A) and Whakakai (B) streams during a flood event in August 2010. Hysteresis patterns are also shown for the same flood event (Reproduced from Hughes *et al.* (2012)).

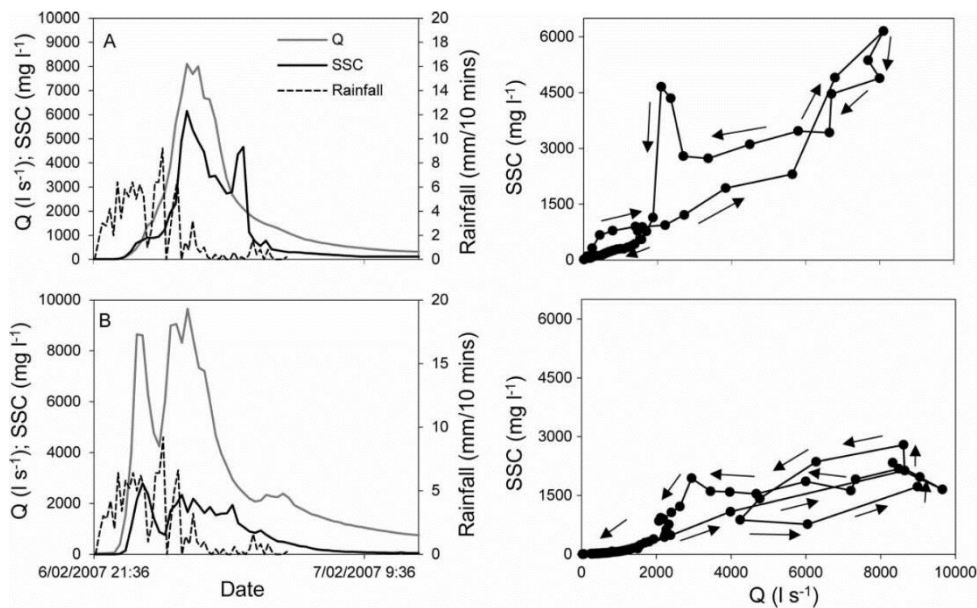


Figure 2.12. Peak discharge (Q), suspended sediment concentrations (SSC) and rainfall in the Mangaotama (A) and Whakakai (B) streams during a flood event in May 2010. Hysteresis patterns are also shown for the same flood event (Reproduced from Hughes *et al.* (2012)).

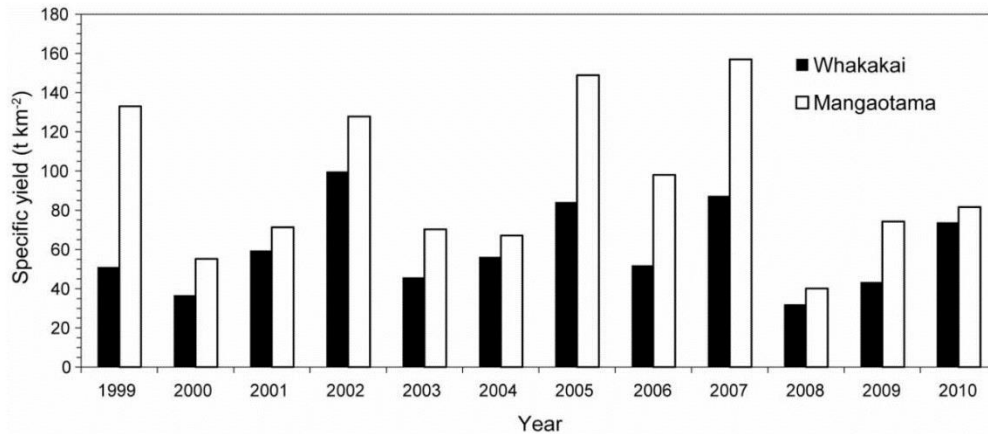


Figure 2.13. Comparison of the annual specific yields in the Mangaotama and Whakakai catchments from 1999 to 2010 (Reproduced from Hughes *et al.* (2012)).

This thesis will compare the past research undertaken by Hughes *et al.*, 2012 to SSC and Q relationships in the Mangaotama and Whakakai catchments (Whatawhata) for the year 2017 (see chapter five).

2.6 Field survey methods

Field surveys can be used to assess streams and banks (Lawler, 1993). One such method is the Pfankuch method, which is specifically designed to assess the bank stability in streams (Pfankuch, 1975). Parameters such as slope length/class, mass wasting (upper bank) and bank rock content are assessed based on their condition (poor to good) and assigned a score. At the end of the assessment, the scores are totalled and a ranking is assigned to the site (poor to good) (Pfankuch, 1975). The Pfankuch method has also been used in New Zealand catchments (Parkyn *et al.* (2003) and Collier (1992) made recommendations to adapt the method for New Zealand streams.

There are also a number of survey methods that have been developed specifically for New Zealand catchments. Harding *et al.* (2009) describes three general methods (i.e. protocols) to assess stream habitat. Protocol 1 is the fastest method (20 minutes) to implement and is similar to a methodology called the Riparian Management Classification (RMC) method used by NIWA (see next paragraph) (Quinn, 2009b).

The other two methods (i.e. Protocol 2 and 3) take longer (i.e. 45 mins – 180 mins) as they involve a more detailed assessment (e.g. Protocol 2 includes taking cross sectional measurements of the channel). Protocols should be chosen based on the purpose of the study. For example, Protocol 1 is best suited for State of the Environment reporting (SOE), while Protocol 2 is better suited for an Assessment of Environmental Effects (AEE) and consent monitoring. Finally, Protocol 3 is better suited for habitat modelling as this methodology is the most detailed (Harding *et al.*, 2009).

Waikato and Auckland (Neale *et al.*, 2009) Regional Councils use similar methods to assess riparian characteristics in their respective regions (Neale *et al.*, 2009). The method that both councils use is not very detailed and is intended for monitoring large rivers and reaches (e.g. 0.5 to 1 km). For example, there is only one section that addresses bank erosion in the Waikato Regional Council survey, where the erosion options are recent, active, pugging and no erosion (Hill & Kelly, 2002; Storey, 2010; Jones *et al.*, 2015).

2.6.1 Riparian Management Classification (RMC)

The Riparian Management Classification (RMC) (Quinn, 2009a, 2009b) is a field assessment tool used by NIWA to assess and enhance the riparian zone of streams. Survey sites are selected at random and reaches are surveyed at 50 – 100 m length intervals. The RMC form (Appendices Figure A.1) is completed for each survey reach. Attributes that are in the form are as follows (Quinn, 2009a);

- GPS coordinates (top and bottom of reach)
- Land use (general and riparian land use, left and right side)
- Stream and valley widths
- Channel plan shape
- Valley form
- Stream flow preference
- Stream shade
- Reach sketch and photographs
- Streambed substrate type
- Flow habitat classification

- Streambank height
- Streambank stability
- Macrophytes
- Periphyton
- Wood
- Live-stock access and damage
- Riparian vegetation cover
- Local land slope angle and length, and
- Riparian wetlands

Land use provides information on the local pressures potentially influencing the stream. For example, land uses like dairy and sheep and beef are potentially damaging to the stream and banks if the stock have access to those areas. If banks are unstable and erode, sediment delivery into the streams that can affect the in-stream habitat (e.g. macrophytes, periphyton, streambed substrate)(Quinn, 2009b). Vegetation in the riparian zone and banks acts to stabilize the bank area and riparian wetlands filter nutrients and sediment from overland flow (largely determined by valley form and local land slope angle and length) (Quinn, 2009b). Riparian vegetation can influence in-stream habitat, but the degree of influence is determined by factors such as stream width. Channel widths, valley widths and bank heights are important factors during flood events and high flows (Quinn, 2009b). Wood plays an important role in geomorphic and ecological habitat in the stream. Flow habitat classification provides information on the slope of the stream and the types of habitat available in the stream (Quinn, 2009b).

2.6.2 Three-dimensional (3D) models for surveys

Terrestrial photogrammetry is a technique that uses photographs to create 3D models (Lawler, 1993). There are numerous benefits and implications of this technique for bank erosion research, including wide spatial coverage, minimal impact on the site, time-efficient method and possible measurements of sediment deposition. However, there are concerns with this method, including the accuracy of the image hindered by poor lighting, erosion rates may not be detected in smaller streams and also that this method is most suitable over short periods of times (Lawler, 1993).

Terrestrial photogrammetry has evolved from the need to use purpose-built photogrammetry scanner (Lawler, 1993; Barker *et al.*, 1997) to the use of any digital camera (Pix4D, 2017; Agisoft LLC, 2018). Pix4D mapper is a software that creates 3D models, from photographs taken by either a digital camera to photographs taken by a drone. There are no specific requirements for the camera, any digital camera can be used (e.g. compact camera, DSLR), any lens can be used (e.g. fisheye, wide focal length), any camera platform can be used (e.g. helicopter, terrestrial vehicles) and any spectral specifications can be processed (e.g. RGB cameras, thermal cameras). Specifications for camera settings should have stabilization turned off and shutter, aperture and ISO on automatic, however manual selection of these values can be applied if images are not clear. The sharper and clearer the images the more accurate the results. Images are then loaded into the Pix4D mapper software where three phases occur; (1) the initial processing phase (quality of data check); (2) the creation of a point cloud and mesh and (3) the creation of a DSM, Orthomosaic and index.

There is another software called Agisoft Photoscan that had the potential to be used for this research but Agisoft Photoscan was created for modelling only (Agisoft LLC, 2018), whereas Pix4D was created specifically for mapping areas with real-world coordinates. This is evident as upon importing images to the software, the user is asked to verify the coordinates of the photographs (Pix4D, 2017).

In theory, terrestrial photogrammetry could be used to estimate eroded volumes (or bank erosion rates), from changes in stream banks over time. Once, a baseline has been established (3D models created for eroding bank sites), the photogrammetry surveys can be repeated over time (e.g. annually, or after large flood events). Previous studies have used terrestrial photogrammetry (structure from motion) to measure erosion rates in coastal environments (James & Robson, 2012) and glaciers (Whitehead *et al.*, 2013).

Prosdocimi *et al.* (2015) tested photogrammetry (structure from motion) to analyse bank erosion within a small agricultural floodplain catchment (916 km) in Veneto, Italy. Two digital reflex cameras ((1) Cannon 22.3 MP resolution, 35 mm focal length, (2) Nikon 10.2 MP resolution, 35mm focal length) and a smartphone camera (iPhone5), were used to test the structure from motion method, and the results were

compared with terrestrial laser scanning (TLS) data. The study was carried out in 2014, where there was a large part flood event in the catchment in 2010.

Stream bank erosion volumes were estimated using a reconstructed digital elevation model (DEM) (based on the geometry of the undisturbed channel), and structure from motion and TLS models. Stream bank erosion volumes were estimated using the Geomorphic Change Detection tool in ArcGIS. The results showed that bank erosion volumes were similar between using the Cannon camera (34.74m³), Nikon camera (34.71m³), smartphone (35.59 m³) and the TLS laser scanner (36.77m³). There was also minimal error in the structure from motion method (0.001m) (Prosdocimi *et al.*, 2015). Although it is recommended that photographs be taken with the highest quality (> 12 megapixel), and to use digital cameras (e.g. SLR models) (Westoby *et al.*, 2012), Prosdocimi *et al.* (2015) found that using a simple smartphone (8 megapixel) with structure from motion method, produced high-resolution DEMs. Therefore, the structure from motion method (terrestrial photogrammetry method), is a potentially effective tool for farmers and land-users to monitor changes in bank erosion over time.

Hamshaw *et al.* (2017) used unmanned aircraft systems (UAS) to monitor bank erosion in four catchments within the Lake Champlain Basin, Vermont, USA. Seven study sites were chosen within the four catchments, which represented a range of land uses (e.g. forested, agricultural), soil type, bank heights and upstream drainage. The sites were also chosen over a range of bank erosion sensitivity (i.e. visible to minimal erosion). UAS surveys occurred four times over 2 years (2015 – 2016), twice in Spring and once in Summer and Autumn. The USA survey data was compared to terrestrial land survey (TLS) and GPS data for validation purposes. Hamshaw *et al.* (2017) found that UAS data correlated well with TLS and GPS data. However, the accuracy of the UAS data was limited by the presence of vegetation (i.e. more accurate when there is less vegetation). Thus, the UAS methodology for bank erosion measurements is not suitable for areas that have year-round vegetation growth (e.g. tropics and the sub-tropics). Further, for small bank sections, TLS data is more accurate than UAS data (Hamshaw *et al.*, 2017).

Thus the advantages of using digital cameras and smartphones are that the method is more cost-effective, requires little technical knowledge, and are lightweight tools to be used in the field (Prosdocimi *et al.*, 2015). On the other hand, the structure

from motion method requires more time in the field, and cannot cover large areas such as those with drones (e.g. large catchments) (Hamshaw *et al.*, 2017).

2.7 Discussion and synthesis

There are few New Zealand studies that have researched the contribution of bank erosion to stream sediment (Hicks *et al.*, 2011). Previous research by De Rose (1998) at Whatawhata that created an ‘input value’ for ^{137}Cs and showed that ^{137}Cs decreased with depth. However, De Rose (1998) focussed on total erosion, whereas this research will focus on the identifying the dominant erosion processes contributing to sediment yields at Whatawhata. Previous research at Whatawhata by Hughes *et al.* (2012) indicates the Mangaotama and Whakakai catchments are dominated by different erosion processes, and this theory will be tested during this thesis.

In terms of the field surveys, the RMC method developed by (Quinn, 2009a) will be most useful as this method is the most time-effective and has important criteria to assess and compare streambank erosion and catchment characteristics between the Mangaotama and Whakakai catchments.

2.8 Conclusions

Soil erosion is a natural process, predominantly dominated by wind or water erosion. However, human activities such as land use changes can accelerate soil erosion, and subsequently increase sediment in streams. Excess sediment in streams can be detrimental to freshwater ecology, amenity values and the connection of indigenous cultures towards freshwater.

Stream bank erosion processes are complex, and drivers for stream bank erosion vary in the catchment (i.e. headwaters, mid-reaches and lower reaches), although these processes can sometimes overlap. Sediment fingerprinting particularly fallout radionuclides (^{137}Cs and $^{210}\text{Pb}_{\text{ex}}$) can be used to determine the relative contribution of sources of sediment within a catchment. Analysing turbidity (as a proxy for suspended sediment) combined with simultaneously recorded flow (Q) data can also provide information on sources of sediment within a catchment. Catchment surveys and terrestrial photogrammetry are also useful methods for monitoring erosion over time.

Very little research has been undertaken to study the relative contribution of stream bank erosion to sediment in streams. In the Whatawhata study site, there has been previous research by De Rose (1998) focusing on total erosion in the catchment, however, this research will focus on identifying the relative contributions of erosion sources to stream sediment. Further, the theory stated by Hughes *et al.* (2012) that stream bank erosion sources dominate the Whakakai and hillslope erosion sources dominate the Mangaotama catchment, will be tested in this thesis. Sediment fingerprinting using fallout radionuclides and catchment surveys using (Quinn, 2009) can help identify the main sources of sediment within both catchments. Terrestrial photogrammetry also has the potential to be used as a monitoring tool for stream bank erosion.

Chapter 3

Catchment Surveys of Stream Bank Erosion

3.1 Introduction

Field surveys are a useful method for determining the state of stream and riparian vegetation health. One qualitative method involves using field forms that assess stream and riparian health with a range of criteria such as those defined in Quinn (2009a). In recent years, more quantitative survey methods have become available such as the creation of 3D models from photographs using photogrammetry software.

The overall objective of this chapter was to;

Identify the similarities and differences in potential sediment sources and catchment conditions, between the Mangaotama and Whakakai catchments by conducting field surveys of each stream with a focus on the streambanks and riparian margins.

The specific objectives were to:

- Divide the two streams into similar reaches,
- For each reach record the main characteristics using the Riparian Management Classification (Quinn, 2009a),
- Identify the similarities and differences in the land use, vegetation, channels, topography, and streambanks between the two catchments, and
- Trial the use of terrestrial photogrammetry for potential quantitative monitoring of streambanks.

3.2 Methods

3.2.1 Riparian Management Classification

The Riparian Management Classification (RMC) (Quinn, 2009a) was carried out in the Mangaotama and Whakakai catchments in September and October 2018 and January 2019. The Mangaotama catchment survey was undertaken about 200 m upstream from the NIWA hydrometric site (Site PW5) and continued upstream for 1.3km (pasture: 0.9km and pine: 0.4km) (Figure 3.1). The Whakakai catchment

survey also was undertaken from a NIWA hydrometric site (Site NW5) and continued upstream for 0.9km (Figure 3.1).

The Mangaotama stream was divided into 26 reaches (14 under pastoral land use; 12 under pine land use), and the Whakakai stream was divided into 16 reaches. Reaches in the Mangaotama stream ranged from 20m to 145m, with an average length of 48m. Reaches in the Whakakai stream ranged from 20m to 135m, with an average length of 58m (Table 3.1). In both streams, where one reach ended, a new reach was started so the entire stream length was surveyed.

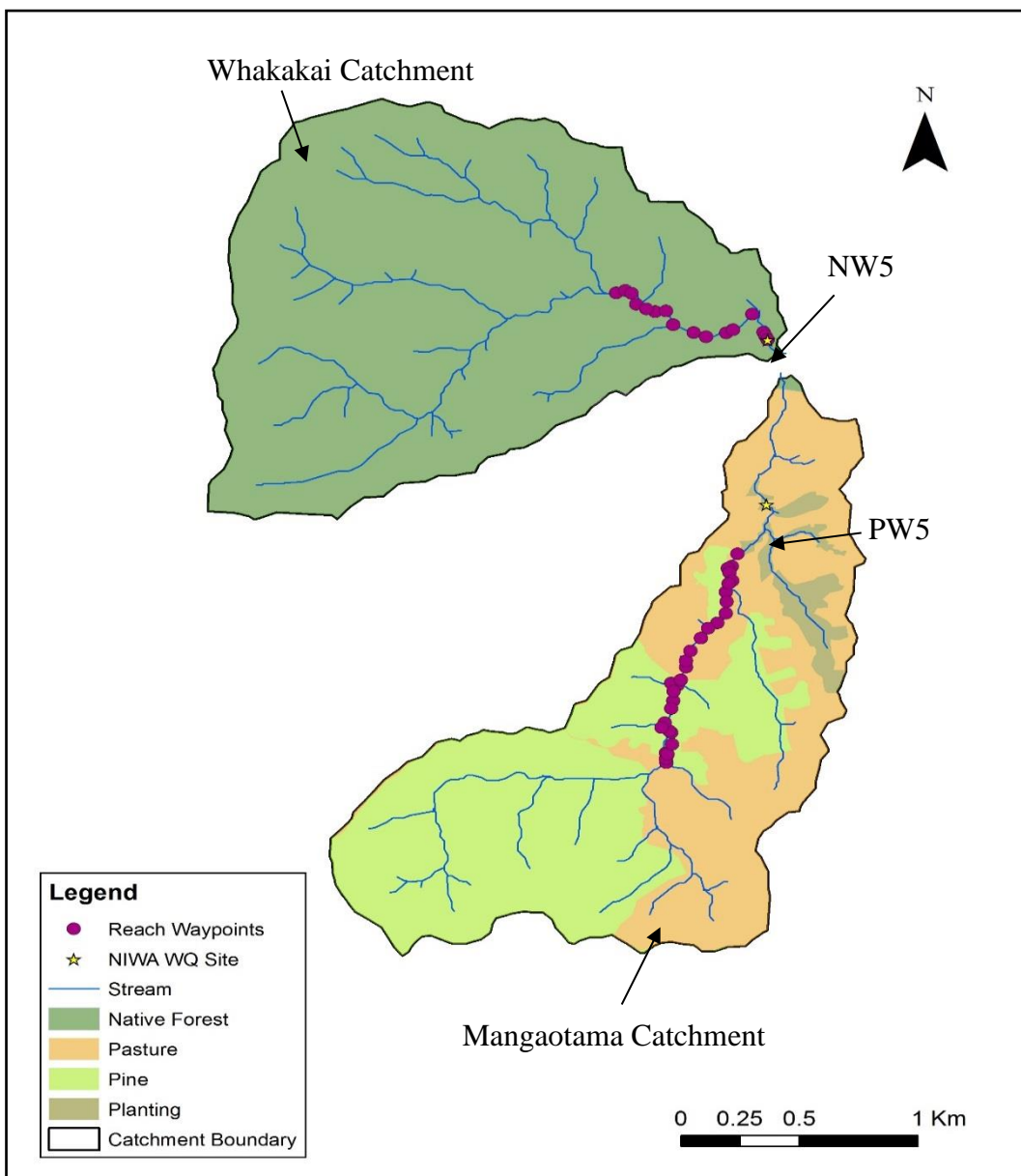


Figure 3.1. GPS points showing the top and bottom of the reaches assessed using the Riparian Management Classification in the Mangaotama and Whakakai Catchments. Note: WQ = water quality

Table 3.1. Reaches in the Mangaotama and Whakakai Streams with GPS locations for the top and bottom of each reach.

Reach	Land Use	Length (m)	Top of reach		Bottom of reach	
			Latitude	Longitude	Latitude	Longitude
Mangaotama Stream						
1	Pasture	60	37° 47' 13.991" S	175° 4' 20.213" E	37° 47' 15.901" S	175° 4' 19.348" E
2	Pasture	25	37° 47' 15.901" S	175° 4' 19.348" E	37° 47' 16.287" S	175° 4' 18.643" E
3	Pasture	35	37° 47' 16.287" S	175° 4' 18.643" E	37° 47' 16.899" S	175° 4' 18.927" E
4	Pasture	30	37° 47' 16.899" S	175° 4' 18.927" E	37° 47' 18.619" S	175° 4' 18.826" E
5	Pasture	80	37° 47' 18.619" S	175° 4' 18.826" E	37° 47' 18.178" S	175° 4' 19.478" E
6	Pasture	70	37° 47' 21.460" S	175° 4' 18.563" E	37° 47' 19.941" S	175° 4' 18.377" E
7	Pasture	60	37° 47' 23.268" S	175° 4' 18.507" E	37° 47' 21.460" S	175° 4' 18.563" E
8	Pasture	60	37° 47' 24.778" S	175° 4' 17.063" E	37° 47' 23.268" S	175° 4' 18.507" E
9	Pasture	60	37° 47' 25.620" S	175° 4' 15.533" E	37° 47' 24.778" S	175° 4' 17.063" E
10	Pasture	60	37° 47' 27.192" S	175° 4' 14.334" E	37° 47' 25.620" S	175° 4' 15.533" E
11	Pasture	145	37° 47' 29.186" S	175° 4' 12.525" E	37° 47' 27.192" S	175° 4' 14.334" E
12	Pasture	70	37° 47' 30.709" S	175° 4' 11.822" E	37° 47' 29.186" S	175° 4' 12.525" E
13	Pasture	40	37° 47' 31.701" S	175° 4' 11.890" E	37° 47' 30.709" S	175° 4' 11.822" E
14	Pasture	60	37° 47' 33.699" S	175° 4' 11.005" E	37° 47' 31.701" S	175° 4' 11.890" E
15	Pine	55	37° 47' 34.235" S	175° 4' 9.345" E	37° 47' 33.699" S	175° 4' 11.005" E
16	Pine	24	37° 47' 35.515" S	175° 4' 9.821" E	37° 47' 34.235" S	175° 4' 9.345" E
17	Pine	42	37° 47' 36.954" S	175° 4' 9.787" E	37° 47' 35.515" S	175° 4' 9.821" E
18	Pine	40	37° 47' 38.177" S	175° 4' 9.496" E	37° 47' 36.954" S	175° 4' 9.787" E
19	Pine	30	37° 47' 40.435" S	175° 4' 8.405" E	37° 47' 38.177" S	175° 4' 9.496" E
20	Pine	33	37° 47' 41.649" S	175° 4' 9.221" E	37° 47' 40.435" S	175° 4' 8.405" E
21	Pine	25	37° 47' 41.909" S	175° 4' 9.555" E	37° 47' 41.649" S	175° 4' 9.221" E
22	Pine	50	37° 47' 43.729" S	175° 4' 9.809" E	37° 47' 41.909" S	175° 4' 9.555" E
23	Pine	40	37° 47' 45.303" S	175° 4' 9.041" E	37° 47' 43.729" S	175° 4' 9.809" E
24	Pine	20	37° 47' 45.095" S	175° 4' 8.755" E	37° 47' 45.303" S	175° 4' 9.041" E
25	Pine	25	37° 47' 46.008" S	175° 4' 8.822" E	37° 47' 45.095" S	175° 4' 8.755" E
26	Pine	30	37° 47' 46.585" S	175° 4' 8.886" E	37° 47' 46.008" S	175° 4' 8.822" E
Whakakai Stream						
1	Native	25	37° 46' 40.102" S	175° 4' 24.164" E	37° 46' 40.695" S	175° 4' 24.473" E
2	Native	24	37° 46' 39.537" S	175° 4' 23.787" E	37° 46' 40.102" S	175° 4' 24.164" E
3	Native	135	37° 46' 36.751" S	175° 4' 21.775" E	37° 46' 39.537" S	175° 4' 23.787" E
4	Native	94	37° 46' 39.250" S	175° 4' 18.534" E	37° 46' 36.751" S	175° 4' 21.775" E
5	Native	28	37° 46' 39.725" S	175° 4' 17.303" E	37° 46' 39.250" S	175° 4' 18.534" E
6	Native	90	37° 46' 40.438" S	175° 4' 13.925" E	37° 46' 39.725" S	175° 4' 17.303" E
7	Native	58	37° 46' 39.782" S	175° 4' 11.741" E	37° 46' 40.438" S	175° 4' 13.925" E
8	Native	80	37° 46' 38.671" S	175° 4' 8.183" E	37° 46' 39.782" S	175° 4' 11.741" E
9	Native	75	37° 46' 36.529" S	175° 4' 6.894" E	37° 46' 38.671" S	175° 4' 8.183" E
10	Native	50	37° 46' 36.693" S	175° 4' 4.972" E	37° 46' 36.529" S	175° 4' 6.894" E
11	Native	50	37° 46' 36.236" S	175° 4' 3.473" E	37° 46' 36.693" S	175° 4' 4.972" E
12	Native	50	37° 46' 35.548" S	175° 4' 1.743" E	37° 46' 36.236" S	175° 4' 3.473" E
13	Native	65	37° 46' 33.897" S	175° 4' 0.854" E	37° 46' 35.548" S	175° 4' 1.743" E
14	Native	45	37° 46' 33.447" S	175° 3' 59.792" E	37° 46' 33.897" S	175° 4' 0.854" E
15	Native	40	37° 46' 33.882" S	175° 3' 58.181" E	37° 46' 33.447" S	175° 3' 59.792" E
16	Native	20	37° 46' 33.882" S	175° 3' 58.181" E	37° 46' 33.882" S	175° 3' 58.181" E

The reaches were determined by changes in the stream characteristics, such as water width, bank heights (e.g. high to low), bank erosion processes and vegetation. Some reaches were simple to group together, as these reaches were straight or semi-straight channel shapes, and the stream characteristics would change around a stream bend (Figure 3.2). However, most reaches were moderate to strongly sinuous and showed a clear change in stream characteristics to distinguish one reach from the next. However, there were two exceptions, in which case it was difficult to determine the beginning and end of these reaches. One reach was in the Mangaotama catchment and one was in the Whakakai catchment. It was difficult to determine where to end these reaches, because they were strongly sinuous and the left bank and right bank heights would change at different parts of the reach, rather than at the same time like the other reaches, thus resulting in longer reaches (Mangaotama: Reach 11 = 145m, Whakakai: Reach 3 = 135m). Further, the dominant bank erosion was the same in each reach (Reach 11 was largely stable and Reach 3 was predominantly stable with small areas of undercut).

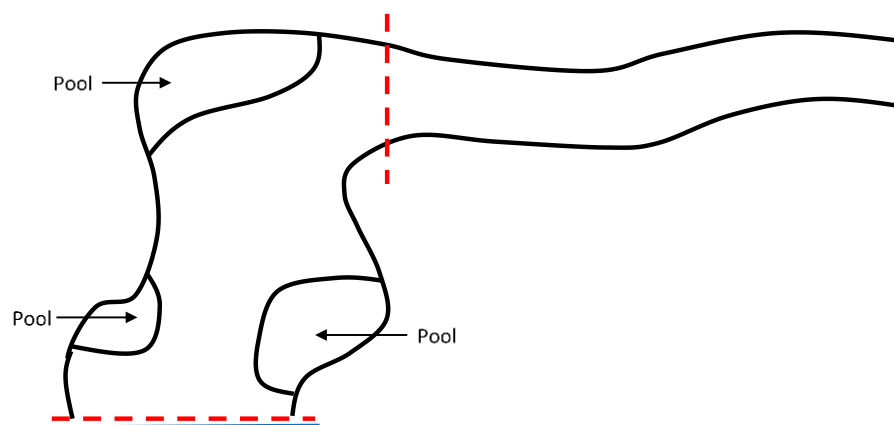


Figure 3.2. Example diagram of how reaches were chosen, where one reach has a wider water width, multiple pools and was sinuous, while the other reach was narrower and semi-straight. The perforated red line represents the separation between two reaches, and the blue line represents a waterfall.

In each reach an RMC form (Appendices Figure A.1) was completed (Figure 3.3), which contained the following categories;

- Site description including name, date, GPS for the top and bottom of the reach and reach length
- General land use (left and right bank)
- Riparian land use (left and right bank)
- Widths for the water, channel, bankfull and valley bottom
- Channel plan shape

- Valley form
- Flow
- Stream shade
- Streambed
- Presence of riffle/run/pools in reach
- Bank stability and heights (left and right)
- Vegetation stabilising the banks (left and right)
- Macrophyte cover and type
- Presence of periphyton
- Presence of wood
- Live-stock access and damage (left and right)
- Riparian vegetation and dominant riparian plant species (left and right)
- Local runoff potential: Slope length and class (left and right)
- Presence of riparian wetlands

The reach lengths were paced by the author and all other measurements (e.g. bank heights, stream widths, valley bottom widths) were estimated by the author. Stream shade was also estimated by the author, using diagram illustrations in Quinn (2009a) and photographs were taken at each reach and GPS points were recorded for the top and bottom of each reach (Table 3.1).



Figure 3.3. Recording stream and riparian characteristics within the pine section of the Mangaotama catchment (Photo: F. Khan, 2019).

3.2.2 Establishment of a photo-based 3D baseline

Eroded bank sites were photographed for 3D modelling purposes on September 20 in the Whakakai catchment and September 29 in the Mangaotama catchment. Two bank erosion sites were photographed in the Whakakai catchment and four bank erosion sites were photographed in the Mangaotama catchment. Three of the Mangaotama sites were in the pine plantation and one was in pasture. Actively eroding bank sites were selected while undertaking the RMC survey in each catchment. Bank sites were chosen that were not too close to each other, to get a spatial representation of each catchment.

Garden stakes were placed on the top of the bank at each site, about 1m back from the edge of the bank (Figure 3.4). The top of the stakes had blue marking tape placed 16 cm from the top of the stake, and yellow surveying paint was sprayed from the top of the marking tape to the top of the stakes (Figure 3.4). The stakes were used as scales for the 3D models and also as reference points for the software.



Figure 3.4. Example of on 3D modelling bank sites (left). Close up of marked garden stakes used for scale during the creation of the 3D models (right).

Photographs were taken using a digital camera (Canon Powershot XS260HS) and photographs were taken in automatic mode. The photographs of each bank site were taken from various angles, perspectives, heights and, where possible, various distances. For example, a photograph would be taken from the left side of the bank and then the photographer would move ~0.5m to the left/right, backwards/forwards (Figure 3.5) or change the vertical height up/down from the original starting

position (Figure 3.5). It was crucial that there was movement between each photograph, as the 3D modelling software is not able to process photographs taken from the exact same position (Pix4D, 2017).

When taking the photographs, care was also taken to include as much of the bank site as possible in each image to ensure that there was a significant overlap between the pictures. Close up photographs were taken to give more details to the models (e.g. underside of overhanging banks). Care was also taken to ensure that photographs of the banks were not over-exposed or too dark.

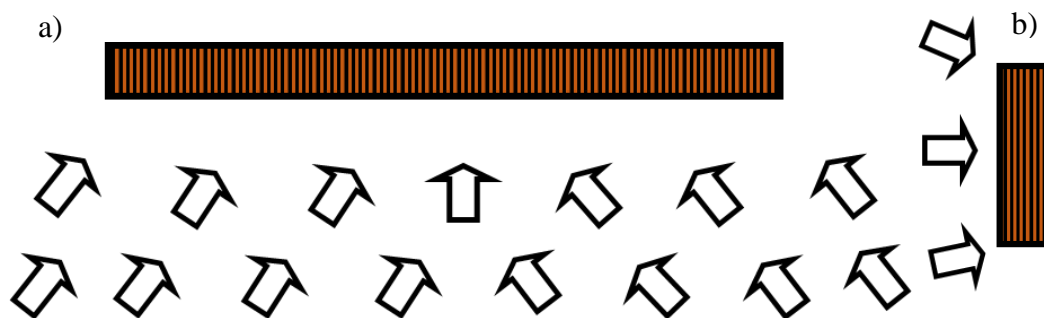


Figure 3.5. Conceptual schematic of the orientation of the photographs (arrows) for 3D modelling of streambanks (rectangle). Birds eye view showing simplified changes in angles and distances used while photographing the banks (a) and a simplified side view of the banks showing (adapted from Agisoft LLC (2018)).

Software

The Pix4D mapper software (Pix4D, 2017) was used to create the 3D models. The first step was to import the photographs into the software. After the photographs were imported for a bank site, the scale was identified and digitally marked on each image (i.e. line marking) using the spray paint on the stakes. The digital line markings were drawn on a few images manually and then the software was able to automatically draw the rest. The line markings were also used to identify the vertical orientation.

Some of the initial survey sites were not staked, and the scale was not determined. The vertical orientation was also not accurately determined at sites with no stakes, therefore best estimates were made (e.g. using a tree that appeared to be vertical). The first model creation step was the initial processing phase (Figure 3.6). The second phase was the construction of the point cloud & mesh and the third phase was forming the Digital Surface Model (DSM) and the ortho-mosaic (Figure 3.6)

(Pix4D, 2017). The bank models were also exported as a fly-through video (.mp4) (for more information re. 3D models e-mail the author at manawa_huirama@hotmail.com).



Figure 3.6. Chart showing the processing steps used by the Pix4D software to create 3D models from terrestrial based imagery (Pix4D, 2017).

3.3 Results

3.3.1 Riparian Management Classification

Land use

The section of the Mangaotama stream that was surveyed had 0.85 km of pastoral land use (Figure 3.7) and 0.4 km of pine plantation land use (Figure 3.7). In the Mangaotama pastoral section, most reaches had general land use of sheep and beef (left and right streambanks) and a riparian land use of sheep and cattle grazing. A smaller proportion of reaches had a general land use of planted pine forest on one side of the stream (22%). Riparian land use consisted of 33% conservation (management practices e.g. poplars planted for bank stability), 16% filter strip (grass area between pine forest and stream) and 5% woodlot (planted forest intended for felling). Stock damage ranged from minor (Figure 3.8) to extensive. In the Mangaotama planted pine section, the general land use was planted forest and the riparian land use was filter strip and woodlot. There was generally no stock access in the planted pine forest section.

There were several bridges in the Mangaotama catchment, some were intact (i.e. stock were able to cross), while others were completely old and broken (Figure 3.8). In some reaches, there were also broken fence posts and wiring (Figure 3.9). The fence posts and wiring appeared to be attempts at preventing the stock from accessing the stream but had not been maintained. There were also fallen pine and poplar trees throughout the pasture reach (Figure 3.9). Some of the fallen pine trees were harvested between 2010 and 2012 (A. Hughes, personal communication,

2018) as there was a pile of pine trees near a shed, other pine trees, much like the poplar trees appear to have fallen naturally.

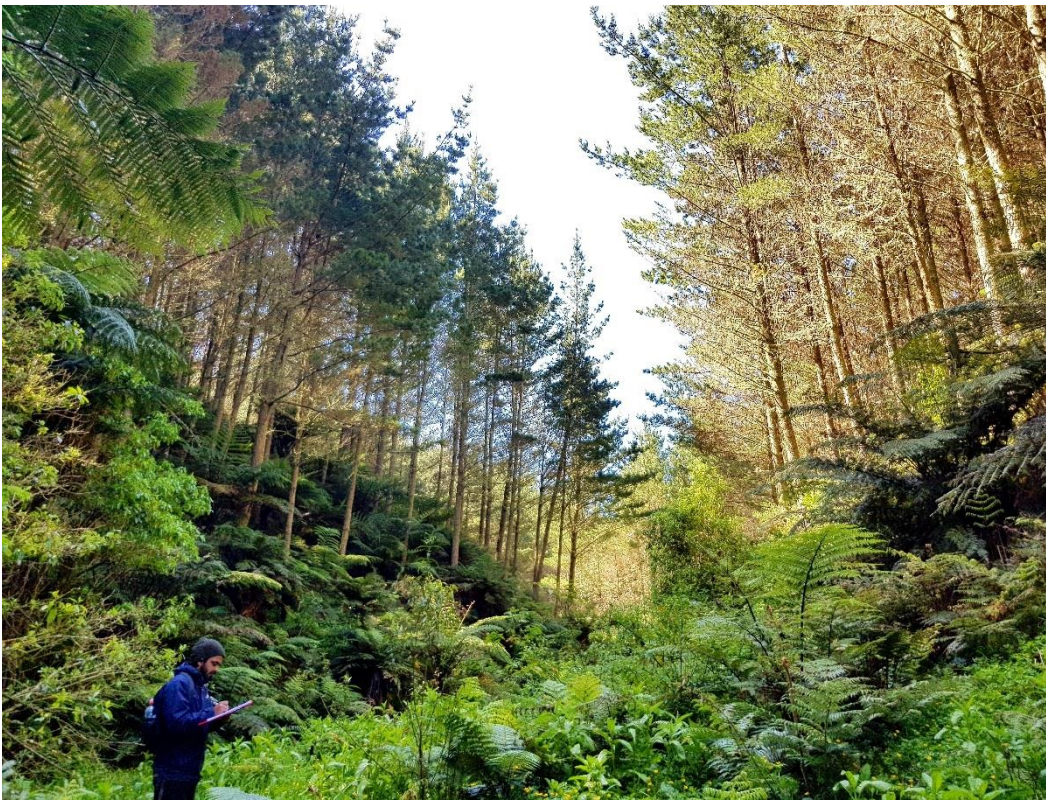


Figure 3.7. Mangaotama catchment (top) pastoral land use (Photo M. Balks, 2018) and (bottom) pine forest.



Figure 3.8. Stock damage on the stream bank in the Mangaotama catchment pastoral section (top) and broken bridge in the Mangaotama catchment pastoral section (bottom).



Figure 3.9. Fallen pine trees (top) and broken fencing (bottom) in the pastoral section of the Mangaotama catchment.

In the Whakakai catchment the general land use in all reaches was native forest (left and right streambanks) (Figure 3.10) and the riparian land use was conservation (left and right streambanks). There was no stock access in the Whakakai catchment. However, there are wild pigs present in the catchment that have been known to wallow near the stream banks (A. Hughes, personal communication, 2019).

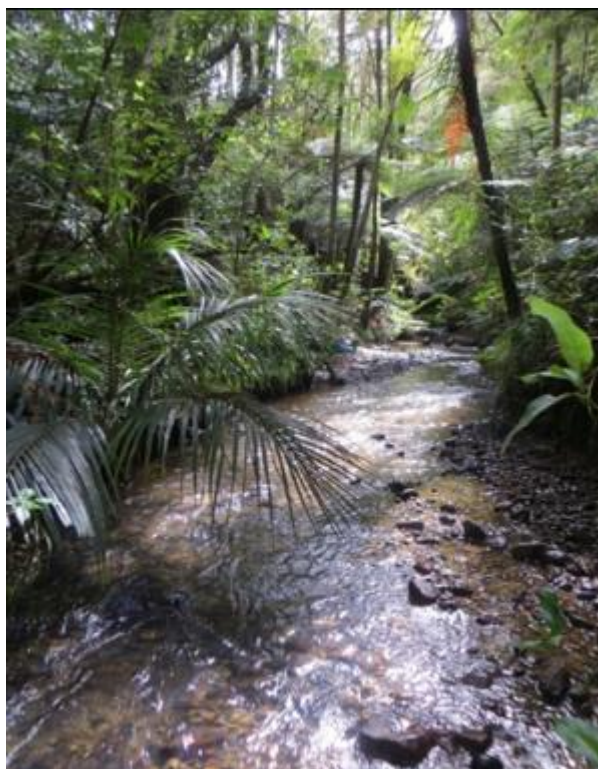


Figure 3.10. Whakakai stream (top) (Photo: M. Balks, 2018).

Vegetation

In the Mangaotama pastoral section, the riparian vegetation included grass, tree ferns, low shrubs, buttercup, native trees and deciduous poplar trees. The dominant plant species were grass and buttercup. Similar riparian vegetation was found in the Mangaotama pine section. The dominant riparian vegetation was grass, buttercup, low shrubs and, in some reaches, tree ferns. There were more riparian wetlands in the pastoral section rather than the pine section. However, both sections had riparian wetlands that ranged from sparse to extensive.

There were also large areas of catchment management interventions observed in both the pasture and pine section of the Mangaotama catchment. These areas were mainly along the stream banks, where poplars were planted on the banks opposite each other (i.e. twin planted poplars) (Figure 3.11). There were also poplars planted in the pasture section on the hills (Figure 3.11), where there appeared to have been earthflows in the past. Past sediment accumulation was evidenced by buried fence posts (Figure 3.12) and batons exposed in the stream banks (Figure 3.12).



Figure 3.11. Conservation management showing twin planted poplars (top) and planting on steep hills (bottom) in the pastoral section of the Mangaotama catchment.



Figure 3.12. Evidence of past sediment accumulation in the Mangaotama catchment (top) Buried posts batons in the stream bank in the pastoral section (indicated by yellow arrows) and (bottom) buried fence post in the pine section (Photos: M. Balks, 2018).

The riparian vegetation in the Whakakai catchment included tree ferns, low shrubs, high shrubs, bare rock and native trees. The dominant riparian vegetation was tree ferns (Figure 3.10). The stream shade ranged from 75 to 95% and there were no riparian wetlands.

Stream shade was the least dense in the pastoral section of the Mangaotama catchment (mean: 64%; std. dev.: 12%). The pine plantation section of the Mangaotama catchment was slightly more dense than the pastoral section (mean:

72%; std. dev.: 10%). The Whakakai catchment had the greatest density of stream shade (mean: 83%; std. dev.: 8%).

Channel descriptions

In both the pastoral and pine section of the Mangaotama catchment, the reaches were mostly sinuous, but some reaches were straight. The periphyton was slippery and obvious, and there were no macrophytes. The wood ranged from sparse to abundant. The streambeds consisted of mud, silt, sand, gravel, cobble, and in some reaches, bedrock and boulders.

Similarly, in the Whakakai catchment, the channel plan shapes were sinuous and straight and the periphyton was slippery or obvious. In-channel woody debris was abundant in most reaches, as there were large fallen trees in the stream throughout the survey length (Figure 3.13). In some reaches, there was evidence of mass wasting (Figure 3.13). However, the mass wasting did not seem to contribute to the sediment within the stream (Figure 3.13). Bedrock outcropped in almost every reach, however, there was a noticeable increase in bedrock exposure in the upper reaches (i.e. reaches near Reach 16). Clay, silt, sand, gravel, cobble and boulders were also in most reaches.



Figure 3.13. Woody debris from fallen trees (a) and mass wasting on hillslope (b) in the Whakakai catchment (Photo: F.Khan, 2018).

Channel and valley bottom widths

The Whakakai stream had generally wider mean water widths (mean: 3m, std: 0.8m) (Figure 3.14a), consistently wider channel (mean 4m, std: 1m) (Figure 3.14b) and bankfull widths (mean: 5m, std: 1m) (Figure 3.15a), compared to the pastoral and pine section of the Mangaotama catchment (Figure 3.14a, 3.14b & 3.15a). The pastoral section had mean water (mean: 2m, std: 0.5m), channel (mean: 2m, std: 0.5m) and bankfull (mean: 3m, std: 0.7m) widths, that were similar to the mean water (mean: 2m, std: 0.3m), channel (mean: 2m, std: 0.4m) and bankfull (mean 4m, std: 0.8m) widths in the pine section (Figure 3.14a, 3.14b & 3.15a).

The pastoral section of the Mangaotama catchment had wider valley bottoms (mean: 12m, std: 5m), than the pine section (mean: 7m, std: 3m) and the Whakakai catchment (mean: 8m, std: 4m). Mean valley bottom widths in the pastoral section of the Mangaotama catchment mean valley bottom width varied with open and narrow width areas. In the pine section of the Mangaotama catchment generally stayed a consistent width with two reaches that were in a particularly open area (reach 9 and 10 in the pine section) and the Whakakai catchment showed an overall decrease in widths, with increased distance from the NW5 monitoring site, particularly in the upper reaches where the stream and banks became steeper. (Figure 3.15b).

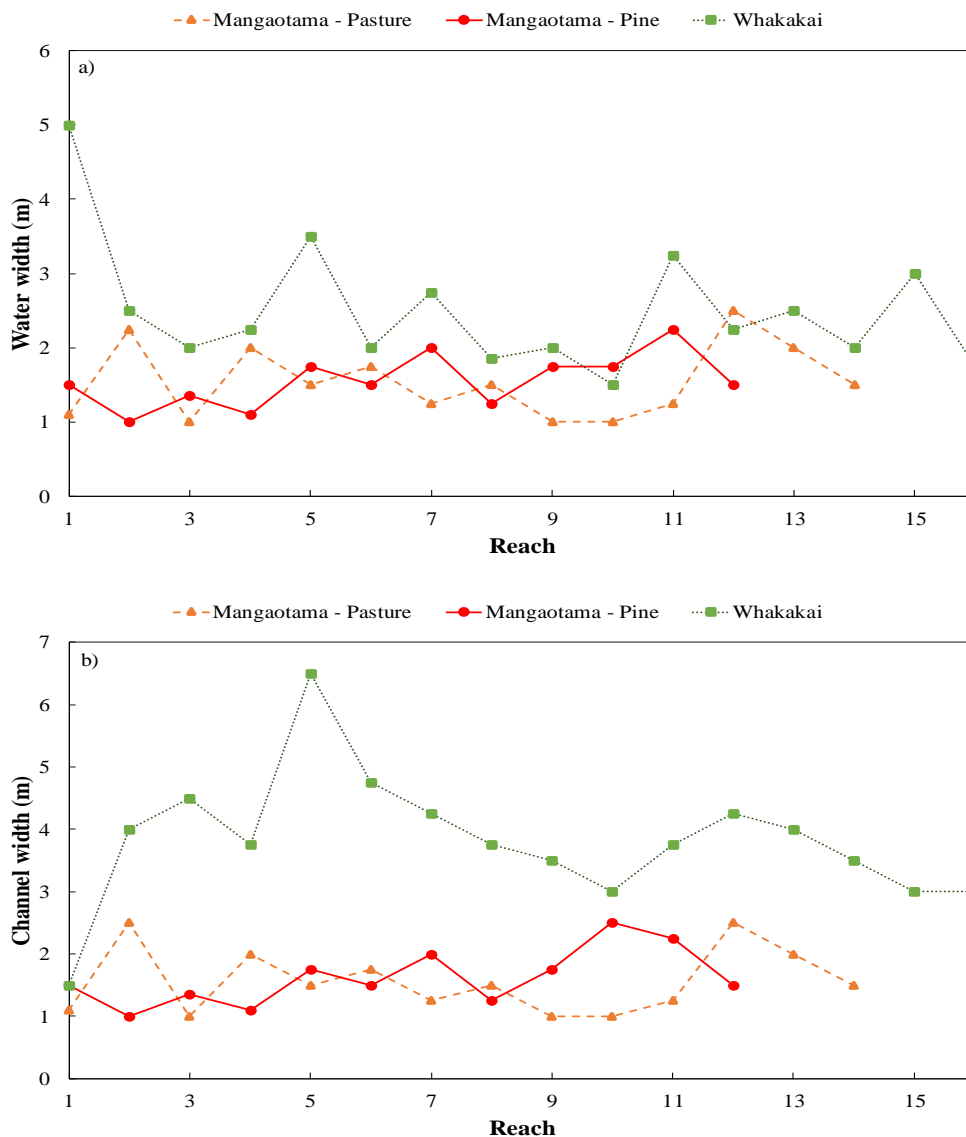


Figure 3.14. Mean water (a) and mean channel (b) widths for the Mangaotama pastoral and pine catchment sections, and the Whakakai catchment. NB. Pine section reaches were changed from reach 15 to 26, to reach 1 to 12 on the graph for comparison with the pastoral section of the Mangaotama catchment and the Whakakai catchment. Mean values were the mean of the smallest to largest width in each reach.

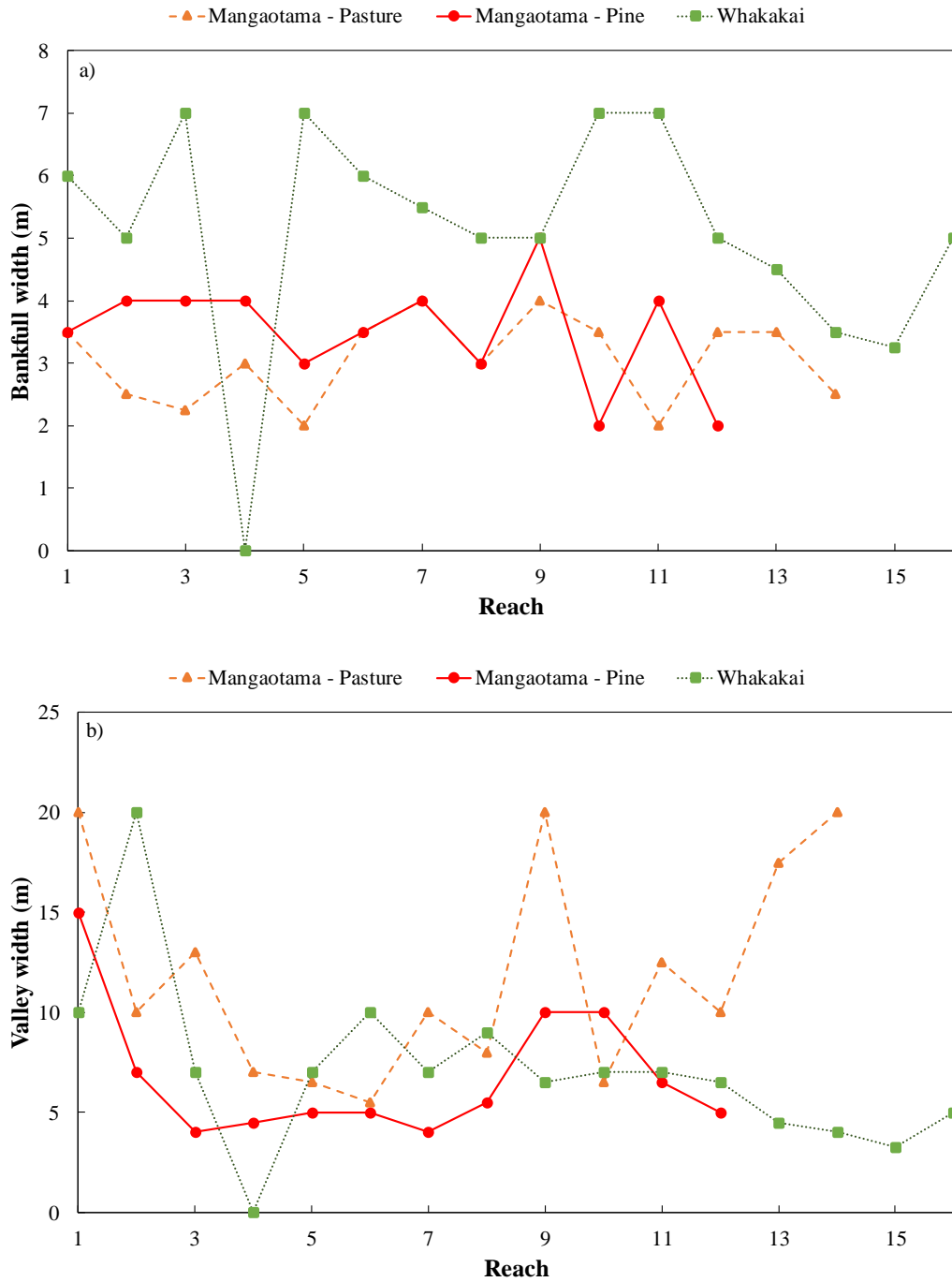


Figure 3.15. Mean bankfull (a) and mean valley (b) widths for the Mangaotama pastoral and pine catchment sections, and the Whakakai catchment. NB. Pine section reaches were changed from reach 15 to 26, to reach 1 to 12 on the graph for comparison with the pastoral section of the Mangaotama catchment and the Whakakai catchment. Mean values were used were widths were recorded as ranges (smallest to largest width in the reach). Gaps in graph represent unrecorded data.

Streamflow preference

In the Mangaotama catchment, both the pastoral and pine section reaches are predominantly run, followed by pools and then riffles (Figure 3.16). Further, there are more reaches with pools, and riffles in the pastoral section rather than in the pine section. The pools in both sections were generally formed due to bank erosion associated with fallen trees (Figure 3.16).

In the Whakakai stream, although runs were dominant, there were more riffles and pools within the reaches compared to the pasture and pine section in the Mangaotama catchment (Figure 3.16). There were also multiple reaches that featured small (Figure 3.17) and large waterfalls.

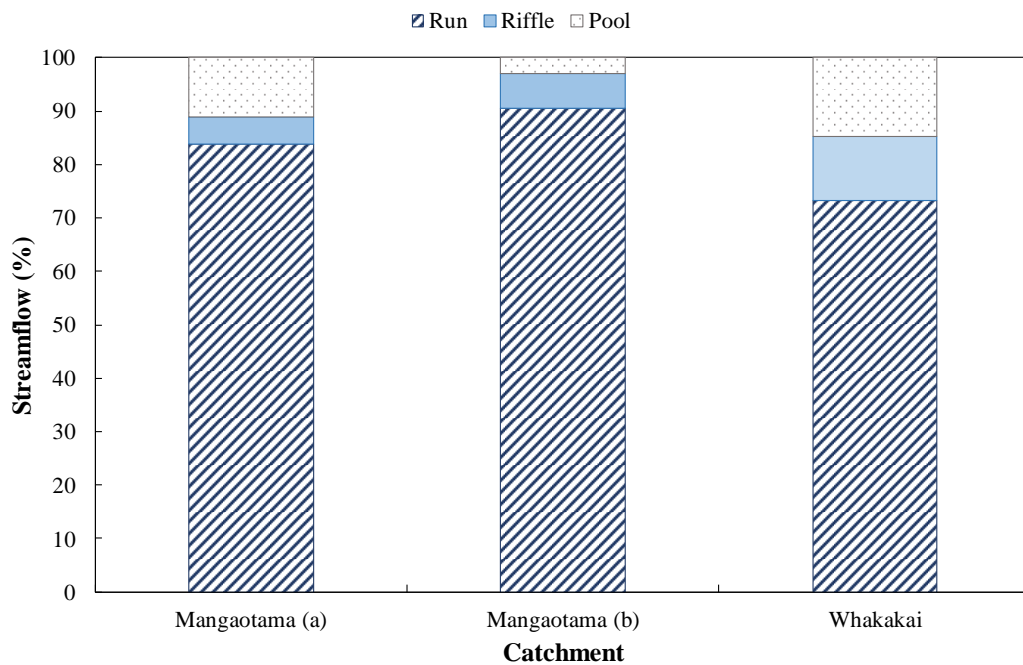


Figure 3.16. Summary of riffle/run/pool in Mangaotama catchment (a = pasture section, b = pine section) and the Whakakai catchment



Figure 3.17. Small waterfall and pool in the Whakakai catchment.

Local runoff potential

The Whakakai catchment had generally steeper left slopes (length: >10 and >20m; class: >15-25°) and right slopes (length: >10m; class: >15-25°), compared to the pastoral and pine sections of the Mangaotama catchment (Figures 3.18 & 3.19). However, the Whakakai catchment was the only catchment that had reaches (reach 1 & reach 2) with a slope length of greater than 100 m (Figure 3.18a & 3.18b).

Most reaches (9 out of 14) in the pastoral section had a slope length of >30m on the left bank and half of the reaches (7 out of 14) had a slope length of >20m on the right bank (Figure 3.18a & 3.18b). Slope classes in the pine section were generally in the 10-15° and 15-25° slope class for both the left and right bank slopes (Figure 3.19a & 3.19b).

In the pine section of the Mangaotama catchment, the slope lengths were generally >10 and >30 on the left bank and >10 and >20m (Figure 3.18a & 3.18b). Slope classes were generally 15-25° and >15-25° for both the left and right banks (Figure 3.19a & 3.19b).

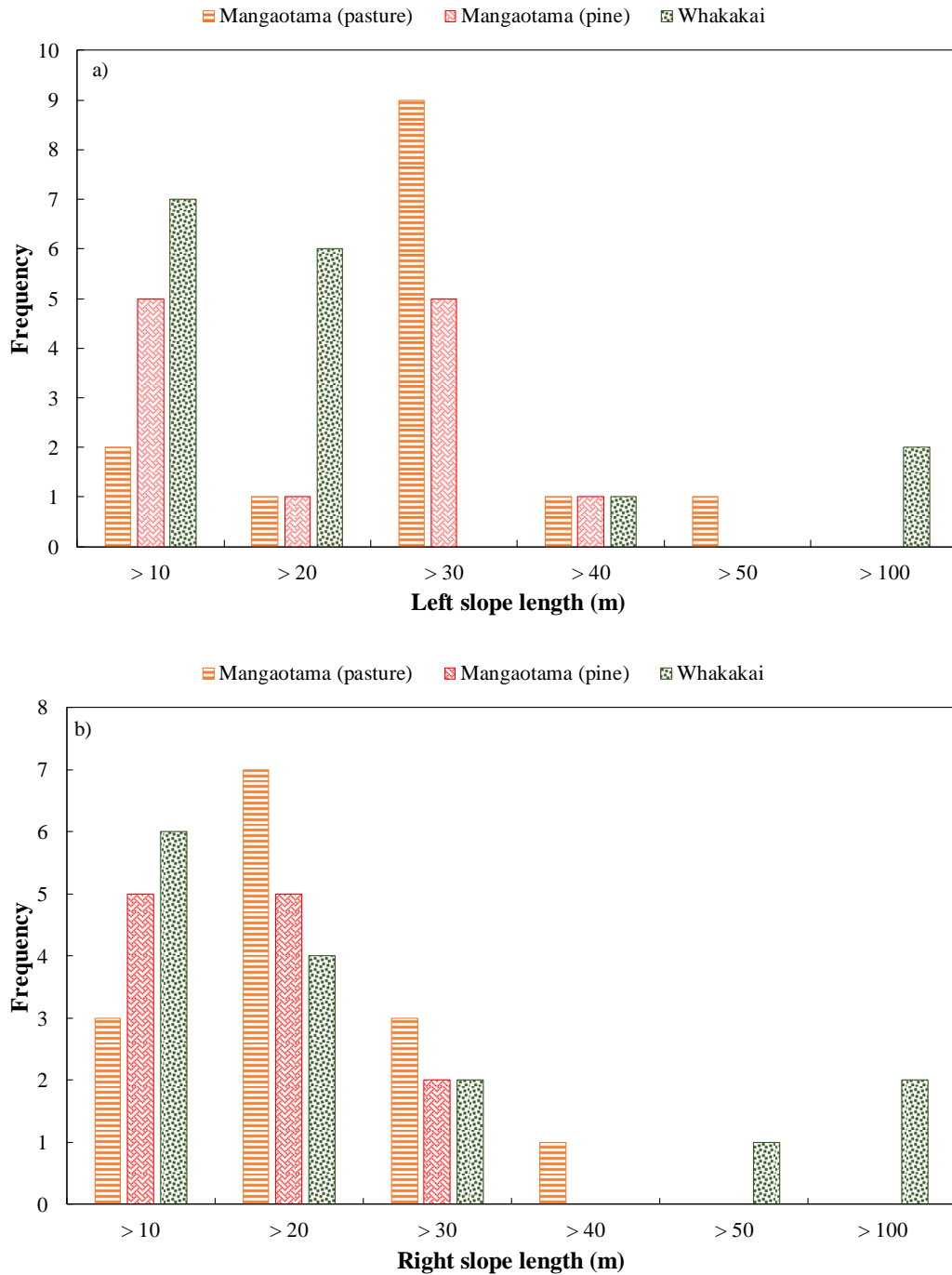


Figure 3.18. Slope lengths in the pastoral and pine sections of the Mangaotama catchment and the Whakakai catchment; left bank (a) and right bank (b). Slope lengths (m) include the number and greater than numbers (e.g. 20m and values greater than 20m). For readability purposes values that were between the selected slope lengths in the graphs were placed in the group with the closest value (e.g. 15 m slope length was placed in the >10m slope length category).

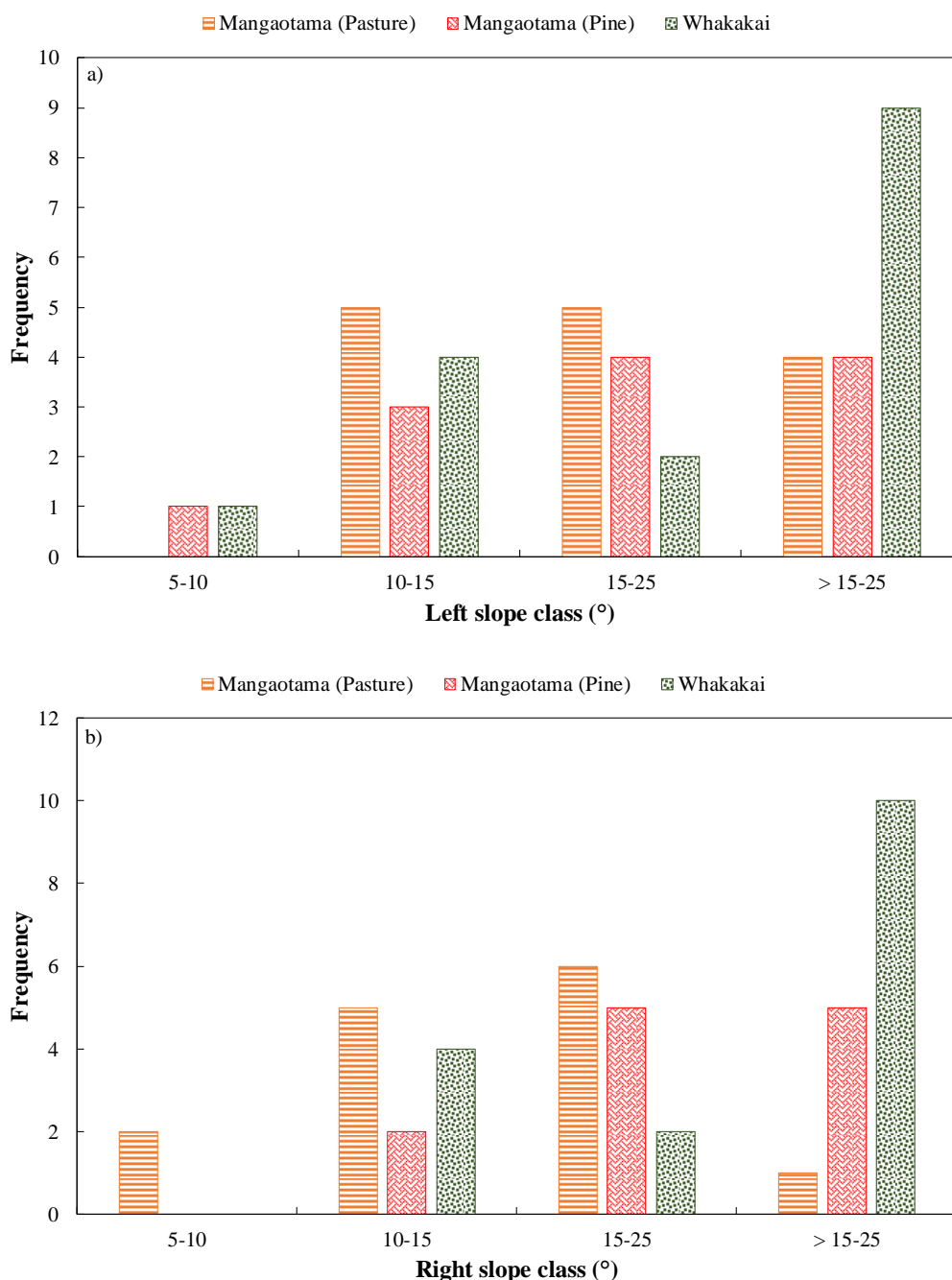


Figure 3.19. Left (a) and right (b) slope classes in the pastoral and pine sections of the Mangaotama catchment and the Whakakai catchment. Some classes have been grouped into the nearest category where values were greater than a particular slope class (e.g. values that were >10-15°, were grouped in the 10-15° category). Where there was more than one slope class recorded (due to the changing topography) the highest slope class value was used (e.g. 10-15°, 15-25°: the 15-25° value was used).

Stream bank heights

Bank heights were generally greater in the Whakakai catchment (in both the left and right banks) than the pastoral and pine section of the Mangaotama catchment (Figure 3.20a & 3.20b).

There were reaches in the pastoral section that had high bank heights (left bank: reach 11; right bank: reach 10 to 12) (Figure 3.20a & 3.20b). The reaches in both the pasture and pine sections were generally similar on both banks of the stream, with slightly higher left bank heights in some reaches of the pine section (reach 4-6), compared to the left bank heights in the pastoral section (Figure 3.20a & 3.20b).

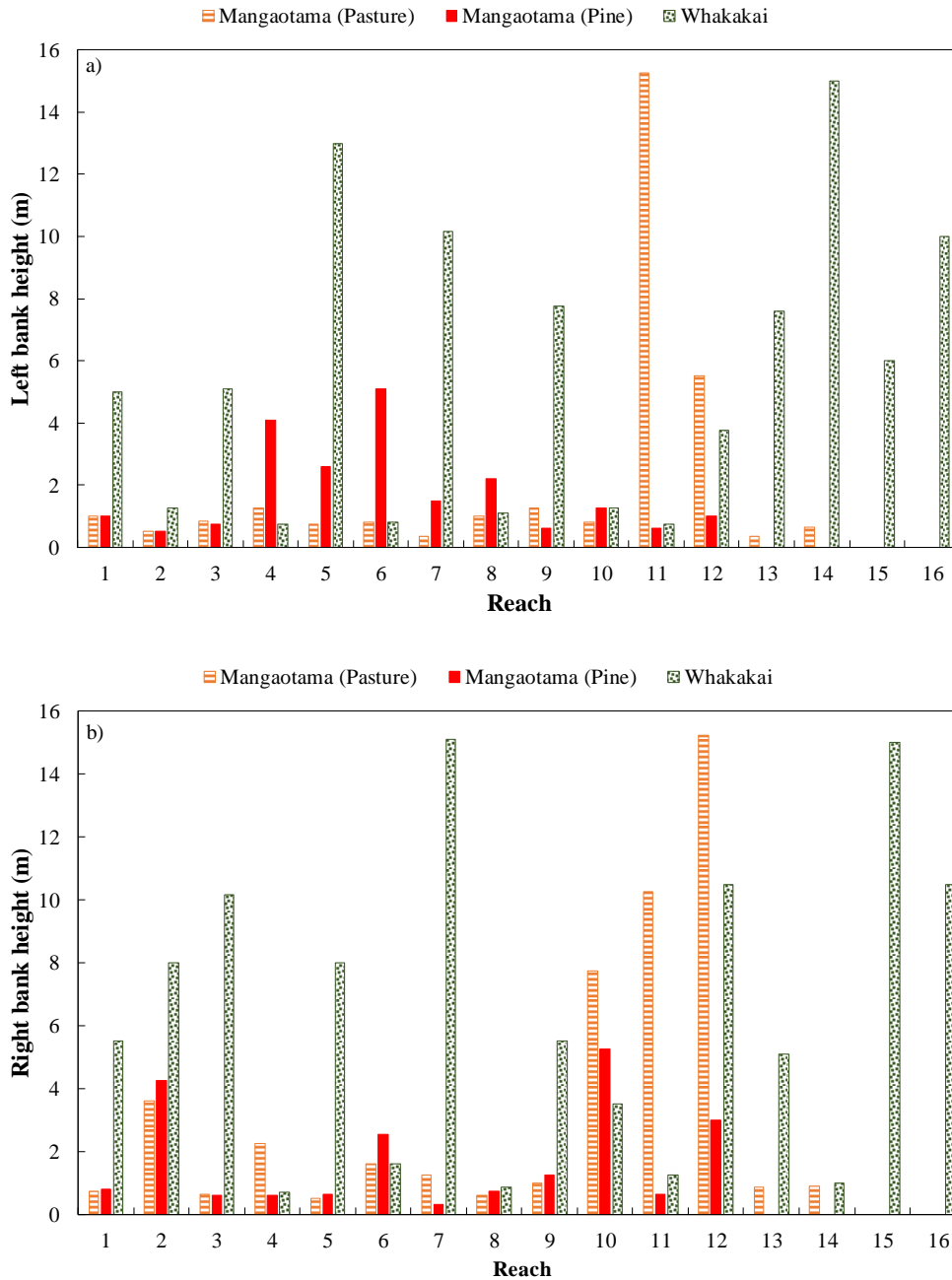


Figure 3.20. Bank heights in the pastoral and pine section of the Mangaotama catchment and the Whakakai catchment; left bank (a) and right bank (b).N.B. Mean values were graphed were lower and upper bank height values were recorded in the Riparian Management Classification field form.

Stream bank erosion

The reaches in the pastoral section of the Mangaotama catchment were generally stable, particularly in the middle reaches (Reach 4 to Reach 11). Stock damage and slumping were the dominant erosion sources in this catchment, with small areas of undercutting (Figure 3.21 & Figure 3.25). The pine section of the Mangaotama section was relatively stable, however, there were some reaches with undercutting (Figure 3.26) and small areas of slumping (Figure 3.22).

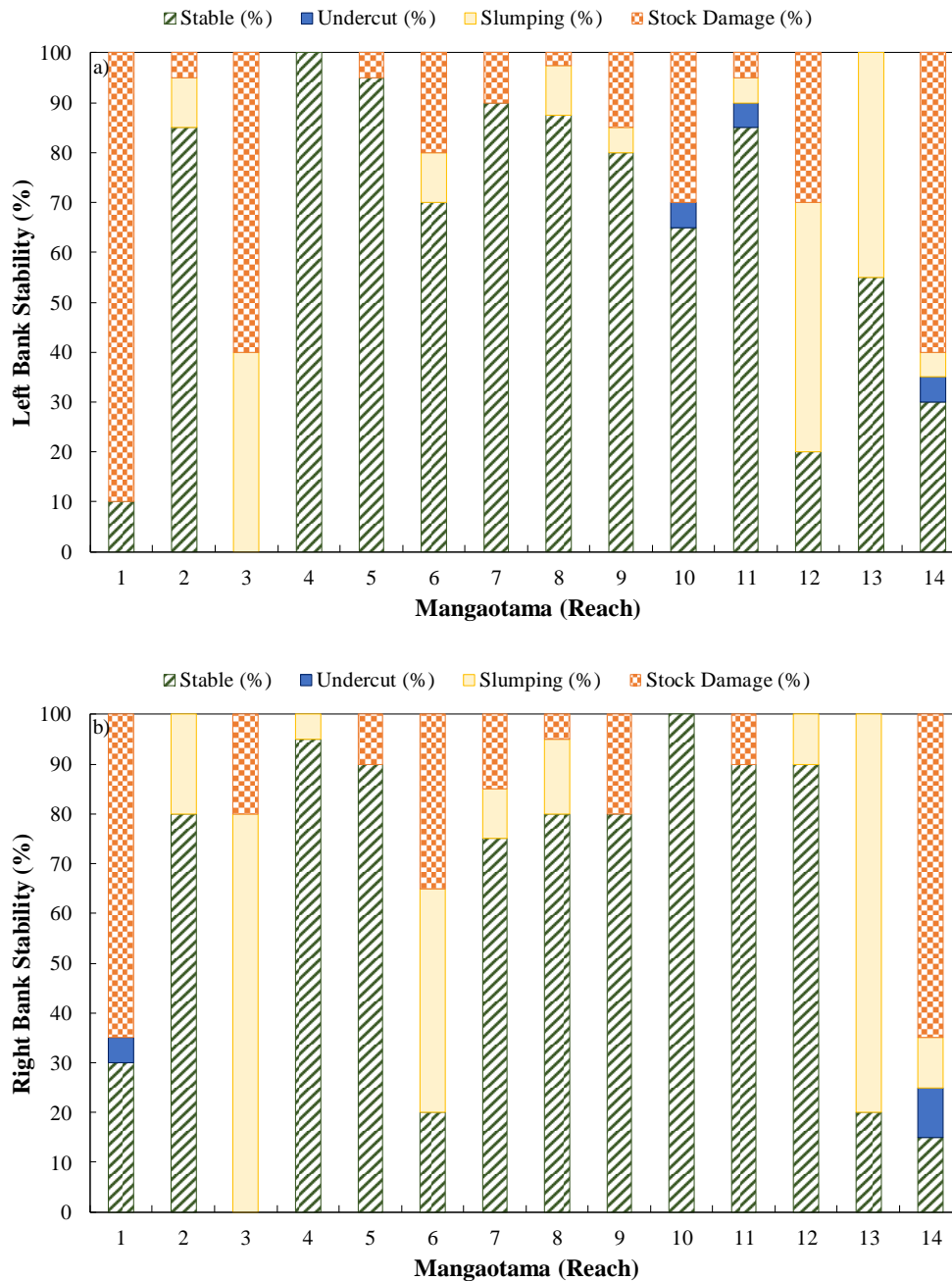


Figure 3.21. Stability (%) in the pastoral section on the left (a) and right (b) banks of the Mangaotama catchment.

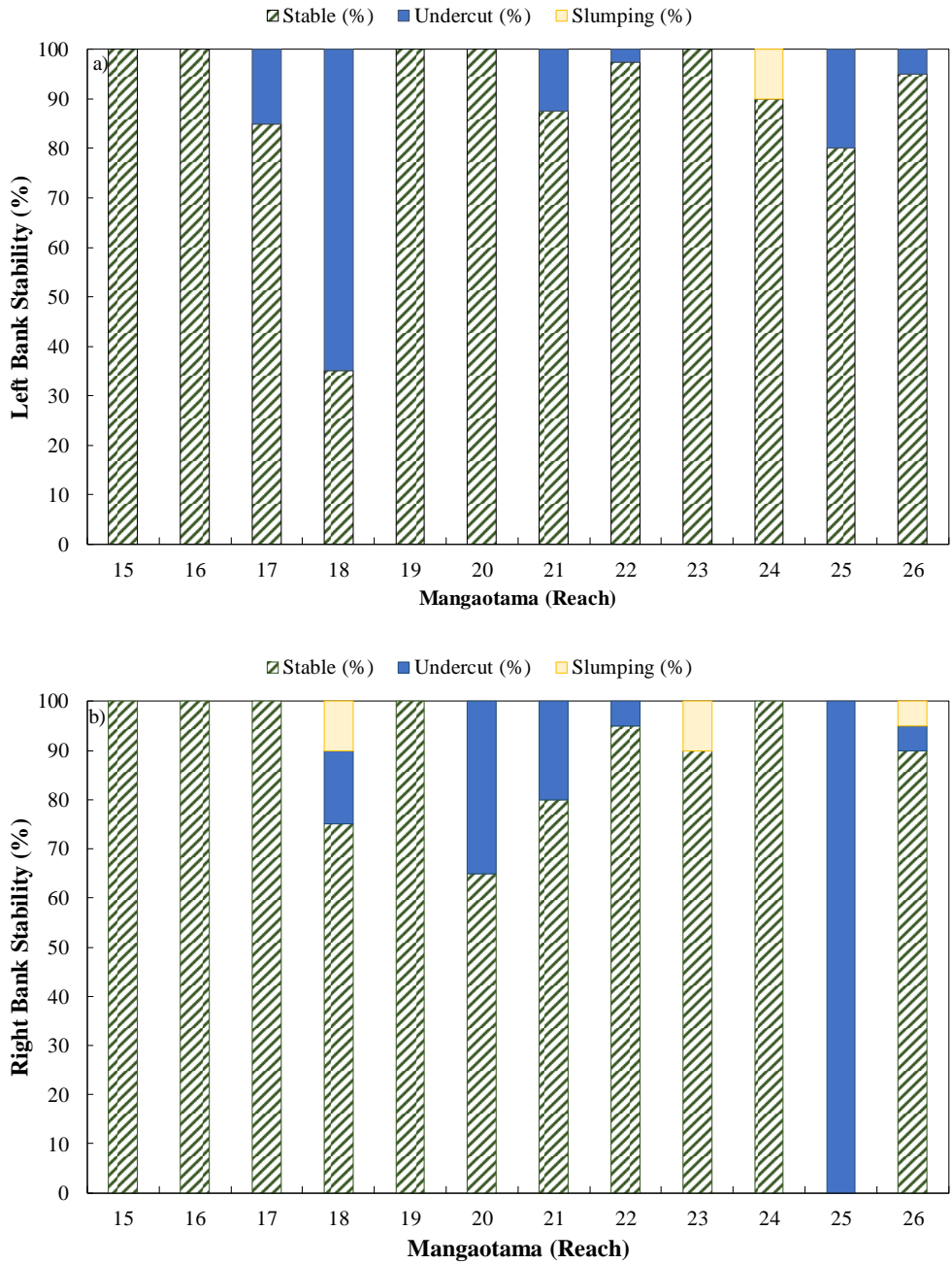


Figure 3.22. Stability (%) in the pine section on the left (a) and right (b) banks of the Mangaotama catchment.

The reaches in the Whakakai catchment were generally stable particularly in most upstream reaches (Reach 15 and 16) (Figure 3.23). Undercut was the dominant erosion source (Figure 3.27), with some undercutting eroding 0.5 to 1m into the stream banks. There were also small areas of slumping, that had been initiated by previous undercut, with some slumps falling into the stream with the whole tree still attached. Also, there were large areas of the stream that had been previously eroded to bedrock or there was old undercut that was currently stable due to the tree roots

(e.g. tree ferns). In the right bank, there was a clear trend of undercutting being more prevalent at the beginning of the survey (first few reaches) and then becoming negligible in the later reaches where bedrock was dominant on the streambanks (Figure 3.23).

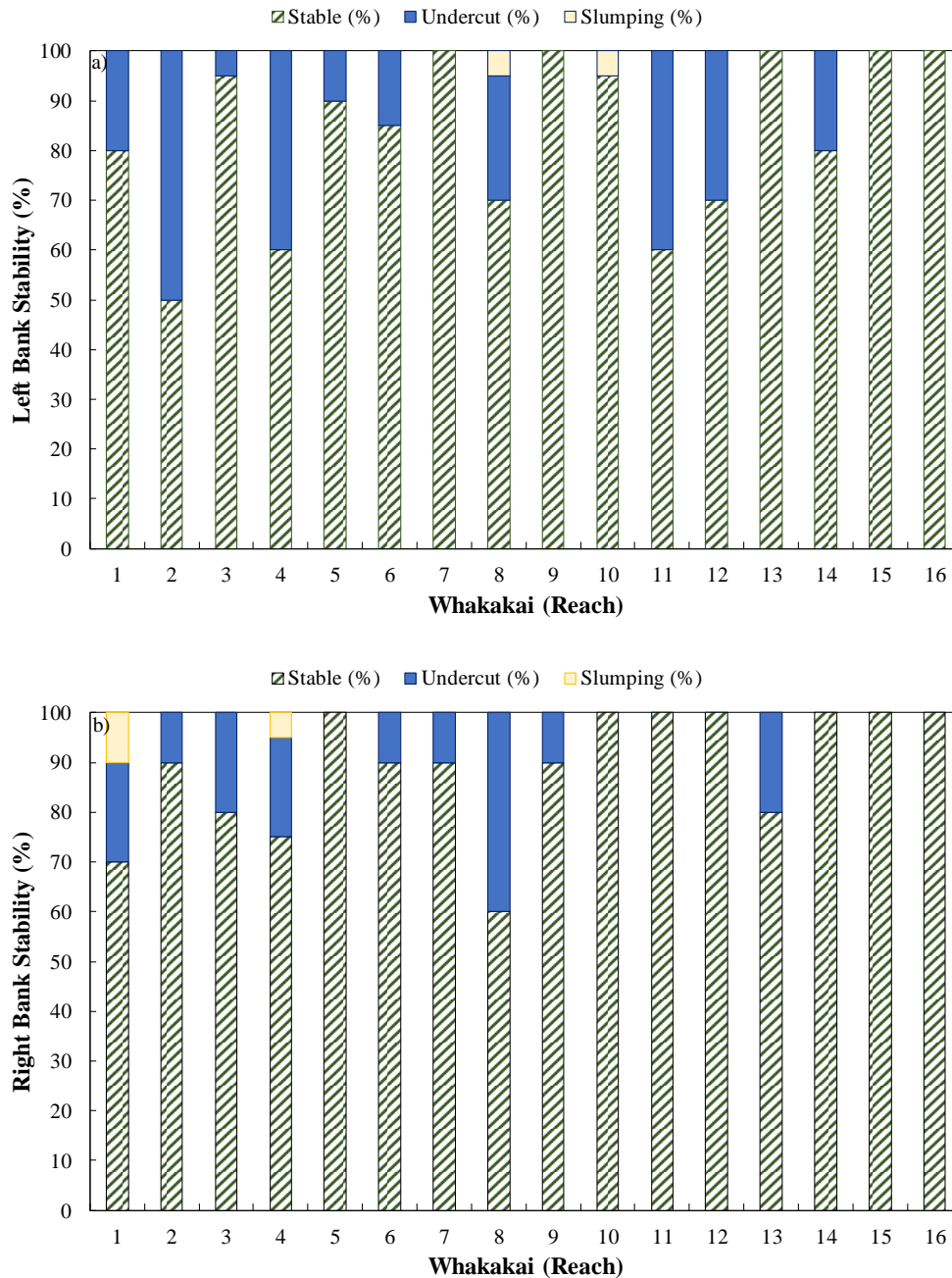


Figure 3.23. Stability (%) of the left (a) and right (b) banks in the Whakakai catchment.

The pasture section of the Mangaotama stream had the greatest stream bank erosion, as compared to the pine section of the Mangaotama stream and the Whakakai stream (Figure 3.24). There were no major differences in the amount of stream bank erosion between the Mangaotama stream pine section and the Whakakai stream (Figure 3.24). In the Mangaotama stream, the banks in the pasture section were predominantly stable (left: 64%, right: 65%), stock damage was the most dominant erosion source (left: 23%, right: 19%), followed by slumping (left: 11%, right: 15%) and finally undercutting (left: 1%, right: 1%). The stream banks in the pine section of the Mangaotama stream were more stable (left: 91%, right: 85%), with undercut being the main source of erosion (left: 9%, right: 13%) with small areas of slumping (left: 0.5%, right: 2%). Similar to the pine section, the Whakakai stream was generally stable (left: 84%, right: 86%). The dominant erosion process is undercut (left: 15% and right: 13%) with small areas of slumping (left: 1% and right: 1%) (Figure 3.24).

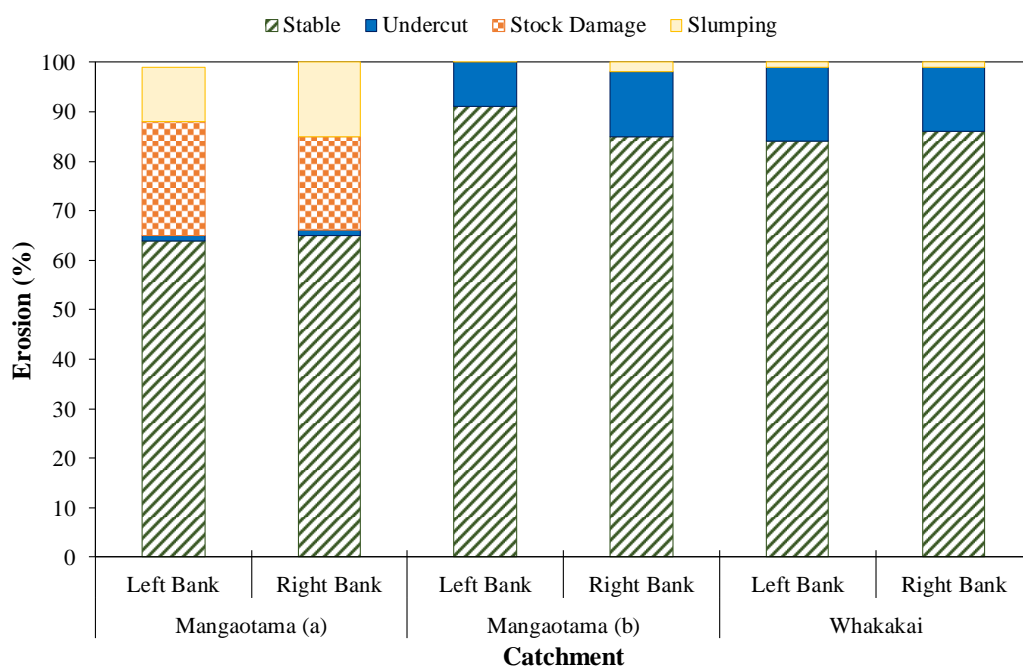


Figure 3.24. Summary percentage (%) of erosion in the Mangaotama (a = pasture section, b = pine section) and Whakakai catchments.



Figure 3.25. Stream bank in the pastoral section of the Mangaotama catchment. Stock damage (top) and a small area of slumping (bottom).



Figure 3.26. Stream bank undercutting in the pine section of the Mangaotama catchment (both pictures).



Figure 3.27. Streambank undercutting in the Whakakai catchment (both pictures) (both photographs taken by M. Balks, 2018).

Hillslope erosion

There was little evidence of hillslope erosion observed during the surveys. There was a small mass movement (around 3 m wide and 10 m tall) event observed before the catchment surveys in May that occurred on a stream bend. There was a noticeable scarp from the mass movement (Figure 3.28). There was also some hillslope erosion observed near the stream in the Mangaotama catchment, however the event was not directly contributing sediment to the stream (Figure 3.28).



Figure 3.28. Hillslope erosion observed in the Mangaotama pastoral section (left) and small mass movement event observed in the Whakakai catchment (right).

3.3.2 Establishment of a photo based 3D baseline

In the Mangaotama catchment four 3D models were created from the photographs taken in the field. In the Whakakai catchment, only one model was created (Model 2) as the first (Native 1) model failed due to inexperience in our first attempt to undertake the photography (Figure 3.29). Many of the photographs taken in the Native 1 model were from the same position with no movement between them, however, the Pine 1 model shows that nearly all the photographs had movement between them (Figure 3.30). In the Native 1, model about 10% out of the total images taken were able to be used (Table 3.29), while the rest of the models used 92 to 100% of the images captured. As a result, the Native 1 model shows significant gaps in the point cloud and the bank is unrecognizable (Figure 3.29), as

compared to the Native 2 model and the four models in the Mangaotama catchment (Figures 31 - 35). For more information re. 3D models e-mail the author at manawa_huirama@hotmail.com.

Table 3.2. Results of the initial processing stage of the 3D modelling software.

Name	Video	Images (Field)	Image quality	Images (Used)	Images (%)
Model 1 - Native	No	126	4093	13	10%
Model 1 - Pine	Yes	24	58332	22	92%
Model 2 - Native	Yes	41	46564	37	90%
Model 2 - Pine	Yes	49	45318	47	96%
Model 3 - Pine	Yes	73	49757	72	99%
Model 4 - Pasture	Yes	40	51541	40	100%

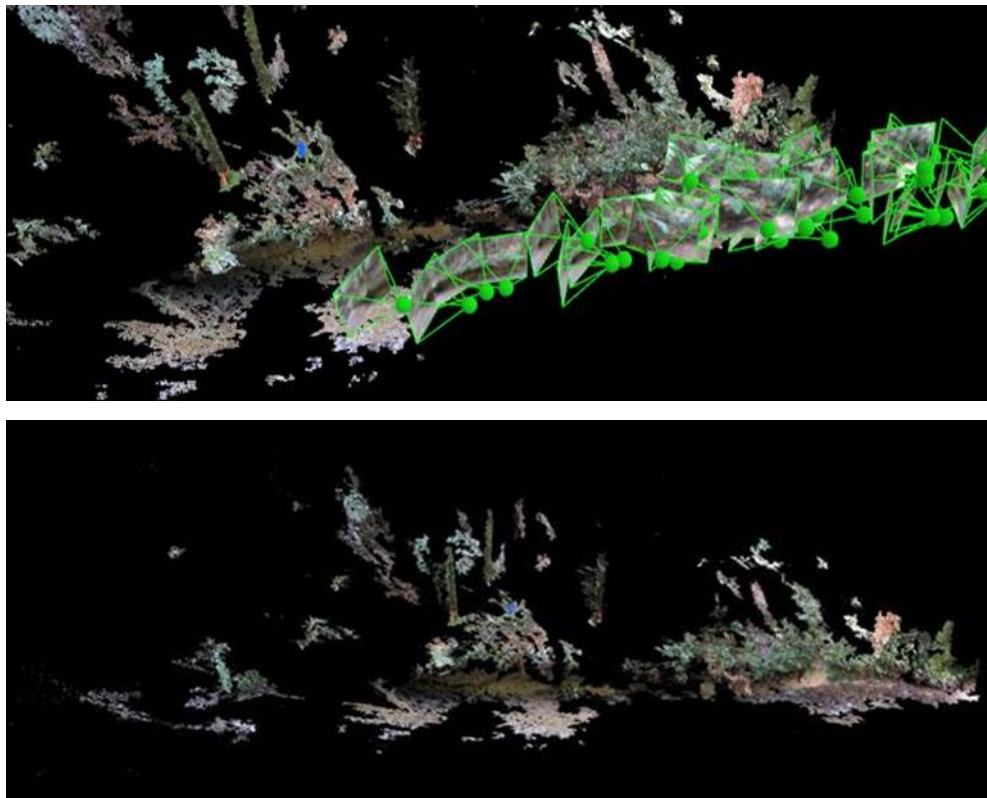


Figure 3.29. The top and bottom images are of the Native 1 3D model. Image top image shows the point cloud 3D model and the photographs used to create the model. Image bottom image shows the final 3D model. Note: There are significant holes in the 3D model.

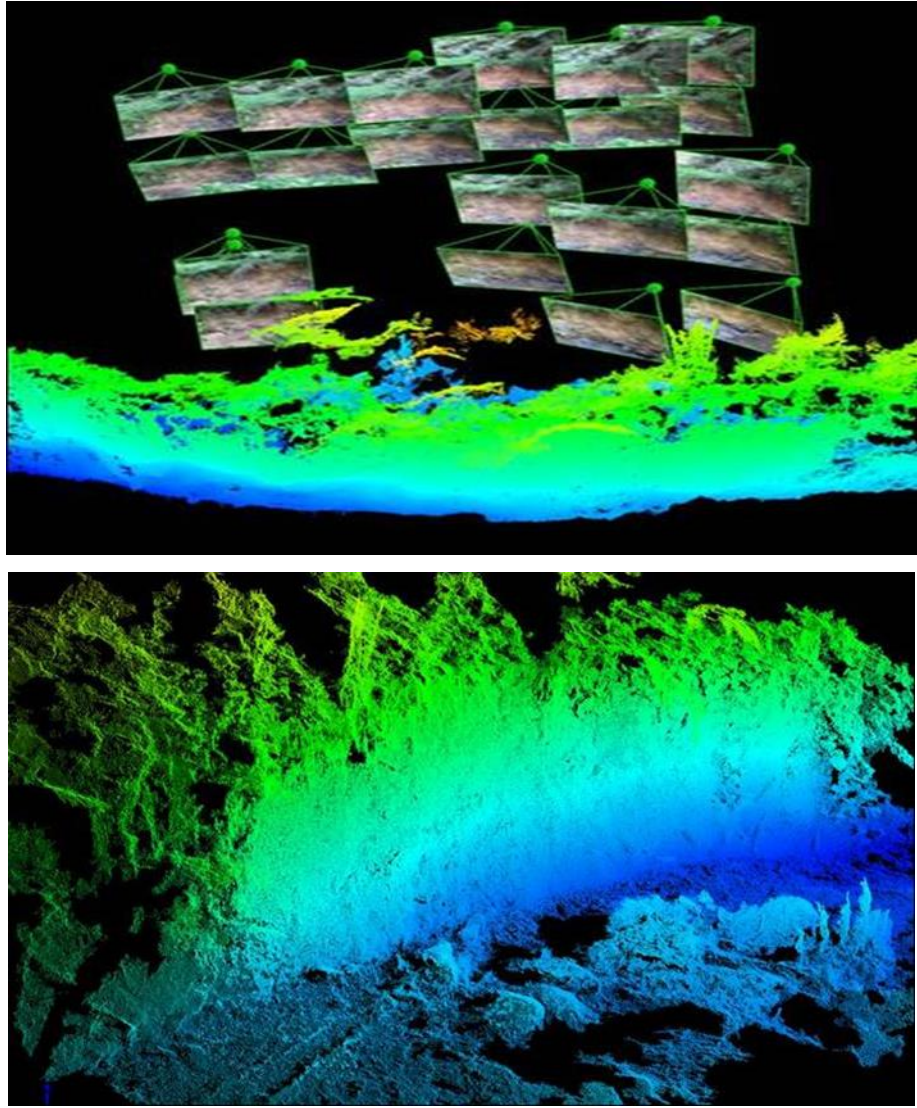


Figure 3.30. Close up images of the point cloud created for the Pine 1 3D model. The top image shows the orientation of the photographs used and the bottom image is a closer image of the model.



Figure 3.31. 3D model of the Pine 1 site in the Mangaotama catchment



Figure 3.32. 3D model of the Pine 2 site in the Mangaotama catchment

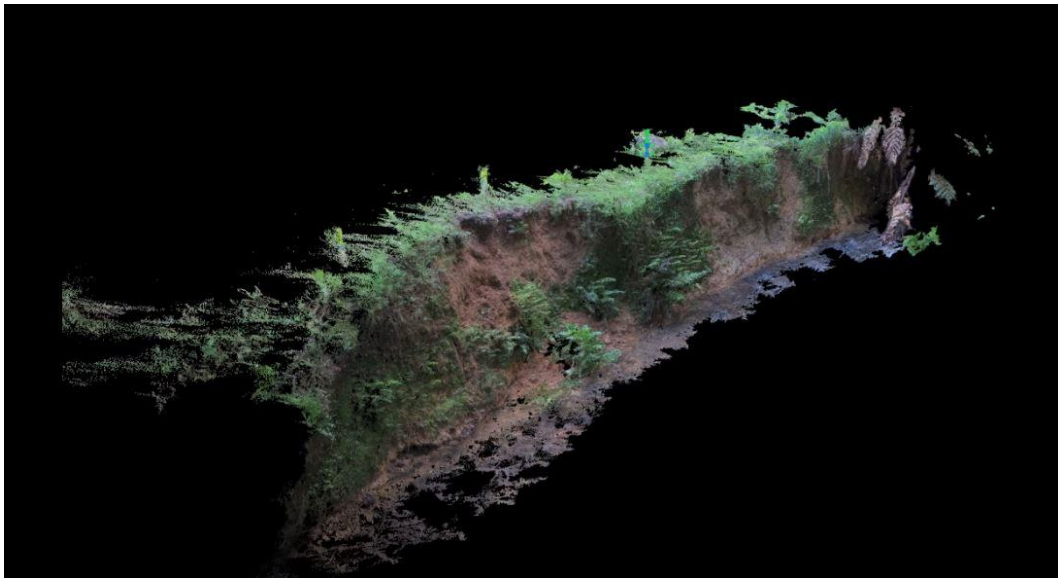


Figure 3.33. 3D model of the Pine 3 site in the Mangaotama catchment



Figure 3.34. 3D model of the Pasture 1 site in the Mangaotama catchment.

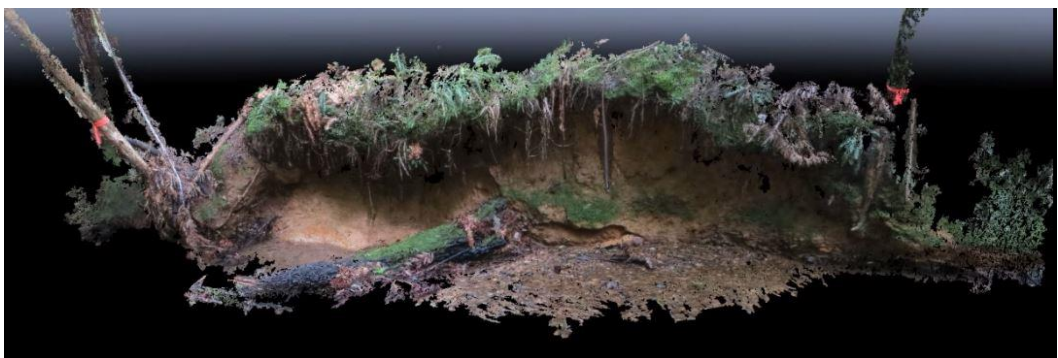


Figure 3.35. 3D model of the Native 2 site in the Whakakai catchment

3.4 Discussion

3.4.1 Riparian Management Classification

Streambank stability

Streambanks within the pastoral section of the Mangaotama catchment were generally stable (left: 64%, right: 65%). The stability of stream banks in the pastoral section could be due to the conservation management observed throughout the pastoral section (e.g. twin planted poplars) the intact bridges allowing for stock crossings and better management practices implemented by the farm manager at the Whatawhata Research Station. For example, there were specific areas that were only used as stock crossings, rather than multiple crossings within a section. However, stock damage was the dominant stream bank erosion process in the pastoral section of the Mangaotama catchment (left: 23%, right: 19%). The stock damaged areas were where the stock crossings were, especially in areas where bridges and fencing were broken. Stock grazing can directly cause damage to stream banks (Trimble & Mendel, 1995; Davies - Colley *et al.*, 2004) resulting in increased turbulence and erosion. Indirect damage can also be caused by stock grazing, due to the removal of vegetation that would otherwise be stabilising the stream banks against erosion (Trimble & Mendel, 1995).

Stream banks in the pine section of the Mangaotama and the Whakakai catchment were also similar in that these catchments were generally stable (pine section: left: 91%, right: 85%; Whakakai: left: 84%, right: 86%) and the dominant erosion process was undercutting (pine section: left: 9%, right 13%; Whakakai: left: 15% and right: 13%). The general stability of stream banks within the pine section and the domination of undercutting in the erosion processes could simply be due to the lack of stock access within the pine section of the Mangaotama catchment (Trimble & Mendel, 1995; Davies - Colley *et al.*, 2004). The general stability of the stream banks within the Whakakai catchment was due to the stream banks being exposed bedrock rather than soil. Where there were banks comprised of soil, there was mostly undercut, this is most likely due to the absence of stock access (Trimble & Mendel, 1995; Davies - Colley *et al.*, 2004) and the dominance of hydraulic power in the Whakakai catchment (Lawler, 1993). Slumping was minimal within the pine section (left: 0.5%, right 2%) and the Whakakai catchment (left: 1%, right: 1%).

The minimal presence of slumping on the stream banks could also be attributed to the lack of stock access, as the weight of grazing stock (Trimble & Mendel, 1995) would be likely able to induce slumping on banks that are already unstable from undercut (Brierley & Fryirs, 2013).

Stream and channel widths

The wider stream, channel and bank-full widths in the Whakakai catchment (as compared to the pastoral and pine section of the Mangaotama catchment) were most likely due to the land use differences between the catchments (Davies-Colley, 1997). For example, Davies-Colley (1997) analysed 20 different streams in the Waikato Region, and found that streams within a forested catchment had channels twice as wide as streams that were in a pasture catchment. The narrower stream banks in the pasture catchment were attributed sediment stored within the stream banks by either (1) sediment from historic hillslope slumping or mass wasting (2) deposition of alluvium during high flows. In the year 1995, a landslide occurred in the Kiripaka catchment of the Whatawhata Research Station (the catchment between the Whakakai and Mangaotama catchments), that deposited soil on the banks for several kilometres downstream of the event (Davies-Colley, 1997).

The theory by (Davies-Colley, 1997) is further supported by the evidence found in this study of the in-filled banks covering the buried batons and in the same area the planted poplars on the slopes (possible historic landslides in the pastoral section of the Whakakai catchment). Trimble (1997) also found that forested streams were wider than grassland streams, but attributed those differences to fallen trees and woody debris concentrating the flow in forested streams and eroding the stream banks. This theory was also seen within the Whakakai catchment (and the pastoral section of the Mangaotama catchment), where bank erosion had occurred due to the concentrated hydraulic power of the stream after a tree or numerous trees had fallen into the channel. Montgomery (1997) noted the contrasting views within the literature where some studies stated that forested catchments stabilize the stream banks while other studies noted that trees falling within forested catchments increase erosion and therefore widening of forested streams (e.g. Trimble, 1997).

Historic mass movement

Deforestation is well known to exacerbate erosion rates, particularly on hill country landscapes with the promotion of mass movement erosion (Basher, 2013). Forest clearance occurred in the Mangaotama catchment in the mid-1920s, and the land was converted to pastoral farming (Dodd *et al.*, 2008). Post-forest clearance there have been numerous mass movement events in the Mangaotama catchment that lead to the majority of sediment within the catchment being derived from landslides (Dodd *et al.*, 2008), particularly a storm event in 1998 (De Rose, 1998), where De Rose (1998) estimated that landslides produced $11,000 \text{ kg}^{-1} \text{ ha}^{-1} \text{ yr}^{-1}$ worth of sediment. However, De Rose (1998) stated that the frequency of landslides had decreased since initial forest clearance.

Vegetation

Davies-Colley (1997) discussed the key role of vegetation in pastoral catchments at storing and trapping transported sediment within the banks particularly after deforestation. Davies-Colley (1997) suggested that converting pasture land into forested land, can increase streambank erosion and widen the stream. The widening of forested streams was by Davies-Colley (1997) attributed to taller forested vegetation shading and eventually inhibiting the growth of pastoral vegetation, leading to exposed bank materials that are susceptible to erosion.

The theory of Davies-Colley (1997) linking vegetation, streambank erosion and the stream channel width is somewhat further supported in this study. The pastoral section of the Mangaotama catchment was dominated by grass and was the least shaded (mean: 64%; std. dev.: 12%). The pine section of the Mangaotama catchment was dominated by a mixture of grass, tree ferns, with some low shrubs present in the riparian zones and was more shaded than the pastoral section (mean: 72%; std. dev.: 10%). Although there was no difference found in this study in the range of mean channel widths between the pastoral (1 to 2.5m) and pine sections (1 to 2.5) of the Mangaotama catchments, Davies-Colley *et al.* (2018) recently found that streams are narrower in the pastoral section of the Mangaotama catchment, as compared to the pine section of the Mangaotama catchment. Finally, the Whakakai catchment in this study was dominated by tree ferns and lacked the solid grass vegetation cover of the Mangaotama catchment.

The Whakakai catchment was the most shaded (mean: 83%; std. dev.: 8%) and had the widest channel widths (1.5 to 6.5m).

Valley widths and slopes

The decline in valley bottom widths in the Whakakai catchment with increased distance from the NW5 monitoring site shows the valleys were steeper in the upper reaches of the survey lengths. The general slope length (left length: >10 and >20m; right length: >10m) and general slope class (left slope class: >15-25°; right slope class: >15-25°) results further show that the Whakakai catchment was steeper than the pastoral and pine section of the Mangaotama catchment. It is suggested that the differences may not be entirely due to land use differences, but rather geological (Hughes *et al.*, 2012). The geology of the two catchments are similar in that the entire Mangaotama catchment is comprised of late Triassic sedimentary rock (siltstone and sandstone). However, there is a geological boundary within the Whakakai catchment, where half of the catchment is comprised of the same late Triassic sedimentary rock as the Mangaotama catchment (survey length within this half), and half is older, early Jurassic sedimentary rock (siltstone and sandstone) (GNS Science, 2014). Further investigation needs to be undertaken to determine whether the two rock units have any physical differences that would influence their susceptibility to erosion.

Improvements for future monitoring

It is recommended that future monitoring, to compare with this record not be carried out when stream levels are high. For example, the streamflow may be 100% run in higher flows, whereas at baseline there would be more riffles and pools evident. The Riparian Management Classification (RMC) method could be further improved by adapting the RMC forms for the particular study area. For example, in this study all streams were perennial and all valleys were 'V' shaped. Removing unnecessary sections would be time-efficient in the field. Additionally, stream shade would have been more easily compared and determined had the photographs in RMC field guide (Quinn, 2009) been taken from within the stream pointing upwards.

In repeating this survey in the future, it is recommended to record the average lower and upper bank height, rather than a total range of bank heights.

Average bank heights are more useful when interpreting the results, rather than recording small areas of low (0.2m) and high banks (>6m), which do not represent an entire reach. These small areas of high and low bank heights should be recorded in the notes.

It is also recommended that percentages be assigned to the lower (if any) and upper values for the stream, channel and bank full widths. Assigning a percentage to the lower and upper width values are more useful for interpreting the results, as a dominant width percentage is more representative of a particular reach during data analysis rather than a mean value.

3.4.2 Establishment of a baseline for 3D monitoring

The Native 2 model created in the Whakakai catchment, and the four models created in the Mangaotama catchment, have the potential to be used for future monitoring of changes in stream bank erosion and potentially to calculate bank erosion rates over time. Additionally more eroding bank sites also can be added in the future.

Improvements for future monitoring

Recommendations for future monitoring include using a camera that takes GPS coordinates (for repeat surveys); creating a consistent photograph plan for every site; using larger stakes (so they remain intact within the bank) and measuring the horizontal distance between the stakes (or other landmarks e.g. trees) rather than the distance between the marking tape and the top of the stake. Scale accuracy can be greatly improved by measuring horizontal distance as opposed to using the masking tape-top of stake distance, as the error is measurement in reduced. It is also recommended that photographs be taken on automatic mode and in a well-lit catchment. The accuracy of the 3D model is dependent on the quality of the photographs used in the software (Pix4D, 2017).

3.5 Summary and conclusion

3.5.1 Catchment surveys

- The Riparian Management Catchment (RMC) survey method was conducted in the Mangaotama catchment (total length 1.3 km with 0.9 km under pastoral land use and 0.4 km under pine plantation) and Whakakai catchment (0.9 km) to assess stream and riparian conditions including stream bank erosion.
- Stream banks over the total survey length were predominantly stable in the pastoral section of the Mangaotama catchment (left: 64%, right: 65%) and stock damage was most dominant erosion source (left: 23%, right: 19%).
- Stream banks over the total survey length were predominantly stable in the pine section of the Mangaotama catchment (left: 91%, right: 85%), with undercut being the main source of erosion (left: 9%, right 13%).
- Stream banks over the total survey length were predominantly stable in the Whakakai catchment (left: 84%, right: 86%), with undercut being the main erosion source (left: 15% and right: 13%). Stream bank undercutting eventually led to occasional bank collapse events resulting in quite large trees falling into the observed stream.
- Catchment management practices such as planted poplars, strong pasture cover and bridges for stock crossings, contributed to stream bank stability within the pastoral section.

The stability of the pine section was attributed to the lack of cattle access in that area, and the Whakakai stream banks were stable due to most of the stream banks being bedrock and the lack of stock access.

- Mean channel widths were narrower in the pastoral (mean: 2m, std: 0.5m) and pine sections (mean: 2m, std: 0.4m) of the Mangaotama catchment, than the Whakakai catchment (mean 4m, std: 1m). Narrower stream widths in the pastoral catchment were attributed to infall from past mass movement in the catchment and other sources of transported (deposited sediment). While wider channel widths in the Whakakai catchment could be due to the shading from trees inhibiting the growth of protective continuous vegetation such as long grass.

- There was little evidence of current mass movement events in either catchment. The pastoral section of the Mangaotama showed buried fencing materials exposed on the bank and cutting through the past in-fill material.
- Future research could re-survey the Mangaotama and Whakakai catchments to compare stream bank erosion over time.

3.5.2 Baseline for 3D monitoring

- Two actively eroding bank erosion sites were selected in the Whakakai catchment, and four bank erosion sites (three in pine plantation and one in pasture) were selected in the Mangaotama catchment.
- Between 24 and 126 photographs (using a digital camera) were taken of eroding stream banks in the Whakakai catchment on September 20 2018, and in the Mangaotama catchment on September 29 2018.
- The photographs were then imported into the photogrammetry software Pix4D (Pix4D, 2017) and the 3D models of the stream banks were created.
- Five successful 3D models were created (one in the Whakakai catchment, and four in the Mangaotama catchment) show that terrestrial photogrammetry is potentially an effective, simple, and cost-effective tool to monitor stream bank erosion over time. A baseline was established which could be re-surveyed though it is recommended that further baseline sites be established to provide improved rigour.
- One attempt in the Whakakai catchment failed to have sufficient overlap in the photographs. It is crucial to take the photographs in a way where common landmarks are noticeable for the photogrammetry software to be successful at creating a 3D model (Pix4D, 2017).
- A baseline has been established that can be resurveyed, however, it is recommended that further baseline sites be established to improve rigour.

Chapter 4

Using Sediment Fingerprinting to Determine the Relative Contribution of Main Erosion Sources

4.1 Introduction

There are many sediment fingerprinting techniques, however the fallout radionuclide method has been demonstrated to be particularly useful for determining the relative contribution of surface sources (i.e. sheet wash and rill erosion) and subsurface erosion (i.e. river bank and gully erosion). Identifying the dominant source of erosion has potential to better prevent and inform, catchment erosion and stream restoration efforts (Walling, 2013).

The overall objective of this chapter was to determine the relative contribution of stream bank erosion and hillslope erosion to the sediment within Mangaotama and Whakakai streams.

The specific objectives were to:

- Distinguish between bank and hillslope sources of erosion in the Mangaotama and Whakakai catchments using fallout radionuclides.
- Determine the relative contribution of bank and hillslope erosion to the suspended sediment within the Mangaotama and Whakakai streams.

4.2 Methods

4.2.1 Soil samples

Soil samples were collected in the Mangaotama and Whakakai catchments in May and June 2018 (Figure 4.1 & Table 4.1). Five stream bank sites and five hillslope sites were sampled in each catchment. Access in the Whakakai catchment was limited, due to the steep hills and bedrock banks (i.e. no soil) further up-stream.

Although access was limited in the Whakakai catchment, radionuclide concentrations of the stream banks and the hillslopes will be similar to the Mangaotama, as radionuclide concentrations are a function of latitude and rainfall (which determine their fallout distribution), rather than soil or geology. Therefore the radionuclide nuclide concentrations will be similar due to the proximity of the two catchments (i.e. same mean annual rainfall) (Basher & Matthews, 1993).

Stream bank sites were selected that were actively eroding over a range of erosion processes (stock damage, undercutting, slumping). At each bank site, samples were taken over five depths on the exposed bank (Figure 4.2) using a small garden shovel. The first sample was taken near the top of the exposed stream bank; the last sample was taken near the water and the other three samples were taken at even intervals in between. The five samples were mixed in a bucket to create a composite sample, while a sub-sample (~1 kg) was placed in a labelled plastic bag and taken to the laboratory. The bucket and shovel were cleaned in the stream after sample collection at each site. GPS coordinates and photographs were taken at each bank site (Table 4.1).

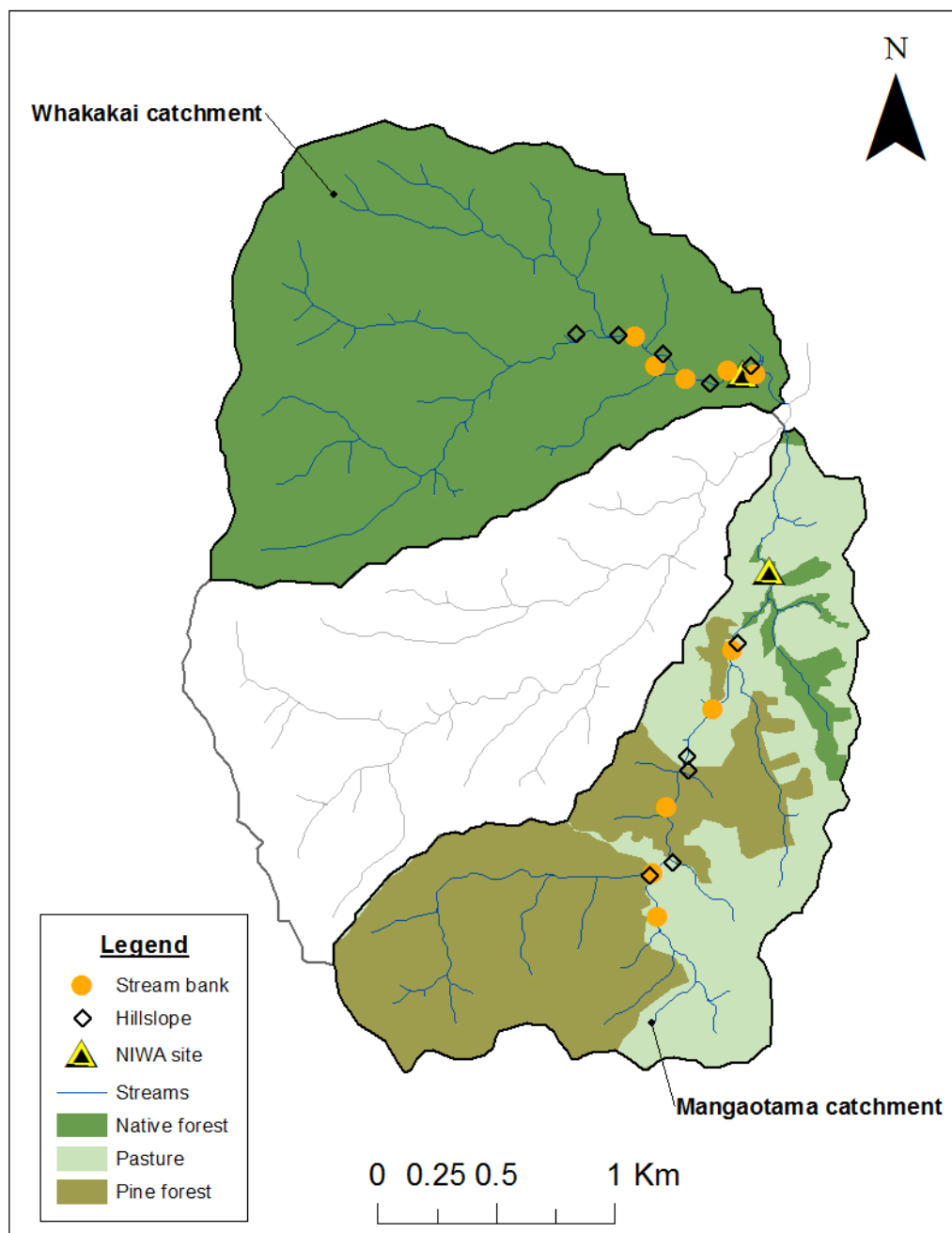


Figure 4.1. Location of stream bank and hillslope sites selected in the Mangaotama and Whakakai catchments for soil sampling and radionuclide analysis

Table 4.1. GPS locations of the stream bank and hillslope sites sampled for radionuclide analysis

Sample ID	Type	Catchment	Landuse	Northing	Easting
WBank 1	Stream bank	Whakakai	Native	37° 46' 37.931"" S	175° 4' 22.181"" E
WBank 2	Stream bank	Whakakai	Native	37° 46' 39.472"" S	175° 4' 10.420"" E
WBank 3	Stream bank	Whakakai	Native	37° 46' 33.773"" S	175° 4' 0.894"" E
WBank 4	Stream bank	Whakakai	Native	37° 46' 39.252"" S	175° 4' 9.984"" E
WBank 5	Stream bank	Whakakai	Native	37° 46' 37.715"" S	175° 4' 19.956"" E
Bank 2M	Stream bank	Mangaotama	Pasture	37° 47' 17.358"" S	175° 4' 19.020"" E
Bank 3M	Stream bank	Mangaotama	Pasture	37° 47' 25.519"" S	175° 4' 15.938"" E
Bank 6M	Stream bank	Mangaotama	Pine	37° 47' 39.322"" S	175° 4' 8.087"" E
Bank 7M	Stream bank	Mangaotama	Pine	37° 47' 48.660"" S	175° 4' 6.143"" E
Bank 11M	Stream bank	Mangaotama	Pasture	37° 47' 54.773"" S	175° 4' 7.122"" E
WHill 1	Hillslope	Whakakai	Native	37° 46' 37.931"" S	175° 4' 22.181"" E
WHill 2	Hillslope	Whakakai	Native	37° 46' 40.163"" S	175° 4' 14.012"" E
WHill 3	Hillslope	Whakakai	Native	37° 46' 36.221"" S	175° 4' 5.729"" E
WHill 4	Hillslope	Whakakai	Native	37° 46' 33.892"" S	175° 3' 59.242"" E
WHill 5	Hillslope	Whakakai	Native	37° 46' 33.440"" S	175° 3' 52.140"" E
Hill 1M	Hillslope	Mangaotama	Pasture	37° 46' 37.931"" S	175° 4' 22.181"" E
Hill 5M	Hillslope	Mangaotama	Pasture	37° 46' 39.472"" S	175° 4' 10.420"" E
Hill 6M	Hillslope	Mangaotama	Pine	37° 46' 33.773"" S	175° 4' 0.894"" E
Hill7M	Hillslope	Mangaotama	Pine	37° 46' 39.252"" S	175° 4' 9.984"" E
Hill 8M	Hillslope	Mangaotama	Pasture	37° 46' 37.715"" S	175° 4' 19.956"" E



Figure 4.2. Example of streambank sites sampled in the Mangaotama (top) and Whakakai (bottom) catchments.

Three hillslope sites near the stream (Figure 4.3) and two colluvial toe slope sites (one in the pine section (Figure 4.4) and the other in the pastoral section) were selected in the Mangaotama catchment. Colluvial toe slopes were selected as they are remnants of past mass movement, and where the soil has collected at the base of the hillslope. Five hillslope sites adjacent to the stream (Figure 4.5) were selected in the Whakakai catchment. Hillslope sites were sampled in the topsoil (0 – 5cm depth) using a soil auger. Before sampling, the grass was cleared to expose the soil for sampling. There were no observed colluvial toe slopes in the Whakakai catchment.

At least seven soil cores were collected along a transect at each hillslope site, depending on the size of the hill (i.e. larger hills had more samples taken). Samples were taken in a straight or semi-straight transect from the bottom of the hill to the top of the hill, and more samples were taken around the top of the hill. The colluvial toe slopes were also sampled with a soil auger (0 – 5cm depth), and at least seven samples were taken at various locations on the colluvial toe slopes.

The transect soil samples from each hillslope site were mixed in a bucket to create a composite sample. The colluvial toe slope samples were also mixed in a bucket to create a composite sample. Sub-samples (~1kg) from the composite sample were placed in a labelled plastic bag and taken back to the laboratory. The bucket and soil auger were cleaned in the stream after the sample collection at each hillslope site. GPS coordinates and photographs were taken at each hillslope site (Table 4.1).



Figure 4.3. Soil sample collection from a hillslope site under pine plantation in the Mangaotama catchment. Soil samples were collected in a semi-straight transect from the bottom of the hill to the top of the hill, and more samples were taken at the apex of the hill (Photo: K. Huirama, 2018).



Figure 4.4. Soil sample collection at one the colluvial toe slope sites in the Mangaotama catchment. The site was located in the pine section.

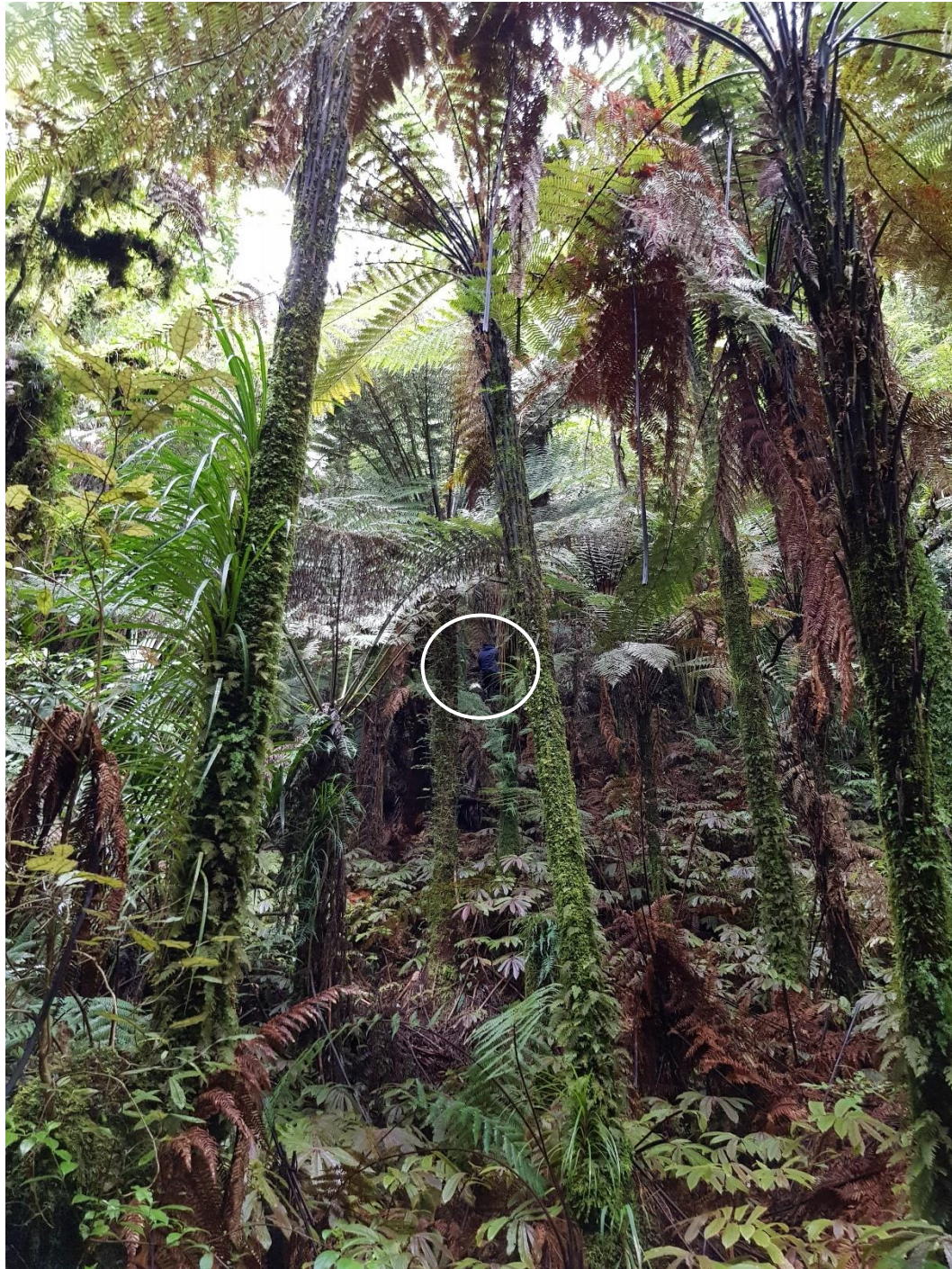


Figure 4.5. Soil sample collection from one of the hillslope sites in the Whakakai catchment. N.B. The circle shows one of the field volunteers (F. Khan) helping to collect the hillslope samples, indicated here to show scale.

4.2.2 Suspended sediment samples

Fine sediment samples were collected using a “Phillips samplers” (Phillips *et al.*, 2000). The samplers were installed on April 12 2018. Samplers were placed at the Mangaotama and Whakakai catchment outlets, near the NIWA water quality monitoring sites (Figure 4.1).

Stage-height discharge data collected by NIWA for 2017 was used to determine the baseflow and discharge during flood events in the Mangaotama and Whakakai streams. It was determined from the stage-height discharge data that the samplers would be placed 15 cm above the baseflow (Figure 4.6) to capture suspended sediment during flood events (Figure 4.7). Two samplers were placed at the same height next to each other to as duplicates. The waratahs that held the samplers were firmly secured in the stream bed and marking tape was used on the waratahs to mark the position of the samplers so that they were returned to their original position after being emptied.

On July 13, the two duplicate samplers in the Whakakai catchment were found washed downstream caused by a bank collapse event that included a fallen tree fern. The samplers were re-installed on July 13 about 40 m upstream from their original installation area (i.e. ~40 m from the NIWA monitoring station) (Costley, 2018). The samplers in both the Whakakai and Mangaotama catchments were emptied (into 5L containers using a funnel) on September 20 2018.

The samplers in the Whakakai catchment had been in operation from July 13 2018 to September 20 2018, and there six events that sub-merged the sampler. The samplers in the Mangaotama catchment had been in operation from April 12 2018 to September 20 2018, and there were 12 events that sub-merged the sampler. Thus, the sediment collected from the Phillips samplers were composite samples representing several of events between the date of installation and the date of emptying.



Figure 4.6. Phillips samples in the Mangaotama (top) and Whakakai catchment (Photo: M. Barks, 2018) (bottom) installed 15cm above base flow. N.B. The photograph was taken after the samplers were re-installed ~40m from the NIWA monitoring station on July 13.



Figure 4.7. Sub-merged Phillips samplers during the same flood event in the Mangaotama (left photo) and Whakakai (right photo) catchments. (Both photographs taken by K. Costley, 2018).

4.2.3 Laboratory work

The soil samples (Figure 4.8) (i.e. five bank and five hillslope sub-samples) from each catchment were wet sieved using tap water in the laboratory to $<63\mu\text{m}$, using 8 sieves ranging from 4 mm to $63\mu\text{m}$ (Figure 4.9). An L-cup was used to scoop the soil samples before placing the sample in the sieve to avoid overloading the sieves and damaging the fine mesh. The suspended sediment samples were wet sieved to $<63\mu\text{m}$, using the three smallest sieves used for sieving the soil samples ($500\mu\text{m}$ and $250\mu\text{m}$) (Figure 4.10). Care was taken when sieving so that particles greater than $63\mu\text{m}$ did not enter the final sample. All tools (including sieves, L-cups, buckets and beakers) were washed before wet sieving the next soil sample to avoid cross-contamination. Finally, the wet sieved samples ($<63\mu\text{m}$) were collected in beakers (Figure 4.11).



Figure 4.8. Some stream bank and hillslope samples collected in the Mangaotama catchment and returned to the laboratory.



Figure 4.9. Wet sieving area in the laboratory, showing sieves ranging from 4mm to <math><63\ \mu\text{m}</math>.



Figure 4.10. Wet sieving a suspended sediment sample (sampler near the left bank) in the Mangaotama catchment.



Figure 4.11. Example of a wet sieved stream bank soil sample ($<63\mu\text{m}$), 20 minutes after sieving and shows the sediment beginning to settle in the bottom of the beaker.

The beakers containing the final wet sieved samples ($<63\mu\text{m}$) were then dried in a 60°C oven, for 5 to 7 days. After drying the samples were crushed with a mortar and pestle (Figure 4.12), and sieved to less than $500\mu\text{m}$. All tools were wiped with paper towels between each sample. Notes were also taken at each step of the laboratory process to record any noticeable differences between samples. Finally the dried and crushed samples (size: $<63\mu\text{m}$, weight: $>30\text{g}$) (Figure 4.12) were sent to the Institute of Environmental Science and Research for gamma spectrometry analysis.

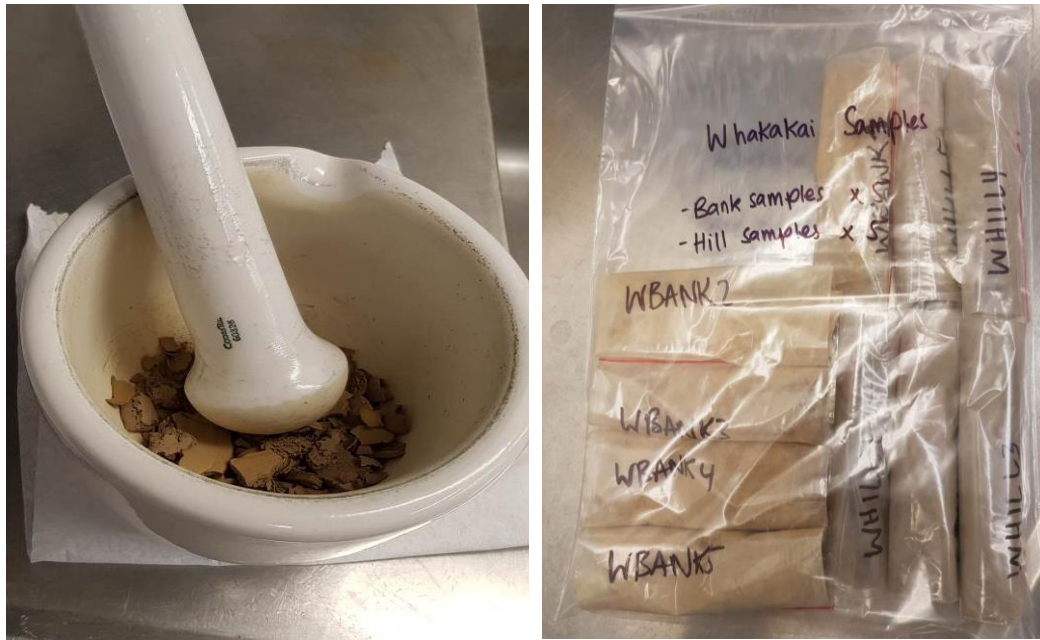


Figure 4.12. Example of dried soil sample being crushed by mortar and pestle (left) and final stream bank and hillslope soil samples from the Whakakai catchment, post drying and sieved to $<500\ \mu\text{m}$ before being sent to ESR for radionuclide analysis (right).

4.2.4 Laboratory analysis

The radionuclides chosen for analysis were caesium-137 (^{137}Cs) (derived from atmospheric nuclear testing (Longmore, 1982)) and lead-210 (^{210}Pb), radium-226 (^{226}Ra) and radium (^{228}Ra) (all derived from the decay process of ^{238}U in rocks and soils (Mabit *et al.*, 2014)). Excess lead-210 ($^{210}\text{Pb}_{\text{ex}}$) which was created in the atmosphere (from radon-222, a daughter isotope ^{238}U that diffused into the atmosphere) and was deposited back on earth as wet and dry fallout (Mabit *et al.*, 2014), cannot be analysed directly in soil, but is instead calculated from ^{210}Pb and ^{226}Ra (i.e. $^{210}\text{Pb}_{\text{ex}} = ^{210}\text{Pb} - ^{226}\text{Ra}$) (Mabit *et al.*, 2014).

The activity concentrations (Bg kg^{-1}) of the radionuclides were determined using a Hyper Pure Germanium (HPGe) and Multi-Channel Analyser detector system.

The soil samples were cast into polyester resin moulds with pre-determined geometries for each specific sample mass. The samples were left for approximately 23 days before gamma spectrometry analysis, to allow elements in the uranium decay process to reach equilibrium. Sample masses were all $> 30\ \text{g}$ and count times were typically 48 hours (A. Hughes, personal communication, 2018) (Appendices Table A.1).

4.2.5 Numerical mixing model

Numerical mixing models are commonly utilized in sediment fingerprinting studies, to estimate the relative contribution of potential erosion sources (from collected soil samples) to suspended sediment samples collected downstream (Haddadchi *et al.*, 2013; Walling, 2013). There are many mixing models available (see Haddadchi *et al.* (2014)) and the model variations are chosen based on the nature of the study and fingerprinting properties being used (Walling, 2013).

The numerical mixing model used in this study was a variant of the Monte Carlo mixing model used by Olley and Caitcheon (2000) and is the same numerical mixing model used in Hughes *et al.* (2009). The numerical model was run by Dr Andrew Hughes of NIWA, and was selected as it was easy to use (runs in Microsoft Excel using the Solver add-in function) and has been shown to produce robust and accurate results (Haddadchi *et al.*, 2014).

The key components of the numerical mixing model used in this study were:

- Radionuclide concentrations from the hillslopes and stream bank samples (sources of erosion)
- Radionuclide concentrations from the suspended sediment samples in each catchment

The numerical mixing model calculated the average concentration of the radionuclides over 1000 iterations (Hughes *et al.*, 2009). An optimisation procedure was then used, and the relative source of erosion was determined by minimising the sum of squares of deviations between the estimated relative contributions of the erosion sources, and the measured radionuclide concentrations in the suspended sediment (Mukundan *et al.*, 2012).

The relative contributions of the sources of suspended sediment (in this case hillslope erosion and stream bank erosion) must meet the following constraints (Hughes *et al.*, 2009; Mukundan *et al.*, 2012; Walling, 2013).

- The contribution from hillslope and stream banks must each be between 0 and 1 (i.e. 0 and 100%)

- The sum of both hillslope and stream bank erosion must be 1 (i.e. 100%)

In other words, the constraints act as boundaries for the numerical mixing model, to provide a realistic measure of the contribution of each erosion source. For example, if one erosion source contributes to 50% of the stream sediment, the other source would be 50% as well.

4.2.6 Statistical analysis and calculations

Basic statistical analysis (minimum, maximum, mean, standard deviation), as well as student t-tests and Man-Whitney tests, were used to determine the significant differences in the hillslope and stream bank radionuclide concentrations of the Mangaotama and Whakakai catchments.

4.3 Results

4.3.1 Soil descriptions

The stream bank samples had were similar in both the Mangaotama and Whakakai catchments, where the soil was light brown predominantly clay soil. The hillslope sample in the Mangaotama catchment were also similar in colour (light brown clay soil) to the stream bank samples from both catchments, whereas the hillslope samples in the Whakakai catchment had a darker brown/black soil colour, appeared to have a lower clay content and was more friable. The hillslope samples in the Whakakai catchment also had more organic matter and roots in the topsoil (i.e. roots had to be removed before soil could be sampled).

During sieving fewer amounts of raw stream bank samples in both catchments was needed, to gain enough fine sediment samples (<63 μ m). However, 2-3 times more raw samples were needed in order sieve enough fine sediment samples (<63 μ m) from the hillslope sites, especially in the Whakakai catchment. When the samples would not pass through the sieves easily (due to sieving too much raw sample at once), a metal rod was used to tap the sieve and move the sediment through the sieves. During sieving of the suspended sediment samples small stones and clumps of sediment would not pass through the 250 μ m sieve, and as such the sieves needed to be tapped by a metal rod for sediment to pass through (Figure 4.10).

Post-drying in the 60°C oven, most of the dried soil samples still had a light brown colour (stream banks in both catchments and Mangaotama hillslope samples), while some of the hillslope samples in the Whakakai catchment had a darker medium brown colour. However, one sample in the Whakakai catchment (WHILL1) had a darker black colour (7.5 YR 1.7/1) (Munsell, 1975), compared to the stream bank and hillslope samples in the Whakakai catchment (Figure 4.13).



Figure 4.13. A hillslope soil sample from the Whakakai catchment (WHILL1 Appendices Table A.1) that developed a dark black colour post drying in the 60°C oven, compared to other stream bank and hillslope samples from the Whakakai catchment, which had a light brown colour post drying.

4.3.2 Caesium-137 and Excess lead-210

The concentrations of ^{137}Cs were higher ($P < 0.001$) in the hillslope samples of both the Mangaotama and Whakakai catchments, than the stream bank samples (Table 4.2 & Figure 4.14). There was no significant difference ($P 0.60$) between the hillslope samples of the Whakakai catchment and the hillslope samples of the Mangaotama catchment. However, there was a higher concentration of ^{137}Cs ($P 0.03$) in the stream bank samples in the Whakakai catchment, than the stream bank samples in Mangaotama catchment.

The concentrations of $^{210}\text{Pb}_{\text{ex}}$ were higher ($P < 0.001$) in the hillslope samples of both the Mangaotama and Whakakai catchments, than the stream bank samples

(Table 4.2 & Figure 4.14). There was no significant difference ($P > 0.25$) between the hillslope samples of the Mangaotama and Whakakai catchments. There was also no significant difference ($P > 0.17$) between the stream bank samples of the Mangaotama and Whakakai catchments.

Table 4.2. Summary of the mean, minimum, maximum and standard deviation of radionuclide concentrations (^{137}Cs , $^{210}\text{Pb}_{\text{ex}}$, ^{226}Ra & ^{228}Ra) in stream bank and hillslope samples collected from the Mangaotama (M) and Whakakai (Wh) catchments. N.B. Data is the mean of 5 samples.

	Mean	Min	Max	Std
^{137}Cs (Bg kg⁻¹)				
Stream bank (M)	0.7	0.4	0.8	0.2
Stream bank (Wh)	1.1	0.8	1.9	0.4
Hill (M)	6.1	3.3	9.8	2.4
Hill (Wh)	5.5	3.1	9.1	2.3
$^{210}\text{Pb}_{\text{ex}}$ (Bg kg⁻¹)				
Stream bank (M)	5.9	-3.1	14.5	5.7
Stream bank (Wh)	10.8	5.4	14.4	3.5
Hill (M)	33.7	10.9	86.6	27.5
Hill (Wh)	31.3	23.2	36.9	4.5
^{226}Ra (Bg kg⁻¹)				
Stream bank (M)	26.6	22.6	28.3	2.1
Stream bank (Wh)	31.1	29.4	33.1	1.4
Hill (M)	24.0	20.4	26.9	2.3
Hill (Wh)	25.9	22.1	27.6	1.9
^{228}Ra (Bg kg⁻¹)				
Stream bank (M)	46.1	42.4	50.2	2.8
Stream bank (Wh)	48.4	45.3	49.9	1.6
Hill (M)	38.0	33.3	41.3	2.9
Hill (Wh)	32.5	25.1	40.0	5.1

One hillslope sample (WHILL1) in the Whakakai catchment can be considered an outlier as the concentrations of ^{137}Cs were 9.8 Bg kg⁻¹ and $^{210}\text{Pb}_{\text{ex}}$ were 86.6 Bg kg⁻¹. The ^{137}Cs was slightly higher, but the $^{210}\text{Pb}_{\text{ex}}$ value was over twice the concentrations of the other samples (Figure 4.14).

The concentrations of ^{137}Cs in the suspended sediment samples of the Mangaotama (0.86 Bg kg⁻¹) and Whakakai (0.91 Bg kg⁻¹) catchments had similar concentrations to the stream bank samples (Figure 4.14). The concentrations of $^{210}\text{Pb}_{\text{ex}}$ in the

suspended sediment samples of the Mangaotama (23.2 Bg kg^{-1}) and Whakakai (25.4 Bg kg^{-1}) were also similar (though elevated in $^{210}\text{Pb}_{\text{ex}}$) to concentrations found in the stream bank samples (Figure 4.14).

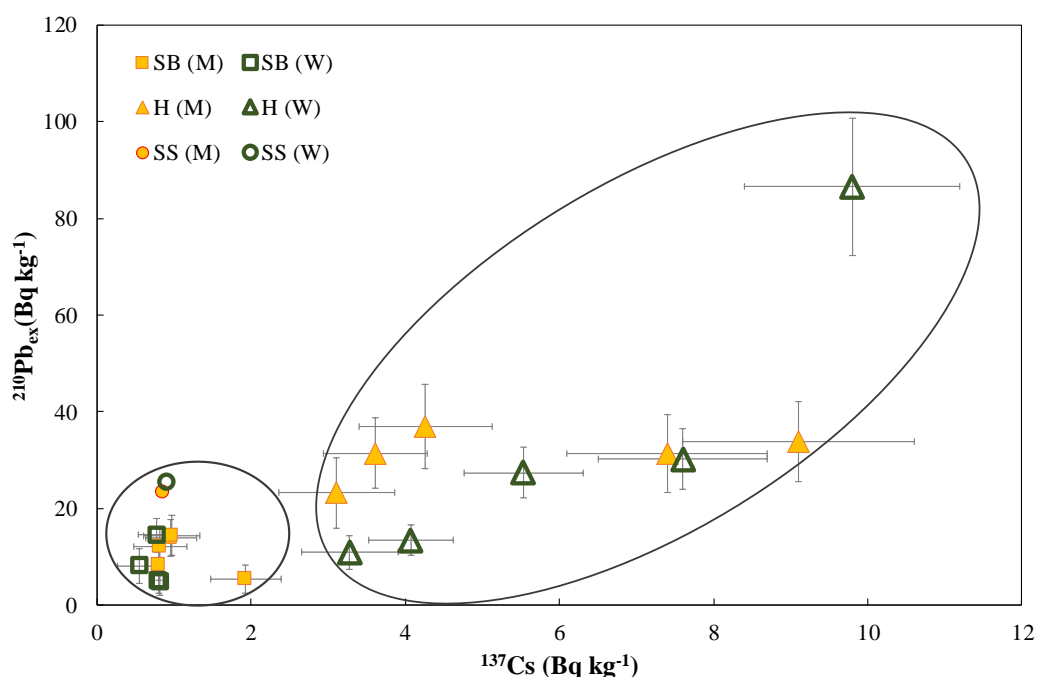


Figure 4.14. Radionuclide concentrations of ^{137}Cs and $^{210}\text{Pb}_{\text{ex}}$ in the stream bank and hillslope samples collected in the Mangaotama (M) and Whakakai catchments (W). N.B. SB = stream bank samples, H = Hillslope samples and SS = Suspended sediment samples. The error bars were results from the gamma analysis.

4.3.3 Radium-226

The concentrations of ^{226}Ra were higher ($P < 0.001$) in the hillslope samples of both the Mangaotama and Whakakai catchments, than the stream bank samples (Table 4.2 & Figure 4.15). There was no significant difference ($P > 0.25$) of ^{226}Ra concentrations between the hillslope samples of the Whakakai catchment, and the hillslope samples of the Mangaotama catchment. However, there was a higher concentration of ^{226}Ra ($P < 0.01$) in the stream bank samples of the Whakakai catchment, than the stream banks in the Mangaotama catchment.

The concentrations of ^{226}Ra in the suspended sediment samples of both the Mangaotama (30.1 Bg kg^{-1}) and Whakakai (23.3 Bg kg^{-1}) had similar concentrations to the stream bank samples (Figure 4.15).

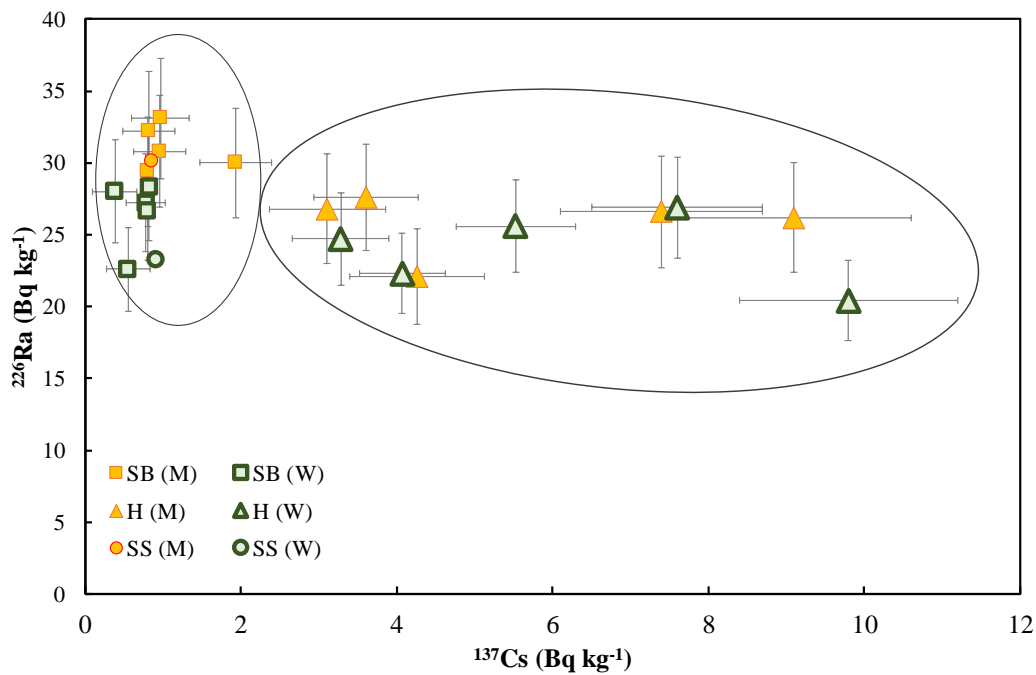


Figure 4.15. Radionuclide concentrations of ^{137}Cs and ^{226}Ra in the stream bank and hillslope samples collected in the Mangaotama (M) and Whakakai (W) catchments. N.B. SB = stream bank samples, H = Hillslope samples and SS = Suspended sediment samples. The error bars were results from the gamma analysis.

4.3.4 Radium-228

The concentrations of ^{228}Ra were higher ($P < 0.001$) in the hillslope samples of both the Mangaotama and Whakakai catchments, than the stream bank samples (Table 4.2 & Figure 4.16). There was no significant difference ($P = 0.17$) of ^{228}Ra concentrations between the hillslope samples of the Whakakai catchment, and the hillslope samples of the Mangaotama catchment. There was also no significant difference ($P = 0.25$) between the concentrations of ^{228}Ra in the stream bank samples of the Mangaotama and Whakakai catchments.

The concentrations of ^{226}Ra in the suspended sediment samples of both the Mangaotama (45.9 Bq kg⁻¹) and Whakakai (45.8 Bq kg⁻¹) catchments had similar concentrations to the stream bank samples (Figure 4.16)

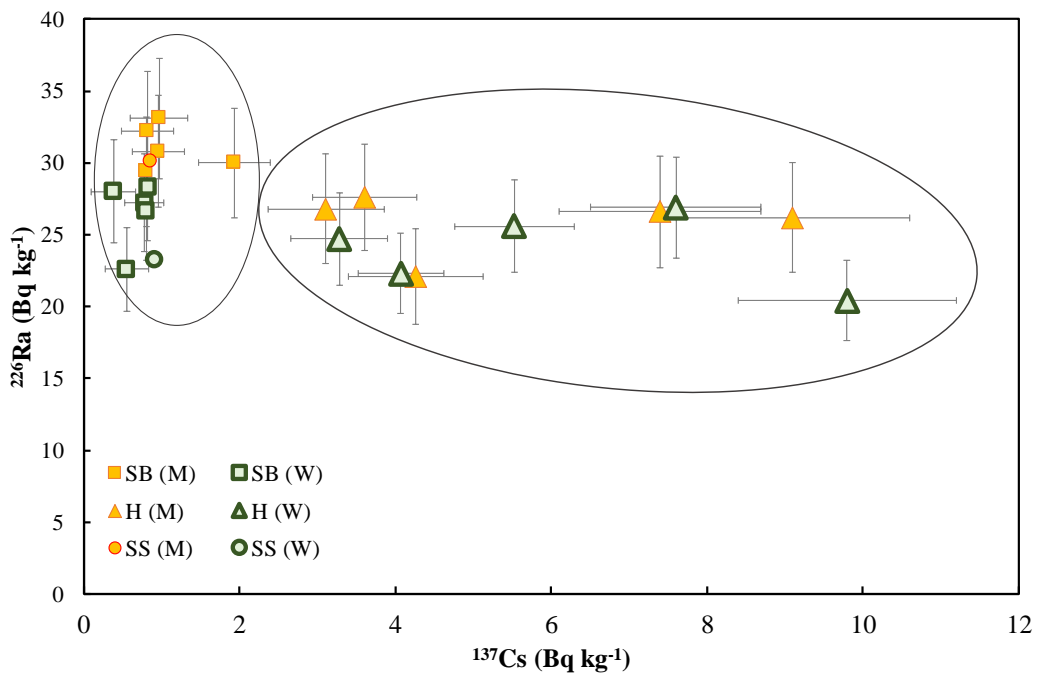


Figure 4.16. Radionuclide concentrations of ^{137}Cs and ^{226}Ra in the stream bank and hillslope samples collected in the Mangaotama (M) and Whakakai (W) catchments. N.B. SB = stream bank samples, H = Hillslope samples and SS = Suspended sediment samples. The error bars were results from the gamma analysis.

4.3.5 Numerical mixing model

Finally, the numerical mixing model results determined that in both the Mangaotama and Whakakai catchments, 90% of the suspended sediment samples matched the stream bank samples, and 10% of the suspended sediment samples matched the hillslope samples.

4.4 Discussion

4.4.1 Radionuclide concentrations

All radionuclides (^{137}Cs , $^{210}\text{Pb}_{\text{ex}}$, ^{228}Ra and ^{226}Ra) had higher ($P < 0.001$) concentrations in the hillslope samples of both the Mangaotama and Whakakai catchments, than the stream bank samples of both catchments (Figures 14-16 & Table 2). Thus, clearly distinguishing both sources of sediment. The biggest difference between hillslope and stream bank samples was in the ^{137}Cs .

There have been two New Zealand studies by Hughes and Hoyle (2014) and A. Hughes (personal communication, 2018) that have used similar sediment

fingerprinting methods. Much like this study, Hughes & Hoyle (2014) were able to distinguish between hillslope and stream bank radionuclide concentrations (^{137}Cs , $^{210}\text{Pb}_{\text{ex}}$, ^{226}Ra and ^{228}Ra) within the Kopurererua catchment, a tributary of Tauranga Harbour. A. Hughes (personal communication, 2018) was also able to distinguish between hillslope and stream bank radionuclide concentrations (^{137}Cs , $^{210}\text{Pb}_{\text{ex}}$, ^{226}Ra and ^{228}Ra) with sediment deposits from the Hoteo river, that discharges to Kaipara Harbour (Auckland). Stream bank and hillslopes were similarly separated in ^{137}Cs and $^{210}\text{Pb}_{\text{ex}}$ between stream banks and the hillslopes in Hughes (unpublished).

4.4.2 Statistical results

The t-test and Man-Whitey tests showed that ^{137}Cs (P 0.03) and ^{226}Ra (P 0.01) was higher in the Mangaotama stream bank samples than the Whakakai stream bank samples. The significant difference in concentrations may indicate either a land use or physiograph difference influencing the concentrations of ^{137}Cs and ^{226}Ra in the stream banks of both catchments, or the differences could be a false result influenced by the small sample size used in this study (five hillslope and five stream bank sites in each catchment).

However, there was no significant difference in the stream bank concentrations of ^{228}Ra (P 0.25) and $^{210}\text{Pb}_{\text{ex}}$ (P 0.17) between the Mangaotama and Whakakai catchments. There was also no significant difference in all the radionuclide concentrations ($^{137}\text{Cs} = P$ 0.60, $^{210}\text{Pb}_{\text{ex}} = P$ 0.25, $^{226}\text{Ra} = P$ 0.25 and $^{228}\text{Ra} = 0.17$) in the hillslope samples between the Mangaotama and Whakakai catchments. Thus suggesting in this study that land use has no significant effect on radionuclide concentrations in the hillslopes (all radionuclides) and stream banks (^{228}Ra and $^{210}\text{Pb}_{\text{ex}}$).

4.4.3 Outlier

The outlier sampled in the hillslopes of the Whakakai catchment with elevated levels of $^{210}\text{Pb}_{\text{ex}}$ (Figure 4.14) was sampled at a steep site, with tree ferns and large amounts of forest litter. Sample collection was also difficult due to the abundance of roots in the topsoil. Upon drying, the outlier soil sample (Figure 4.5) was a dark black colour, while all the rest of the dried soil samples (hillslope and stream banks of both catchments) were a brown colour. The darker black colour of the outlier,

indicates the soil sample had a higher organic matter than the rest of the soil samples (Munsell, 1975). Previous research had found that organic matter in soils can have a high affinity for $^{210}\text{Pb}_{\text{ex}}$ (Mabit *et al.*, 2014). Another possibility could be that the soil sample was more untouched (less eroded) than the rest of the samples, as the sample was taken on a hillslope that was well-vegetated and located on a steep slope.

The outlier had considerably higher concentrations than both the stream bank and hillslopes sites sampled by Hughes and Hoyle (2014) and Hughes (unpublished). Interestingly, the highest concentrations of ^{137}Cs and $^{210}\text{Pb}_{\text{ex}}$ in the hillslopes under native forest land use sampled by A. Hughes (personal communication, 2018) ($^{137}\text{Cs} = ^{210}\text{Pb}_{\text{ex}} = 50.8 \text{ Bq kg}^{-1}$) was similar to the value of the concentration of the outlier (86.6 Bq kg^{-1}), possibly supporting the theory that higher concentrations of $^{210}\text{Pb}_{\text{ex}}$ and ^{137}Cs are due to the higher content of organic matter, particularly within native forested areas.

4.4.4 Source of suspended sediment

The concentrations of all radionuclides (^{137}Cs , $^{210}\text{Pb}_{\text{ex}}$, ^{228}Ra and ^{226}Ra) in the suspended sediment samples, were similar to the concentrations of the stream bank samples of both the Mangaotama and Whakakai catchments, and as such plotted closely with the stream bank samples on all scatter graphs (Figures 14 to 16). Therefore indicating that stream bank erosion was the dominant source suspended sediment in both the Mangaotama and Whakakai catchments during the course of this study. The numerical mixing model further confirmed that stream banks contributed to 90% of the suspended sediment within both catchments, while the remaining 10% of the suspended sediment samples were derived from hillslopes.

Similarly, Hughes and Hoyle (2014) found that 95-99% of river deposited sediment was derived from stream bank erosion, within a tributary of Tauranga Harbour. Several radionuclide studies conducted in Australia have also found subsurface erosion to be the dominant source of sediment within their study catchment (Wallbrink *et al.*, 1998; Wasson *et al.*, 2002; Hughes *et al.*, 2009; Wasson *et al.*, 2010; Caitcheon *et al.*, 2012; Olley *et al.*, 2013). Caitcheon *et al.* (2012) determined that greater than 90% of the suspended sediment with a Northern Territory and

Queensland catchment was sourced from subsurface erosion. Olley *et al.* (2013) found that subsurface erosion was contributing to 94% of the fine sediment within a Queensland catchment, while Wasson *et al.* (2010) found that subsurface erosion was contributing 89 to 97% of the fine sediment within a Northern Territory catchment.

To assess whether it is possible (and reasonable) for the two study catchments to be generating the vast majority of their sediment from stream bank erosion, a coarse estimate of the amount of stream bank erosion (mm y^{-1}) required to produce a 90% contribution was made. Hughes *et al.* (2012) estimated that the Mangaotama Stream has a mean sediment load of 252 t y^{-1} and the Whakakai stream has a mean sediment load of 186 t y^{-1} . Based on a 90% contribution of sediment from bank erosion, this means that the Mangaotama stream banks will contribute $\sim 227 \text{ t y}^{-1}$ while the Whakakai stream banks will contribute $\sim 167 \text{ t y}^{-1}$. The equation below was used to determine how much stream bank erosion (mm y^{-1}) would be required to result in the generation this amount of sediment (Table 4.3).

$$\text{Equation 4.1: } R = s/b*h*l*d*K$$

Where:

- R = bank erosion rate (mm y^{-1})
- s = Volume of sediment derived from banks based off a 90% contribution (m^3)
- b= No. of stream banks
- h = Average stream bank height (m)
- l = Total stream channel length (m)
- d = bulk density of eroded sediment (t m^{-3})
- K = conversion factor to convert m y^{-1} to mm y^{-1}

Several assumptions were made for the course estimates of stream bank erosion, including average stream bank height, channel lengths and the bulk density of eroded bulk material. Channel lengths were estimated from a digital elevation model (DEM) (data sourced from NIWA). The conversion factor ($d= 1.5$) for metres (m y^{-1}) to millimetres (mm y^{-1}) was based on the findings that bulk density of mineral based soils ranges from between 1 to 1.6 t m^{-3} (McLaren & Cameron, 1996).

Stream bank height throughout the entire length of the catchment was estimated to be on average 0.5m, for the Mangaotama catchment, and 1m for the Whakakai catchment. The average stream bank heights were estimated based on bank height

data collected in the catchment surveys in chapter three in the Mangaotama pasture (mean left bank: 2m, std: 4m, mean right bank: 3m, std: 4m) and pine (mean left bank: 2m, std: 1.4m, mean right bank: 2m, std: 1.5m), and Whakakai catchment (mean left bank: 6m, std: 5m, mean right bank: 6m, std: 5). Bank heights were also estimated based on observations of the catchment beyond the survey reach (during ground truthing).

The stream bank heights in the Mangaotama catchment, about 300m upstream of the survey reach, had been flattened, due to stock trampling (0 to 0.2m bank heights). The bank heights in the Whakakai catchment were also bedrock in the upper reaches of the catchment survey reach. The mean bank heights are not entirely indicative of the actual average bank heights in the catchment as the upper limit of bank heights were recorded. For example, where the stream cut into a steep hill, the upper limit of that hill was recorded (e.g. 15m) rather than the height across the stretch of the stream. Thus, lower overall average bank height values have been used (Mangaotama: 0.5 m, Whakakai: 1m), to account for the height of the stream banks in the upper reaches of each catchment. However, the Whakakai catchment had consistently higher stream banks, as such, was assumed to be higher than the Mangaotama catchment (1m) in these calculations.

Table 4.3. Course calculations of stream bank erosion rates to test the reasonability of the numerical mixing model results from this study that both the Mangaotama and Whakakai catchments are dominated by stream bank erosion

	Mangaotama	Whakakai
Channel length (m)	11000	11000
Bank height (m)	0.5	1
Number of banks	2	2
Bulk density of eroded sediment ($t\ m^{-3}$)	1.5	1.5
Sediment mass derived from banks based off 90% contribution (t)	227	167
Calculated erosion rate ($mm\ y^{-1}$)	13.8	5.07

The stream bank erosion rates (Table 4.3) based on equation 4.1 were $14\ mm\ y^{-1}$ for the Mangaotama catchment and $5\ mm\ y^{-1}$ for the Whakakai catchment. These stream bank erosion rates are entirely reasonable and are in fact on the lower end of estimated bank erosion rates from headwater catchments around the world (Prosser *et al.*, 2000). Some headwater catchment studies have found bank erosion rates to be as high as 450 to 600 $mm\ y^{-1}$ (Wolman, 1959), and 100 to 200 $mm\ y^{-1}$ (Knighton, 1973). Some studies more close to the erosion rate estimated in this

study, were 10 to 60 mm y⁻¹ (Lawler *et al.*, 1997) and 30 to 54 mm y⁻¹ (Hill, 1973). Bank erosion rates in this study, are closest to Prosser *et al.* (2000) who used a purpose-built ground profiler and photo-electronic erosion pins to measure bank erosion rate in an incised canal (8.9km long), in Tasmania, Australia. Bank erosion rates were found to be 13.7 ± 2 mm y⁻¹. Stream bank erosion was attributed to sub-aerial processes.

4.4.5 Limitations of sediment fingerprinting

Possible factors that may have influenced the results could be; (1) the placement of the Phillips samplers; (2) the sieving process; (3) no replication of the suspended sediment samples and (4) only analysing soil particle sizes of <63µm. The Phillips samplers in the Whakakai catchment were located 50 m downstream of an existing bank erosion site (Figure 3.35. 3D model of the Native 2 site in the Whakakai catchment) possibly allowing the samplers to collect more stream bank derived sediment. The sieving process of the suspended sediment samples once in the laboratory, could also have been a factor, as the samples had aggregated into lumps before sieving (sample had been sitting in the container for 1 – 2 weeks). A chemical may have needed to be used to disaggregate the suspended samples before sieving. Finally, the suspended sediment results have been influenced by only analysing one set of suspended sediment samples. Further this study did not account for the variation of radionuclide concentrations across particle sizes, as tracer properties (radionuclides) in soil and sediment samples, have been found to influence tracer concentrations (Smith & Blake, 2014).

4.5 Summary and conclusions

- Five stream bank and five hillslope sites were sampled were in the Mangaotama and Whakakai catchments on May and June 2018.
- Suspended sediment samples were collected from both catchment outlets using a “Phillips sampler” (Phillips *et al.*, 2000). Samplers were in operation in the Mangaotama catchment from April 12 2018 to September 20 2018, and the samplers in the Whakakai catchment were in operation from July 13 2018 to September 20 2018.
- Stream bank/hillslope soil samples and the suspended sediment samples were wet sieved to <63µm, dried at 60°C for 5 to 7 days, then further sieved

to $<500\ \mu\text{m}$ and sent to the Institute of Environmental Science and Research for gamma spectrometry analysis.

- A numerical mixing model was used to determine the relative contribution of stream banks and hillslopes to suspended sediment, and student t-tests and Man-Whitney tests were used for statistical analysis.
- The concentrations of all radionuclides were higher in the hillslopes ($P < 0.001$) ((mean ^{137}Cs : $5.8\ \text{Bq kg}^{-1}$, std: $2.4\ \text{Bq kg}^{-1}$); (mean $^{210}\text{Pb}_{\text{ex}}$: $32.5\ \text{Bq kg}^{-1}$, std: $16.0\ \text{Bq kg}^{-1}$); (mean ^{226}Ra : $24.9\ \text{Bq kg}^{-1}$, std: $2.1\ \text{Bq kg}^{-1}$); (mean ^{228}Ra : $35.3\ \text{Bq kg}^{-1}$, std: $4.0\ \text{Bq kg}^{-1}$)) of both the Mangaotama and Whakakai catchments than in the streambanks ((mean ^{137}Cs : $0.9\ \text{Bq kg}^{-1}$, std: $0.3\ \text{Bq kg}^{-1}$); (mean $^{210}\text{Pb}_{\text{ex}}$: $8.4\ \text{Bq kg}^{-1}$, std: $4.6\ \text{Bq kg}^{-1}$); (mean ^{226}Ra : $28.8\ \text{Bq kg}^{-1}$, std: $1.7\ \text{Bq kg}^{-1}$)), clearly distinguishing both sources of sediment.
- The numerical mixing model identified that the suspended sediment from both the Mangaotama and Whakakai catchments were predominantly derived from stream bank erosion (90%) with a smaller portion of sediment derived from hillslope erosion (10%).
- Recommendations for future work are to take more suspended sediment samples, ideally after every major storm event; sort and analyse the suspended sediment samples by particle size, and to possibly disaggregate the suspended sediment samples before sieving.

Chapter 5

Using Turbidity and Stream Flow Data to Identify Sources of Sediment

5.1 Introduction

Simultaneously recorded continuous streamflow (Q) and turbidity (acting as a proxy for suspended sediment concentration) can provide information about the main sources of sediment within a catchment, particularly during storm events. Identifying the main sources of sediment provides useful information for catchment management planning and mitigation efforts (Wasson *et al.*, 2002; Minella *et al.*, 2008).

The overall objective of this chapter was to utilize the long-term NIWA data record of streamflow and turbidity to help identify the main sources of sediment within the Mangaotama and Whakakai catchments.

The specific objectives were to;

- Analyse the relationship between turbidity and streamflow (Q) for the year 2017
- Discuss the differences and similarities between the catchments, particularly the influence of land use
- Compare with earlier data published by Hughes *et al.* (2012)

5.2 Methods

Long-term NIWA water quality monitoring sites are located in the outlet of both the Mangaotama (NIWA site PW5) and Whakakai (NIWA site NW5) catchments (Figure 1.1). At the Mangaotama monitoring site (directly upstream of a rectangular weir), stage height has been recorded since 1994 and turbidity has been recorded (at 15-min intervals) since 1998. At the Whakakai monitoring site (bedrock streambed directly upstream of small waterfall), stage height has been recorded since 1992 and turbidity has also been recorded at (15-min intervals) since 1998.

At both sites, stage height data has been recorded using NIWA Hydrologger water level recorders (1 mm resolution). From the stage height data and manual sampling at various water levels, a stage/discharge rating was developed to determine streamflow (Q) from any given water level for both sites. Forest technology sensors (DTS-12 sensors, back scattering-type; nominal range (0-1600 NTU) were used to record turbidity in both catchments. The turbidity data was converted into suspended sediment concentration (SSC) data using site-specific regression relationships. Turbidity and SSC regression relationships were calculated by NIWA for both sites (Hughes *et al.*, 2012).

Both Q and turbidity data in the Mangaotama catchment spanned from 1 January to 31 December 2017 (Figure 5.1a) with no major gaps. In the Whakakai catchment, Q data ranged from 1 January to 14 November 2017 and turbidity data ranged from 1 January to 4 September 2017 (Figure 5.1b). There was missing turbidity data in the Whakakai catchment from the 2 July to 18 July 2017.

- The streamflow data (determined from stage height/discharge rating) and turbidity data from the Mangaotama and Whakakai catchments were analysed only for the year 2017.
- The base flow was around 20 l s^{-1} in the Mangaotama catchment and around 30 l s^{-1} in the Whakakai catchment.
- There were five flood events with $Q > 500 \text{ l s}^{-1}$ in the Mangaotama catchment and eighteen flood events with $Q > 500 \text{ l s}^{-1}$ in the Whakakai catchment.
- Additionally, there were two flood events with $Q > 1,000 \text{ l s}^{-1}$ in the Mangaotama catchment and eleven flood events with $Q > 1,000 \text{ l s}^{-1}$ in the Whakakai catchment.

5.2.1 Analysis of flood events

Three large flood events ($Q > 1,000 \text{ l s}^{-1}$) were selected in the Whakakai catchment, and the corresponding events were selected in the Mangaotama catchment (Figure 5.1). The event dates were:

- April 5
- July 22
- August 9

Additionally, six smaller flood events (Mangaotama: Q between 127 l s^{-1} to 606 l s^{-1} , Whakakai: Q between 219 l s^{-1} and 1398 l s^{-1}) were selected in the Whakakai catchment, and the corresponding events were selected in the Mangaotama catchment (Figure 5.1). The event dates were:

- February 3
- May 12
- June 23

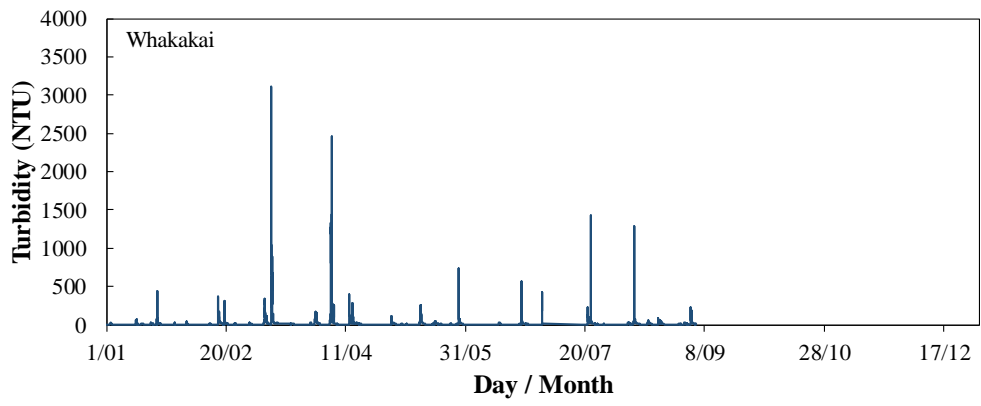
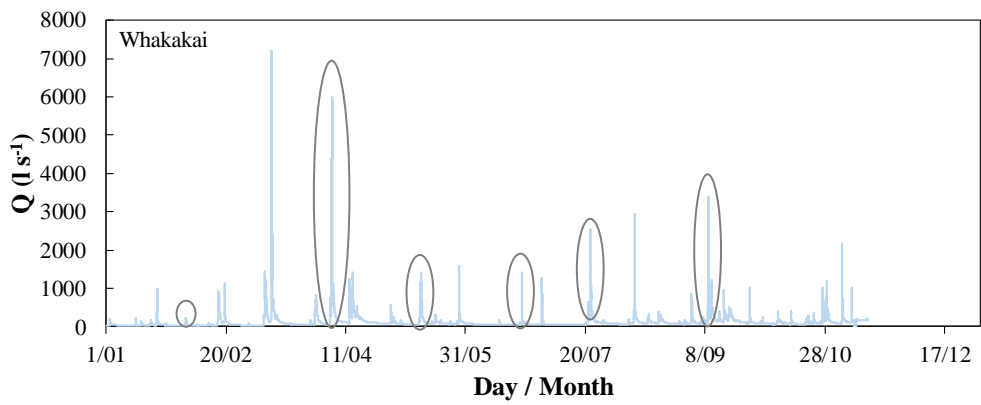
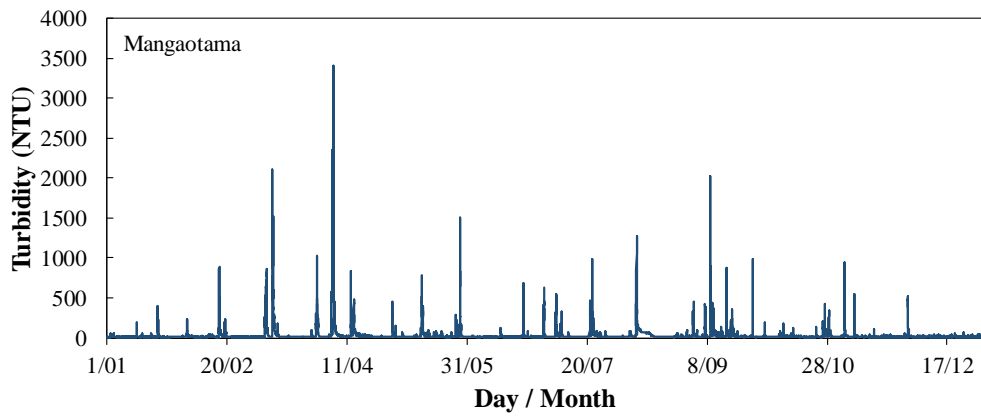
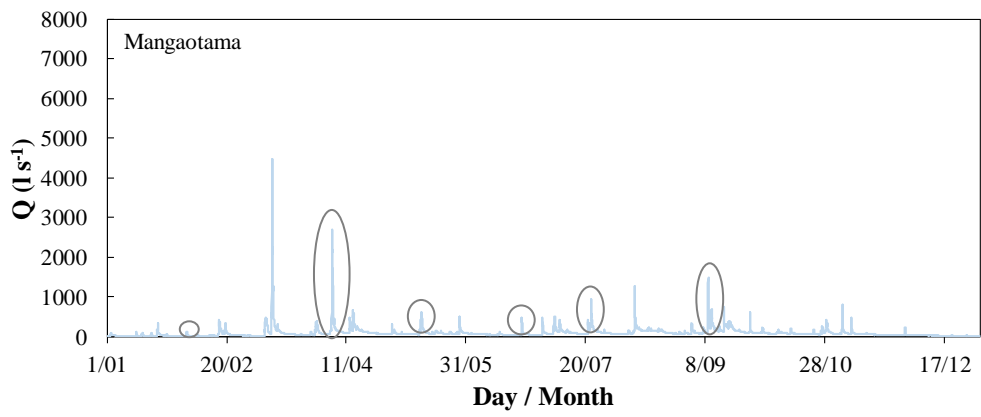


Figure 5.1. Comparison of flow (Q) and turbidity (NTU) data between the Mangaotama catchment and Whakakai catchment from 1 January to 31 December 2017. N.B. The circles on the Q graphs highlight the six flood events analysed in both the Mangaotama and Whakakai catchments.

5.3 Results

The peak Q was greater in the Whakakai catchment (flow events ranged from 219 $l\ s^{-1}$ to 5,982 $l\ s^{-1}$) than the Mangaotama catchment (flow events ranged from 126 $l\ s^{-1}$ to 2,689 $l\ s^{-1}$) for all six events (Table 5.1). Measured turbidity values were greater in the Mangaotama catchment (flow events ranged from 237 NTU, 779 NTU, 689 NTU and 3,402 NTU) for four events and greater in the Whakakai catchment (flow events 1,293 NTU and 1,493 NTU) for two events (two of the largest flood events analysed) (Table 5.1).

Table 5.1. Max Q ($l\ s^{-1}$) and turbidity (NTU) values for the six flood events analysed in the Mangaotama and Whakakai catchments

Flow Event	Mangaotama		Whakakai	
	Q	Turbidity (NTU)	Q	Turbidity (NTU)
5-Apr	2689	3402	5982	2464
22-Jul	949	991	2535	1435
9-Aug	1266	1274	2942	1293
3-Feb	127	237	219	41
12-May	611	779	1411	251
23-Jun	470	689	1399	571

5.3.1 Large flood events analysed

April 5

The storm event on April 5 was a double peaked storm event (one event not long after another), with the highest Q occurring in both catchments during the second event. Whakakai had a greater peak Q ($5,982 \text{ l s}^{-1}$) compared to the Mangaotama catchment ($2,689 \text{ l s}^{-1}$), while the Mangaotama catchment had greater turbidity ($3,402 \text{ NTU}$) than the Whakakai catchment ($2,464 \text{ NTU}$) (Figure 5.2 & Table 5.1).

Closer analysis of the two consecutive flow events on April 5 showed differences in turbidity responses from the first event to the second flow event, in both catchments. During the first event, turbidity peaked before Q in both the Mangaotama and Whakakai catchment (Figure 5.3). Contrastingly, during the second event turbidity peaked after Q in the Mangaotama catchment, while turbidity and Q peaked concurrently in the Whakakai catchment (Figure 5.5).

During the first event, both catchments had clockwise hysteresis, with Mangaotama showing strong clockwise hysteresis, while Whakakai had moderately strong clockwise hysteresis (Figure 5.4). During the second event, the Mangaotama catchment showed moderately strong clockwise hysteresis, while the Whakakai catchment showed no hysteresis (Figure 5.6).

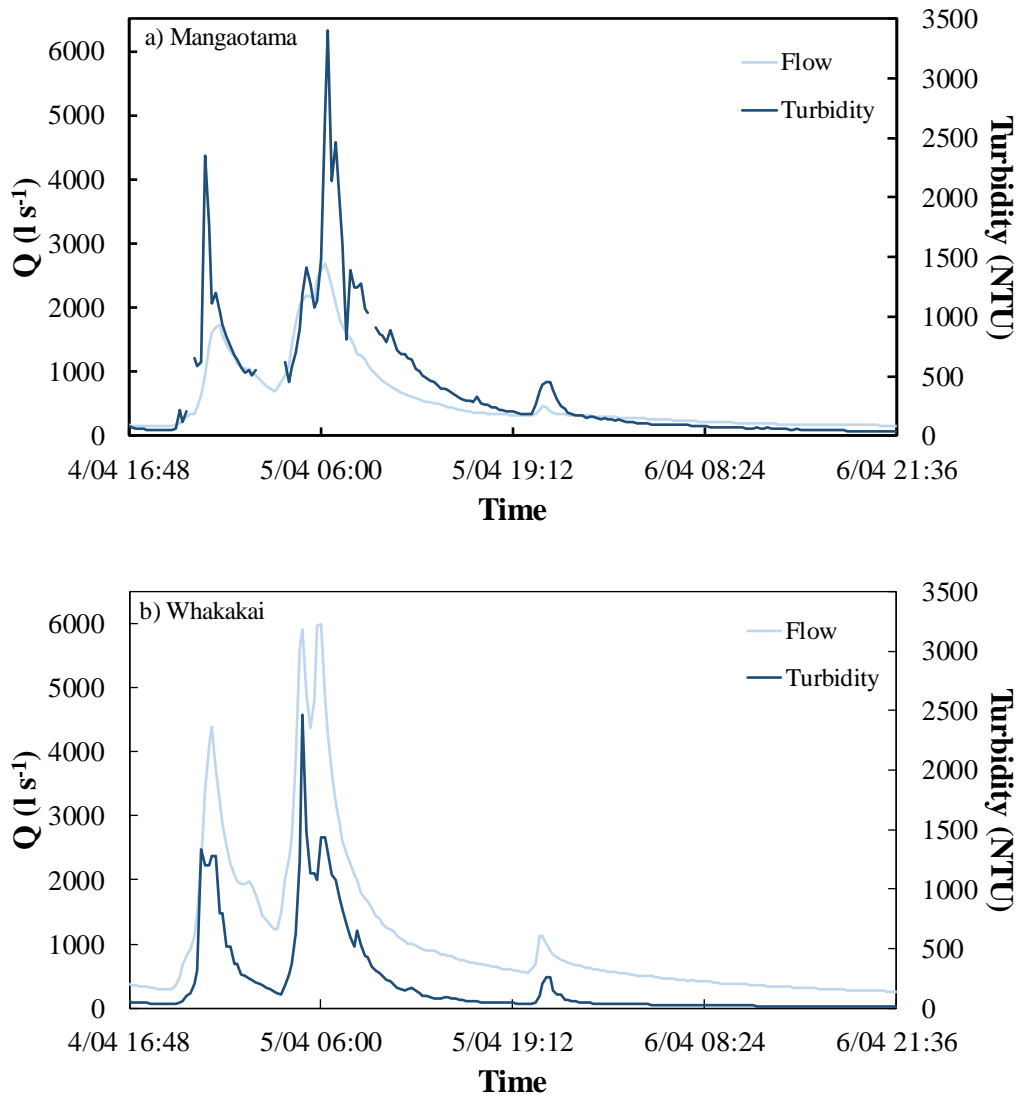


Figure 5.2. Flow (Q) and turbidity data from the storm event on 5 April 2017 in the Mangaotama (a) and Whakakai (b) catchments.

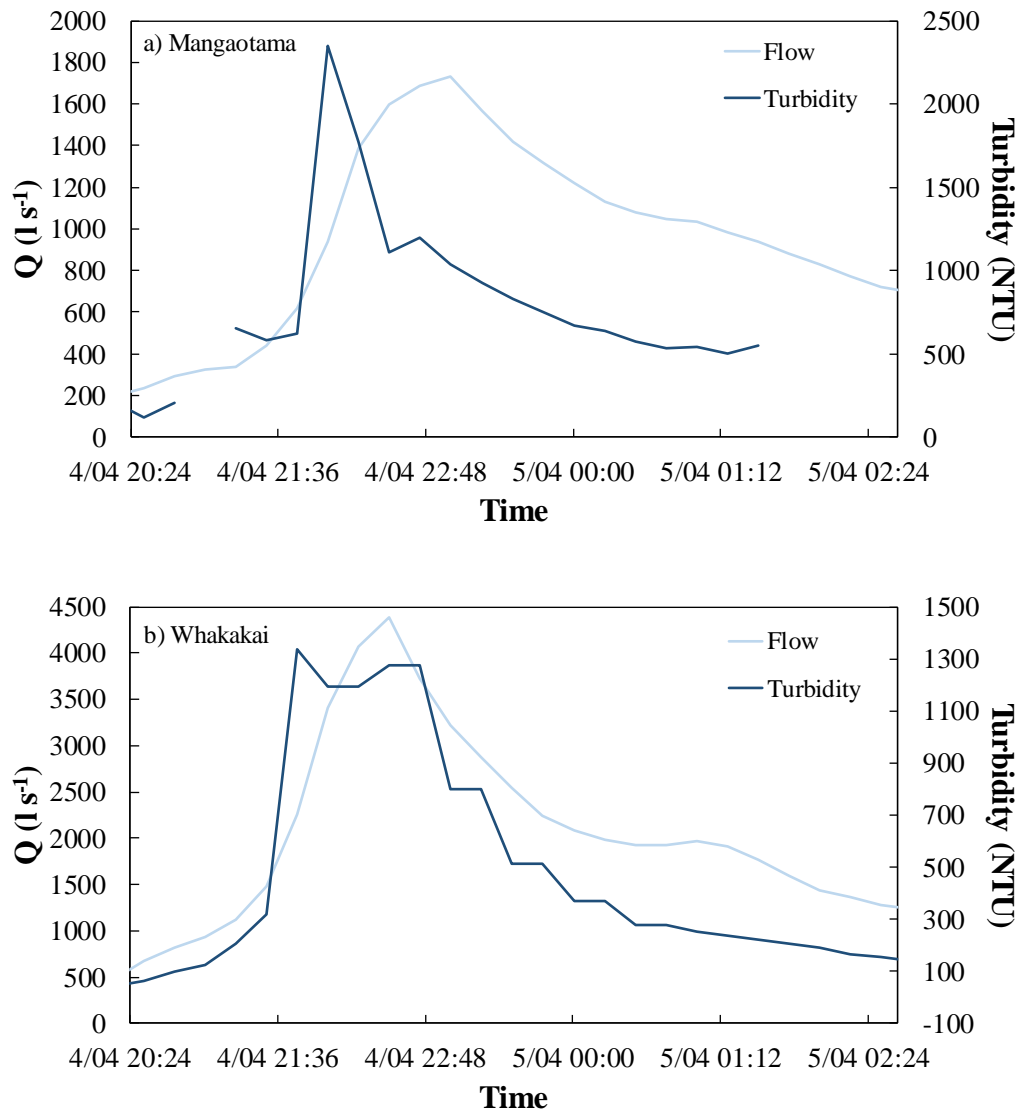


Figure 5.3. Close up view of the first peak of the storm event on 5 April 2017 in the Mangaotama (a) and Whakakai (b) catchments. N.B. The graphs are not plotted on the same y-axis scale (Q and turbidity) and have instead been exaggerated to showcase the Q and turbidity peaks in both catchments.

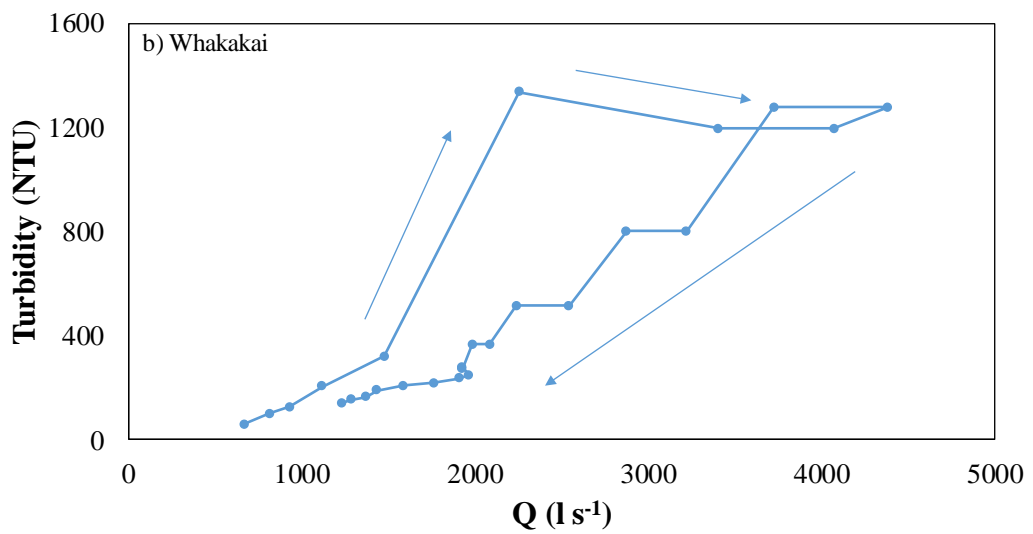
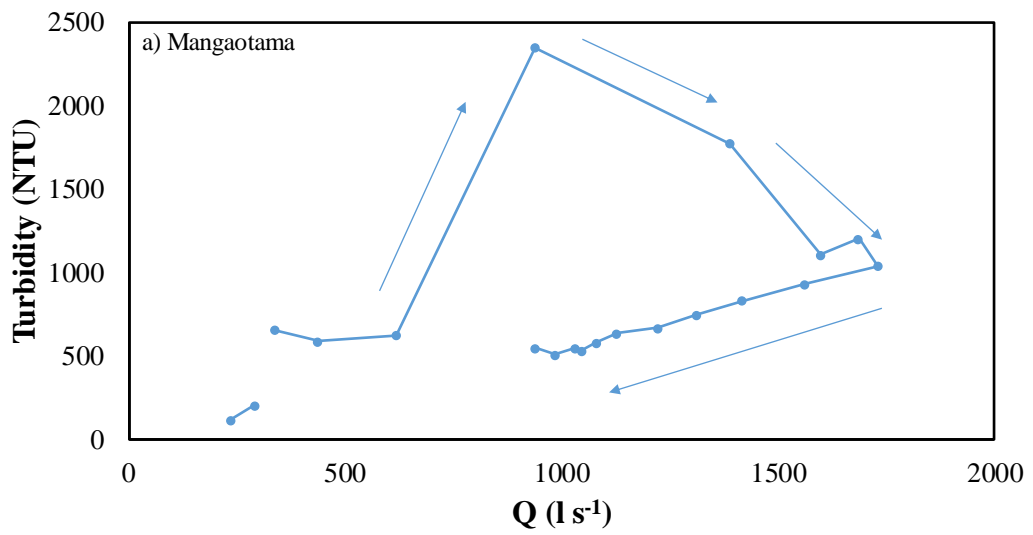


Figure 5.4. Hysteresis graphs for the first peak of the storm event 5 April 2017 in the Mangaotama (a) and Whakakai (b) catchments. N.B. The hysteresis graph scales are not equal and have instead been exaggerated to showcase the hysteresis in each catchment.

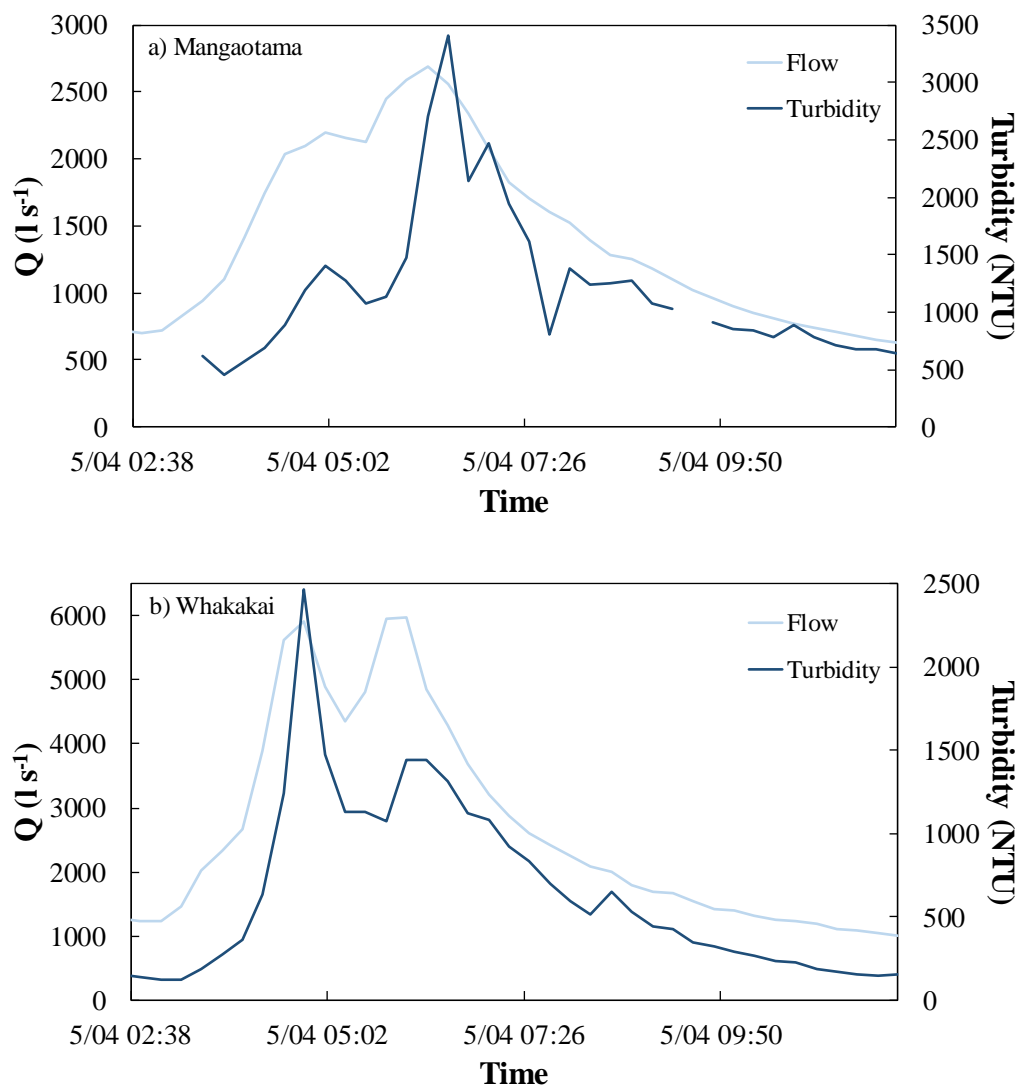


Figure 5.5. Close up view of the second peak of the storm event on 5 April 2017 in the Mangatama (a) and Whakakai (b) catchments. N.B. The graphs are not plotted on the same y-axis scale (Q and turbidity) and have instead been exaggerated to showcase the Q and turbidity peaks in both catchments.

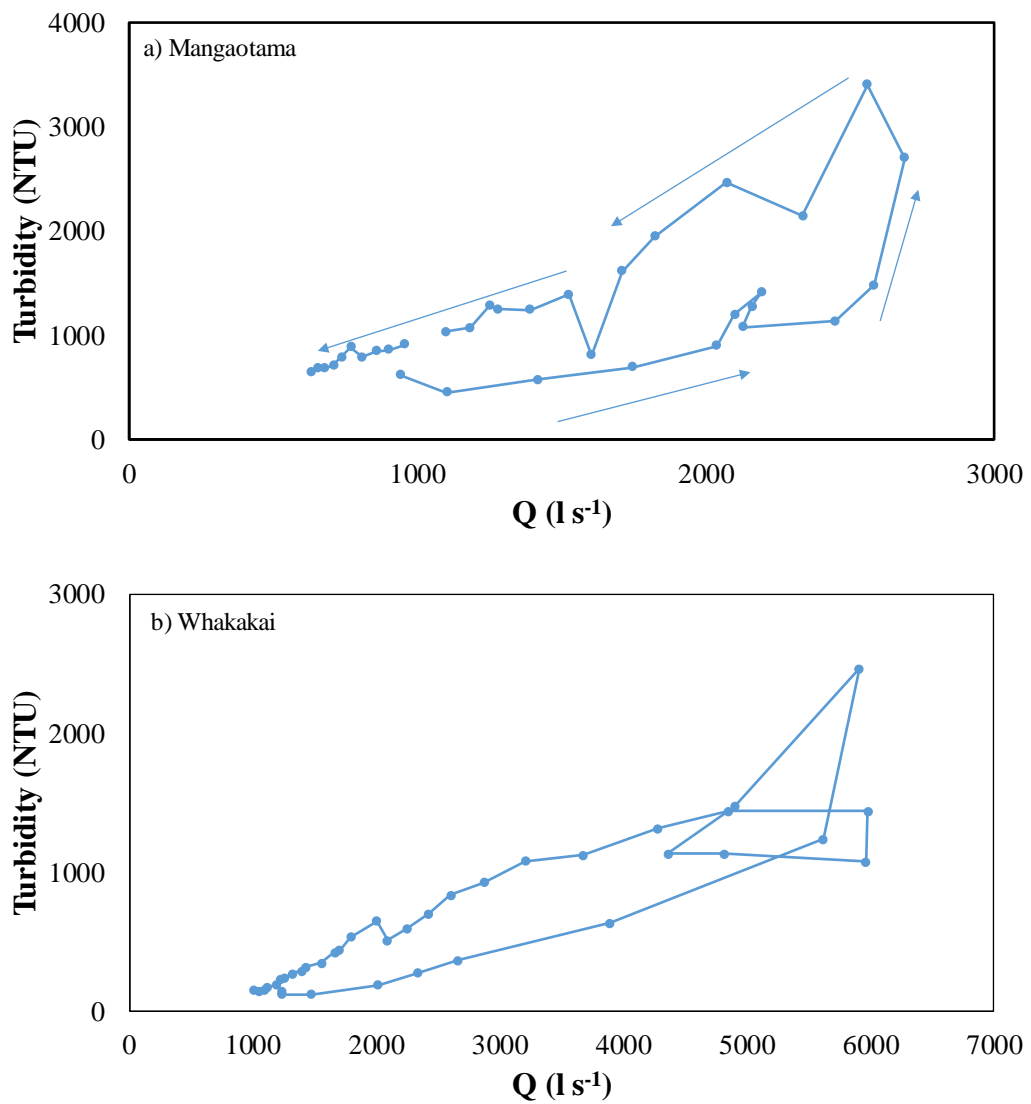


Figure 5.6. Hysteresis graphs for the second peak of the storm event on 5 April 2017 in the Mangaotama (a) and Whakakai (b) catchments. N.B. The hysteresis graph scales are not equal and have instead been exaggerated to showcase the hysteresis in each catchment. No arrows indicates no hysteresis, as Q and turbidity peaked at the same time.

July 22

The July 22 event had greater Q in the Whakakai catchment ($2,535 \text{ l s}^{-1}$) than the Mangaotama catchment (959 l s^{-1}). The Whakakai catchment also had higher turbidity ($1,435 \text{ NTU}$), than the Mangaotama catchment (991 NTU) (Figure 5.7). Closer inspection of the peaks from each catchment shows that turbidity peaks before Q in the Mangaotama catchment and after Q in the Whakakai catchment (Figure 5.8). Strong clock-wise hysteresis was shown in the Mangaotama catchment, while weak anti-clockwise hysteresis was shown in the Whakakai catchment (Figure 5.9).

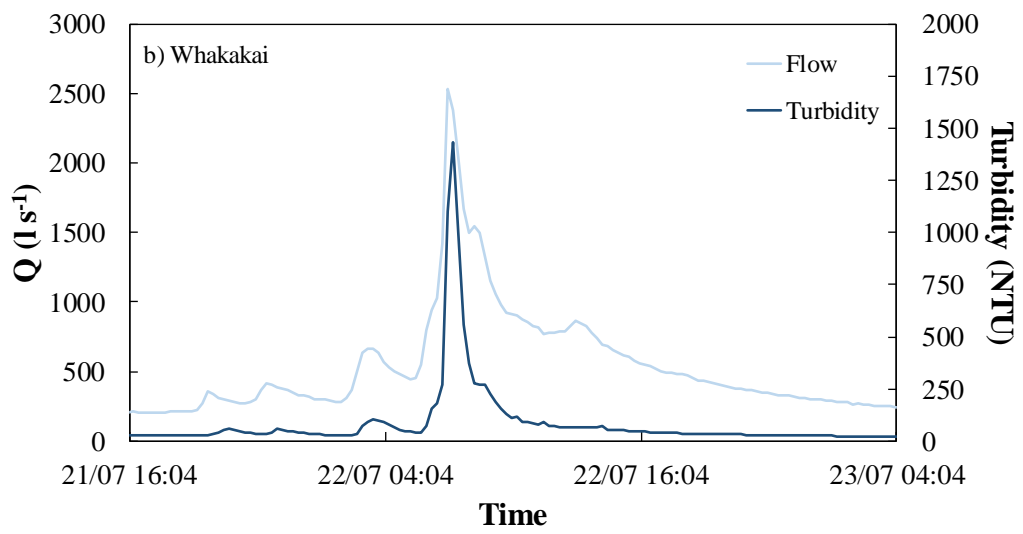
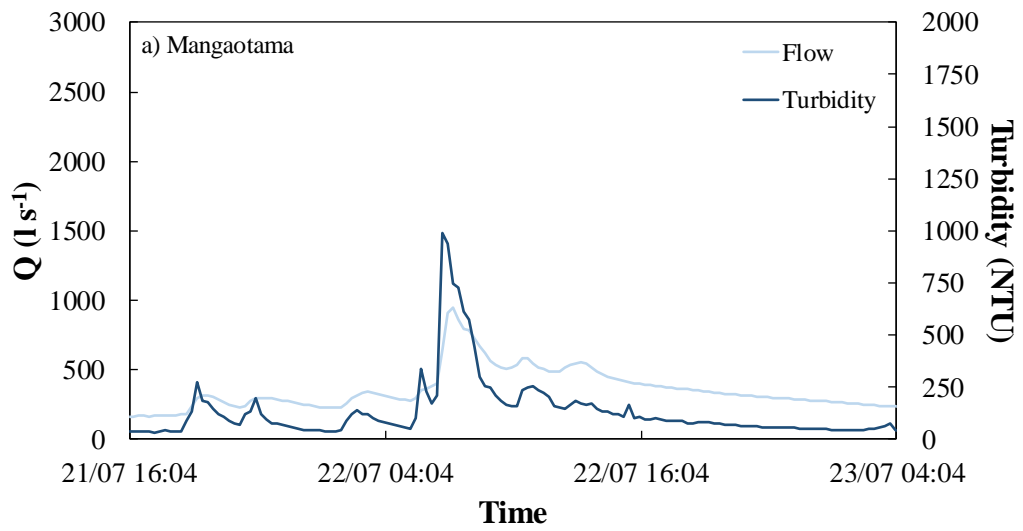


Figure 5.7. Flow (Q) and turbidity graphs for the storm event on 22 July 2017 in Mangaotama (a) and Whakakai (b).

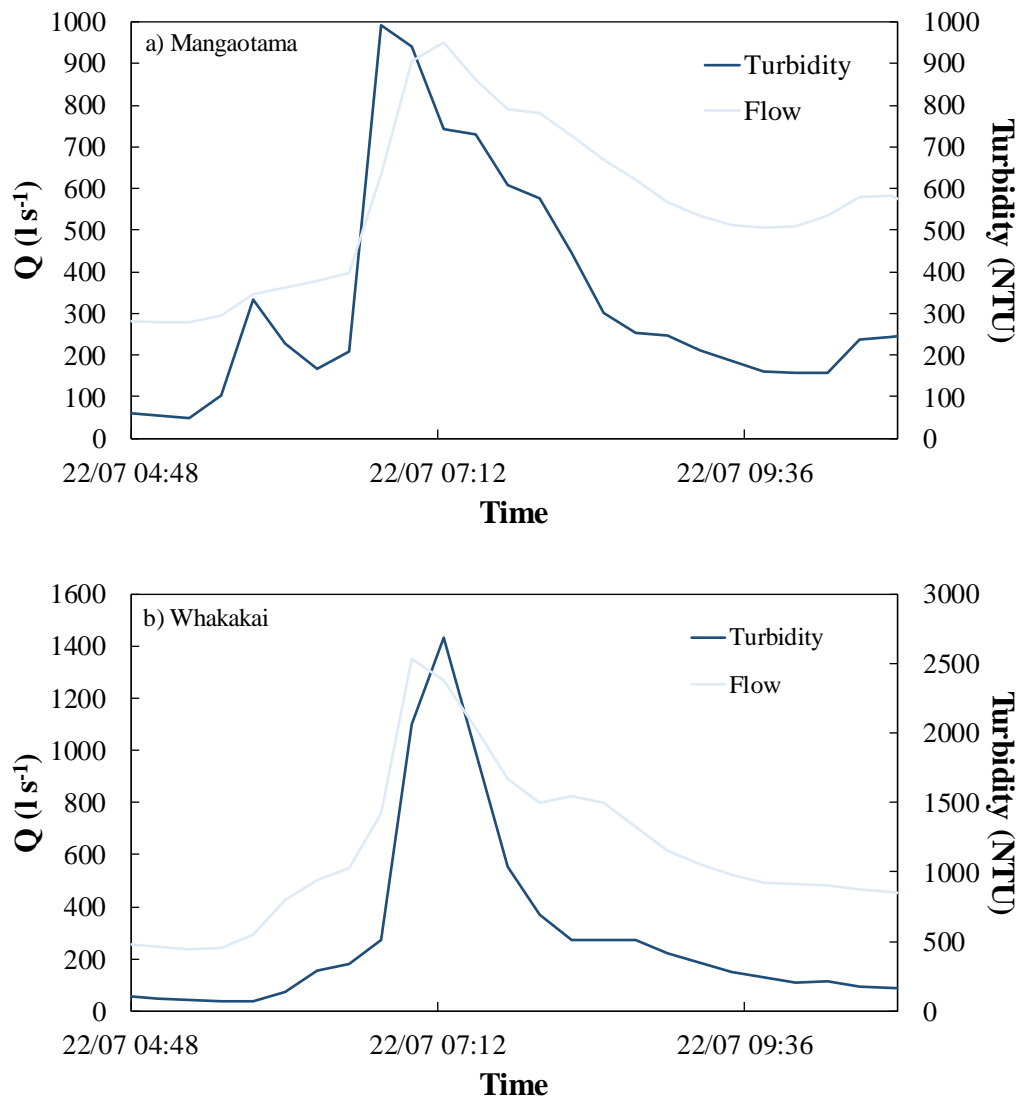


Figure 5.8. Close up view of the storm event on 22 July 2017 in Mangaotama (a) and Whakakai (b). N.B. The graphs are not plotted on the same y-axis scale (Q and turbidity) and have instead been exaggerated to showcase the Q and turbidity peaks in both catchments.

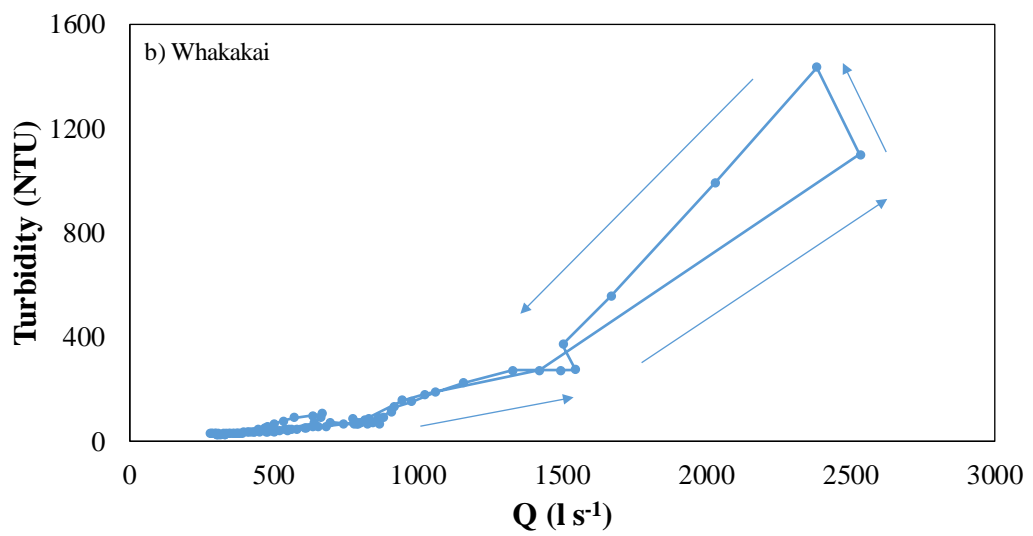
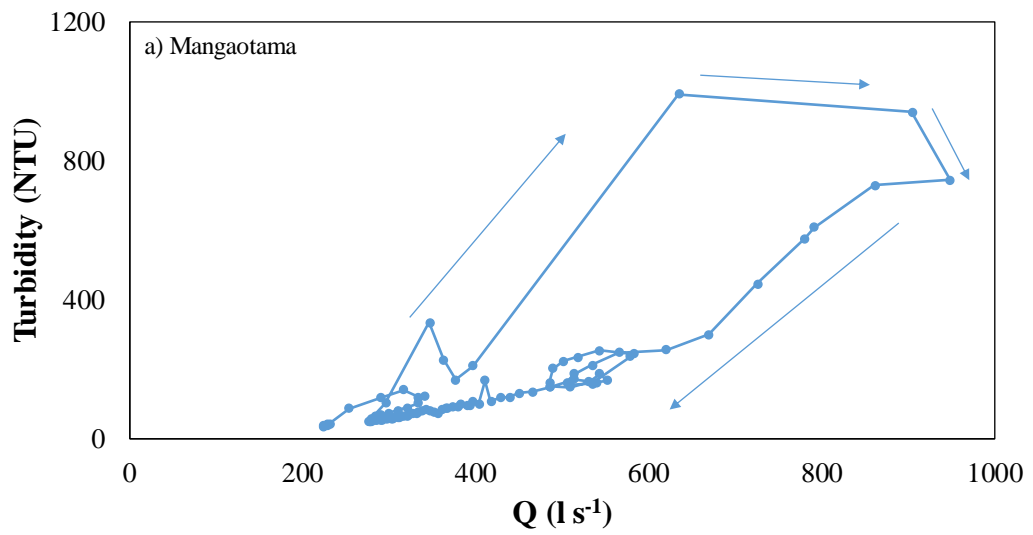


Figure 5.9. Hysteresis graphs for the storm event on 22 July 2017 in the Mangaotama (a) and Whakakai (b). N.B. The hysteresis graph scales are not equal and have instead been exaggerated to showcase the hysteresis in each catchment.

August 9

The August 9 event had greater Q in the Whakakai catchment ($2,942 \text{ l s}^{-1}$), compared to the Mangaotama catchment ($1,266 \text{ l s}^{-1}$) (Figure 5.10). The Whakakai catchment also had higher turbidity (1,293 NTU), than the Mangaotama catchment (Figure 5.10).

A close-up view of the data showed that the Q-turbidity peaked at the same time in the Mangaotama catchment, but turbidity lagged behind Q in the Whakakai catchment (Figure 5.11). There was no hysteresis in the Mangaotama catchment and weak hysteresis in the Whakakai catchment (Figure 5.12)

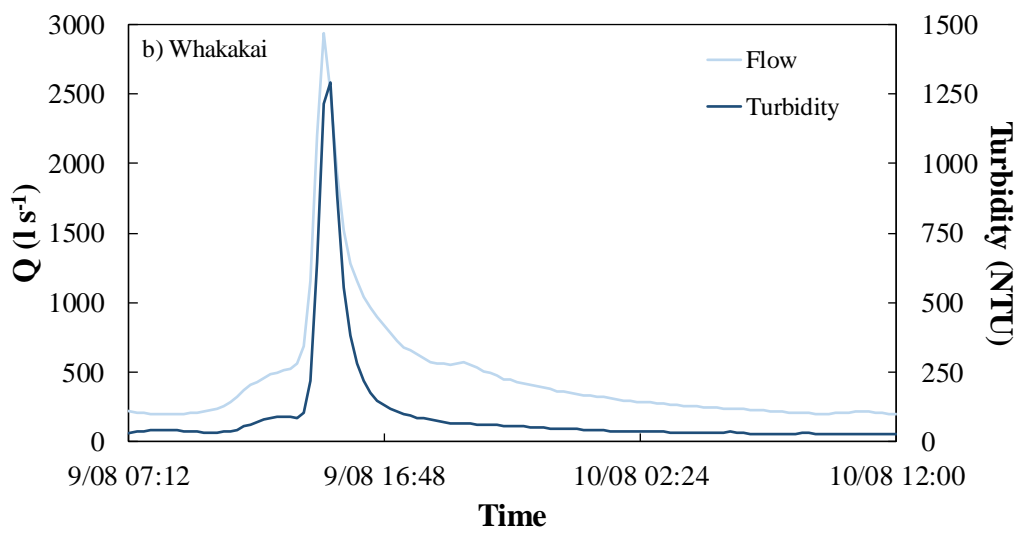
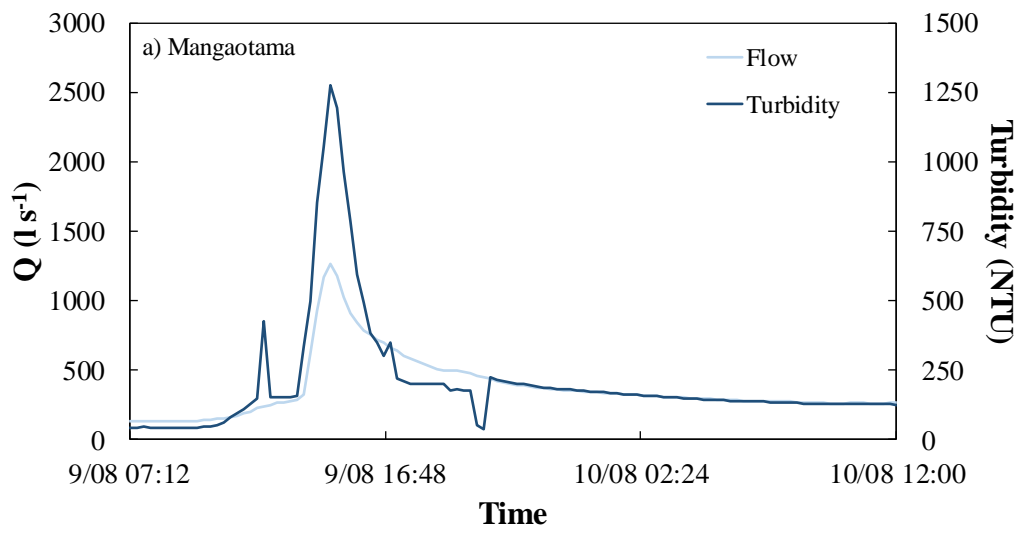


Figure 5.10. Flow (Q) and turbidity data for the storm event on 9 August 2017 in the Mangaotama (a) and Whakakai(b)

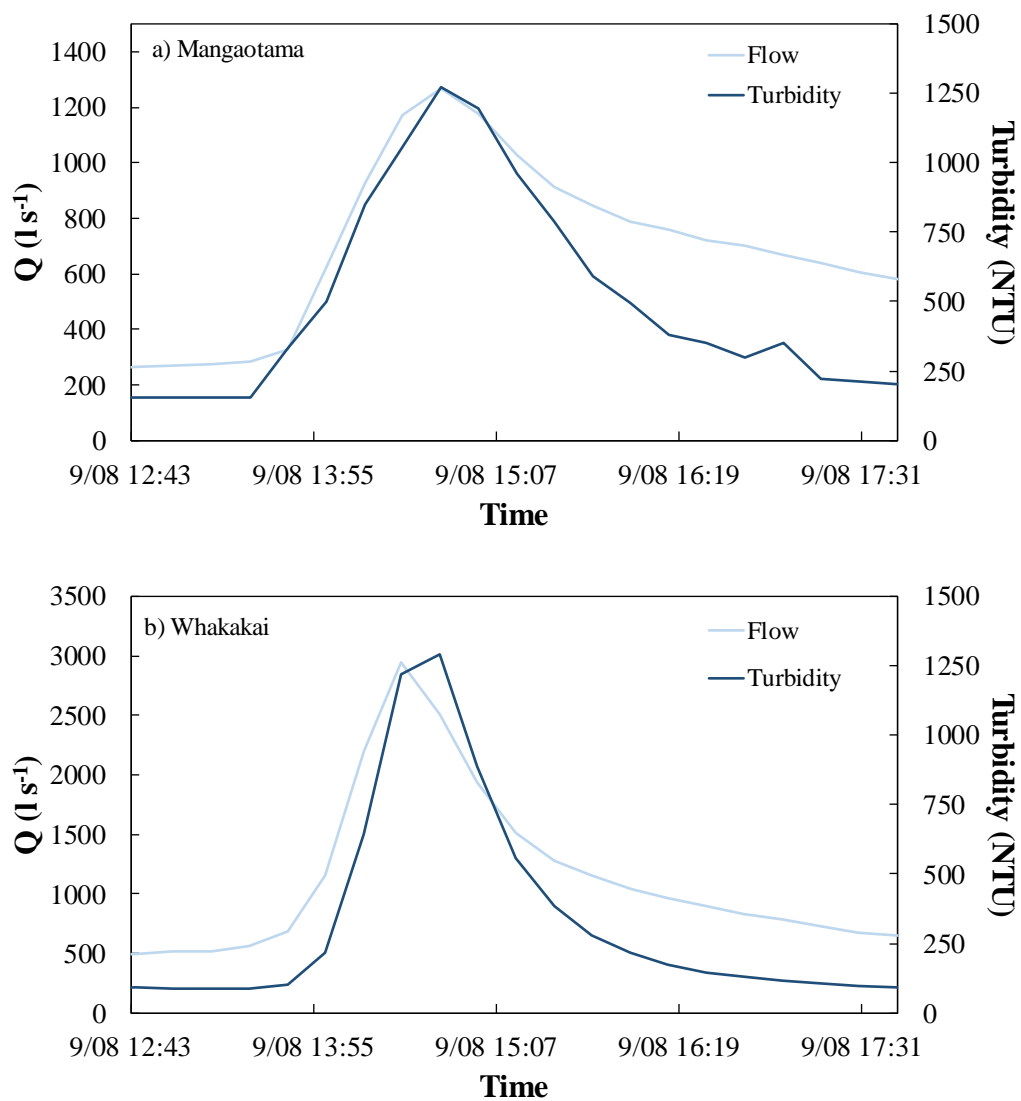


Figure 5.11. Close up view of the storm event 9 August 2017 in the Mangaotama (a) and Whakakai (b). N.B. The graphs are not plotted on the same y-axis scale (Q and turbidity) and have instead been exaggerated to showcase the Q and turbidity peaks in both catchments.

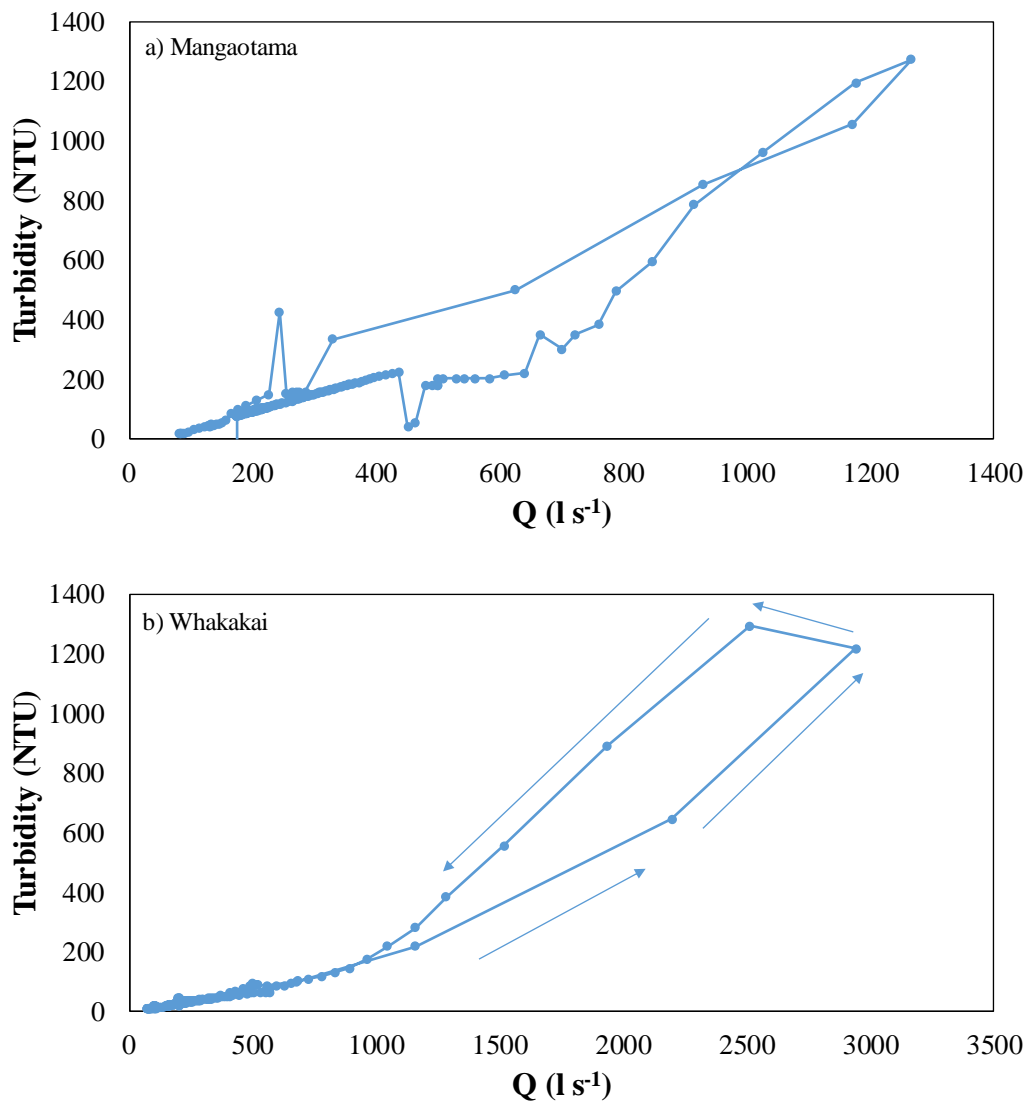


Figure 5.12. Hysteresis graphs for the storm event on 9 August 2017 in the Mangaotama (a) and Whakakai (b). N.B. The hysteresis graph scales are not equal and have instead been exaggerated to showcase the hysteresis in each catchment.

5.3.2 Small flood events analysed

February 3

The February 3 storm event had a higher Q in the Whakakai catchment (219 l s^{-1}) than the Mangaotama catchment (127 l s^{-1}). The Mangaotama catchment also had much higher turbidity (237 NTU) than the Whakakai catchment (41 NTU) (Figure 5.13).

The Mangaotama catchment had a double peak in turbidity and Q data, with turbidity peaking before Q in the first event and turbidity peaking simultaneously with Q in the second. Turbidity in the Whakakai catchment is lagging behind Q (Figure 5.14). Weak clockwise hysteresis was exhibited in the Mangaotama catchment, and moderate hysteresis is shown in the Whakakai catchment (Figure 5.15)

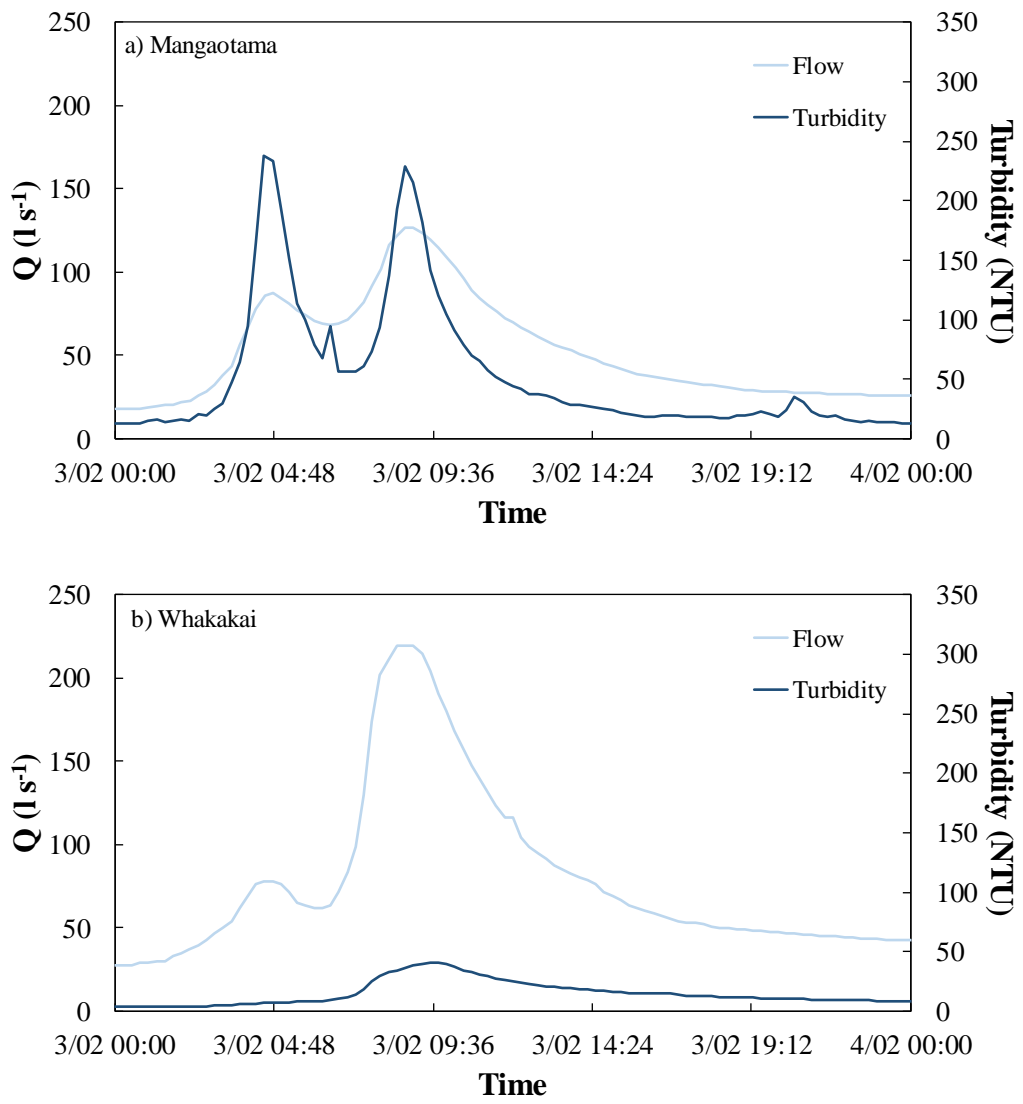


Figure 5.13. Flow (Q) and turbidity data from the storm event on 3 February 2017 in the Mangaotama and Whakakai catchments

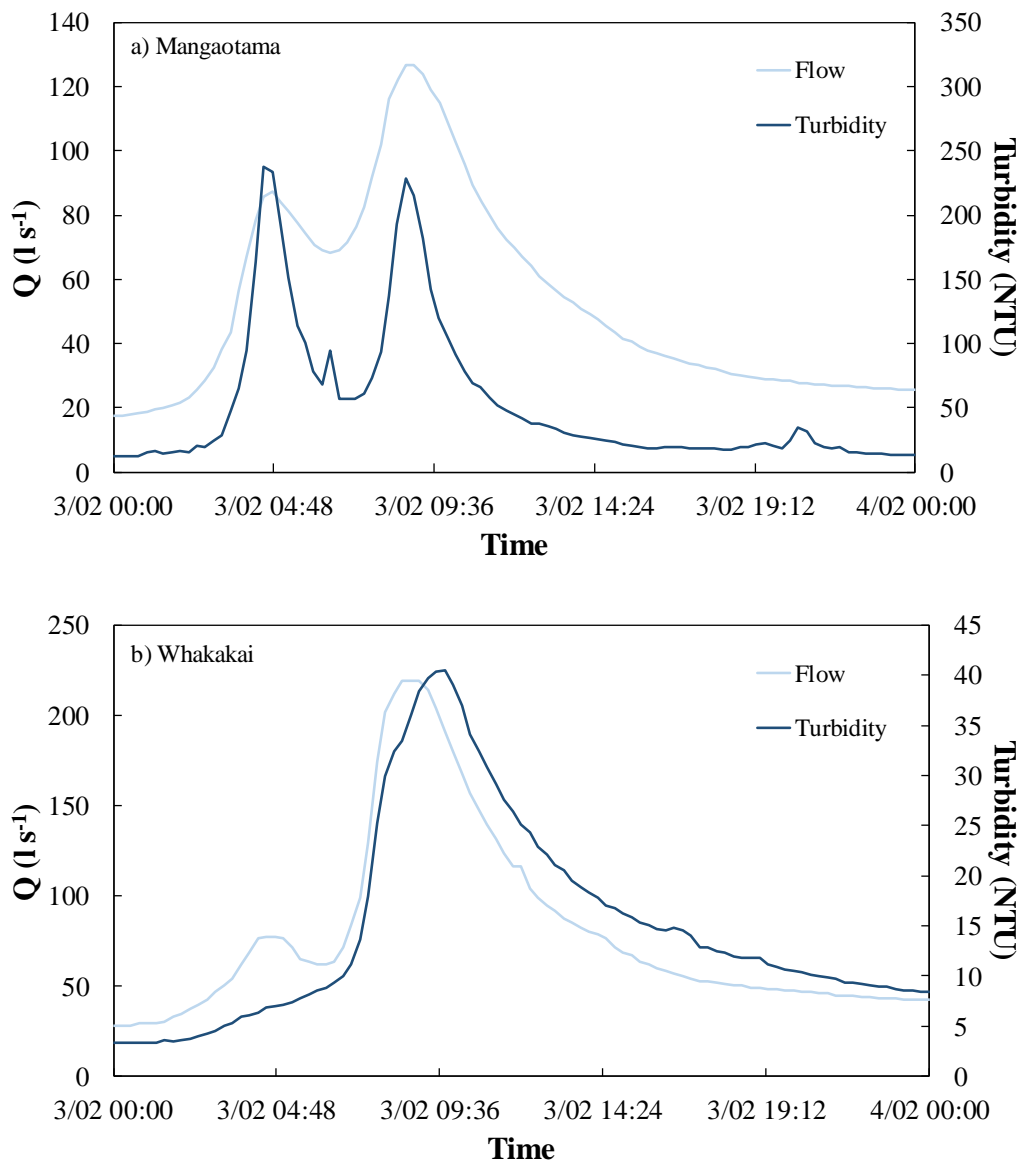


Figure 5.14. Close up view of the storm event on 3 February 2017 in the Mangaotama (a) and Whakakai (b). N.B. The graphs are not plotted on the same y-axis scale (Q and turbidity) and have instead been exaggerated to showcase the Q and turbidity peaks in both catchments.

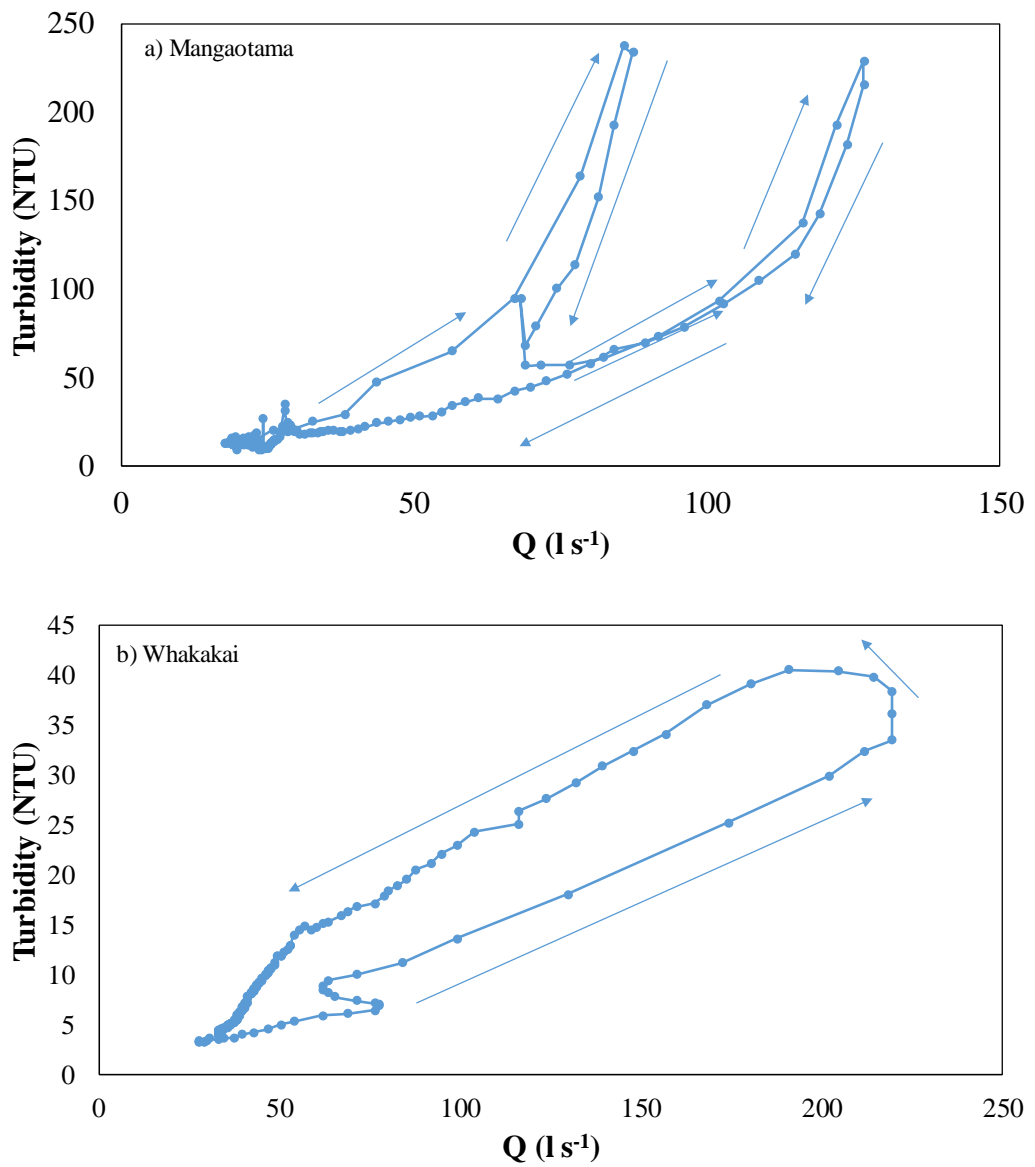


Figure 5.15. Hysteresis graphs for the storm event on 3 February 2017 in the Mangaotama (a) and Whakakai (b) catchments. N.B. The hysteresis graph scales are not equal and have instead been exaggerated to showcase the hysteresis in each catchment.

May 12

The May 12 event had a higher peak Q in the Whakakai catchment ($1,411 \text{ l s}^{-1}$), compared to the Mangaotama catchment (611 l s^{-1}). However, the Mangaotama catchment had greater turbidity (779 NTU), than the Whakakai catchment (251 NTU) (Figure 5.16)

A closer view of the graphs showed that in the first peak, turbidity in the Mangaotama catchment peaked before Q, while in the Whakakai catchment turbidity lagged behind Q (Figure 5.17). During the second peak, turbidity in the Mangaotama catchment peaked at the same time as Q, while in the Whakakai catchment turbidity lagged behind Q (Figure 5.19).

Hysteresis graphs showed that in the first peak the Mangaotama catchment showed weak clockwise hysteresis, while the Whakakai catchment showed anti-clockwise hysteresis (Figure 5.18). In the second peak, the Mangaotama catchment showed no hysteresis, and the Whakakai catchment showed weak anti-clockwise hysteresis (Figure 5.20).

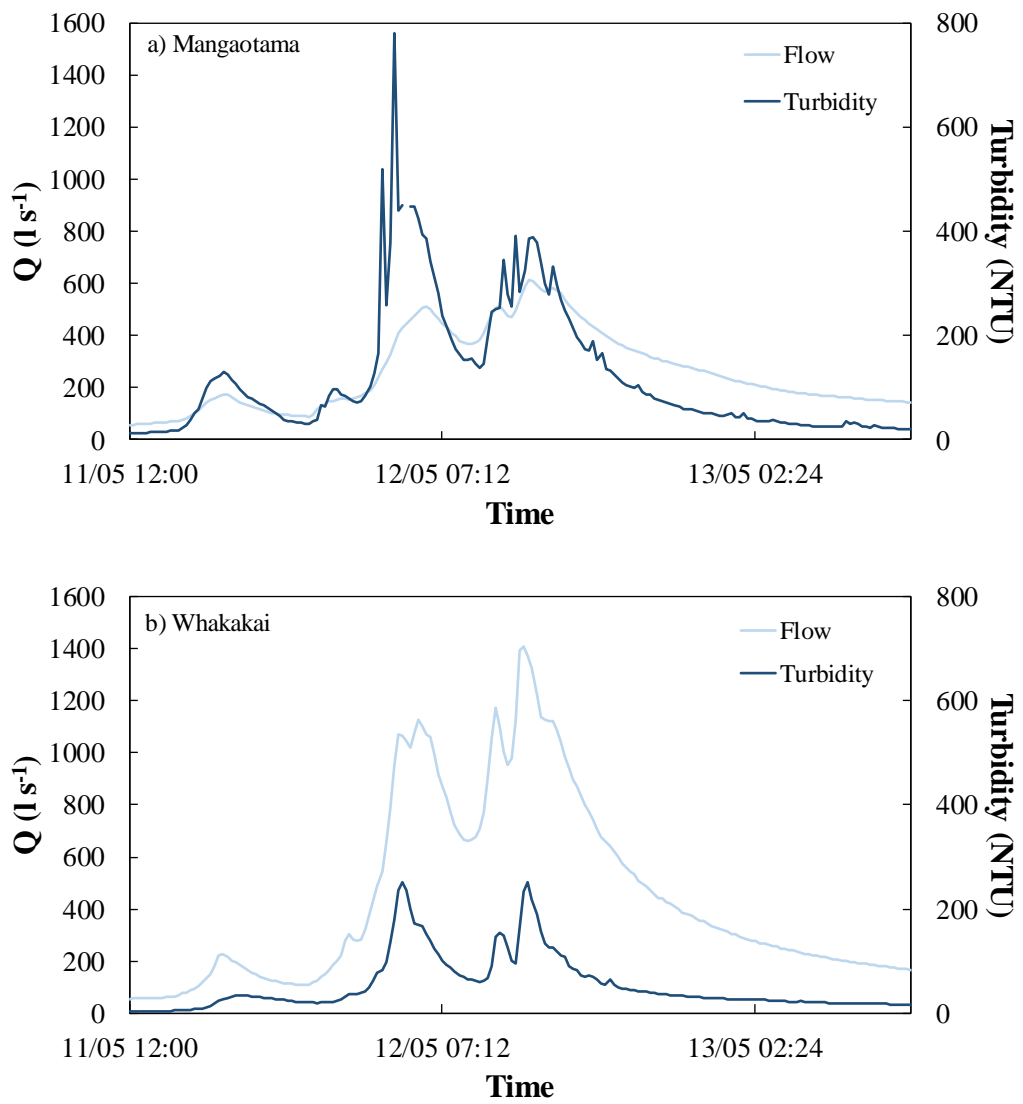


Figure 5.16. Flow (Q) and turbidity data for the storm event on 12 May 2017 in the Mangaotama (a) and Whakakai (b) catchments.

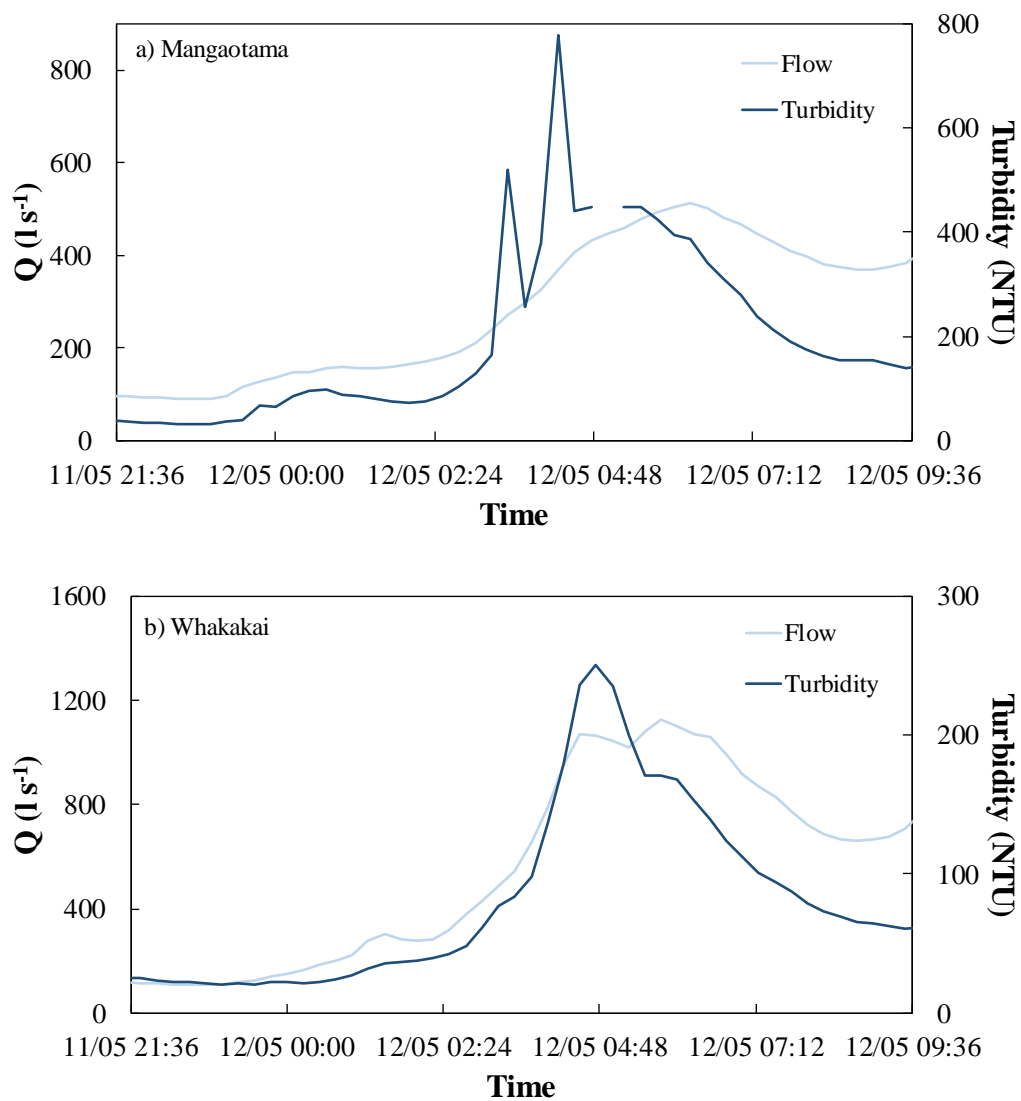


Figure 5.17. Close up view of the first peak of the storm event on 12 May 2017 in Mangaotama (a) and Whakakai (b). N.B. The graphs are not plotted on the same y-axis scale (Q and turbidity) and have instead been exaggerated to showcase the Q and turbidity peaks in both catchments.

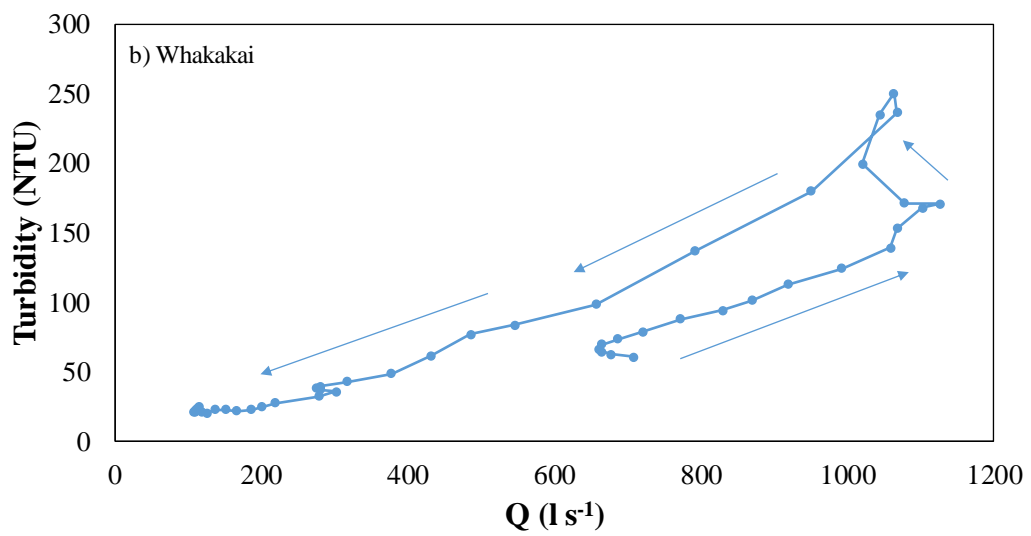
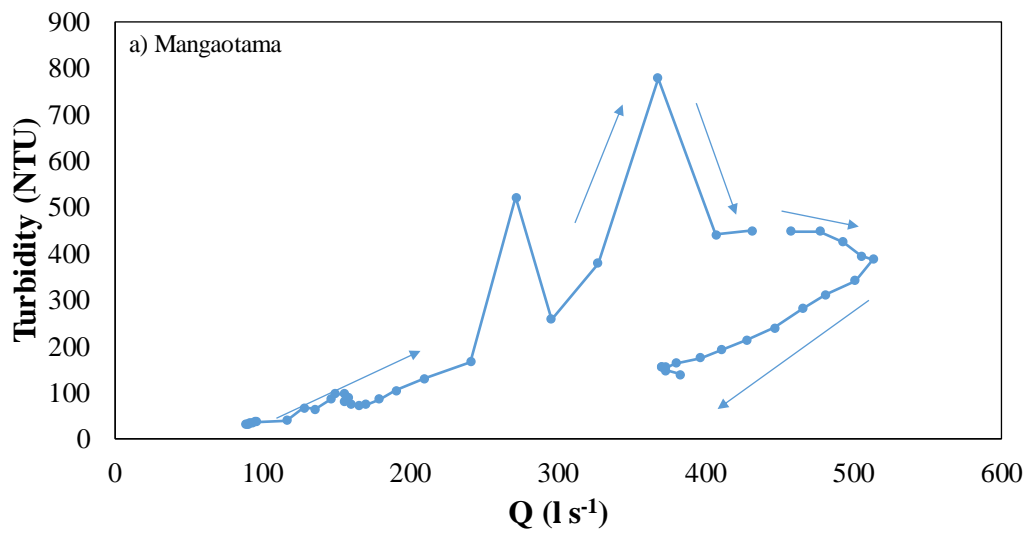


Figure 5.18. Hysteresis graphs for the first peak of the storm event on 12 May 2017 in the Mangaotama (a) and Whakakai (b) catchments. N.B. The hysteresis graph scales are not equal and have instead been exaggerated to showcase the hysteresis in each catchment.

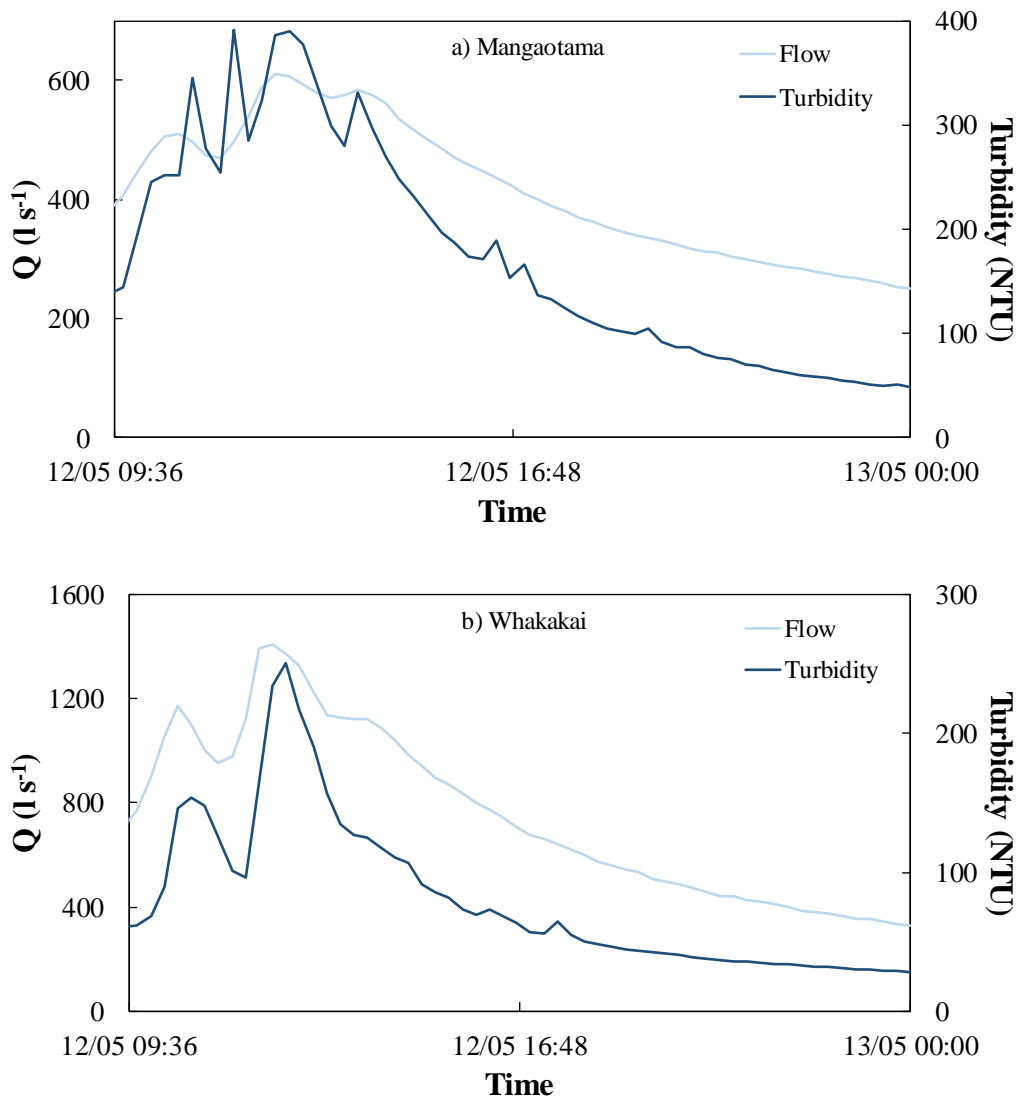


Figure 5.19. Close up view of the second peak of the storm event on 12 May 2017 in Mangaotama (a) and Whakakai (b). N.B. The graphs are not plotted on the same y-axis scale (Q and turbidity) and have instead been exaggerated to showcase the Q and turbidity peaks in both catchments.

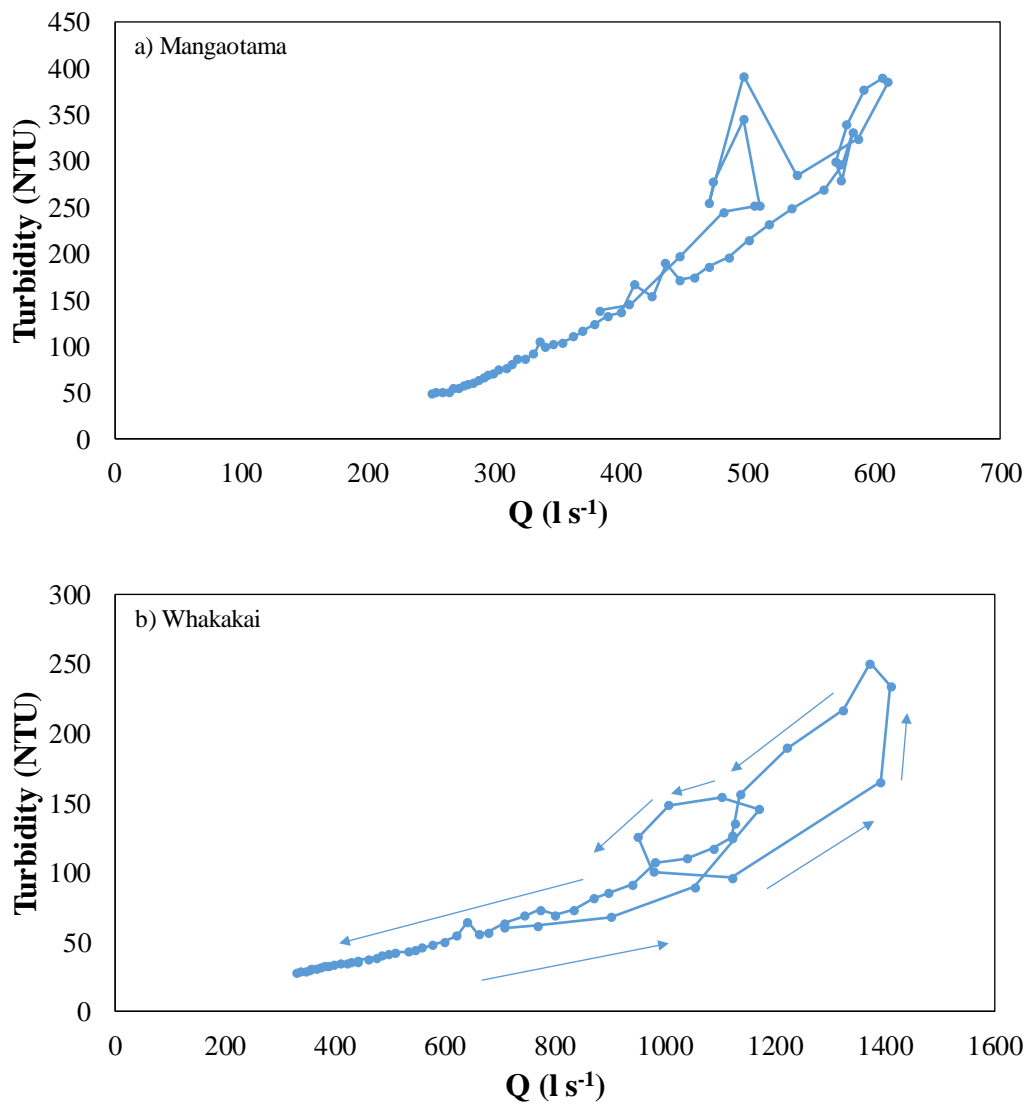


Figure 5.20. Hysteresis graphs for the second peak of the storm event on 12 May 2017 in the Mangaotama (a) and Whakakai (b) catchments. N.B. The hysteresis graph scales are not equal and have instead been exaggerated to showcase the hysteresis in each catchment.

June 23

The June 23 event had a greater Q in the Whakakai catchment ($1,399 \text{ l s}^{-1}$) than the Mangaotama catchment (470 l s^{-1}). However, the turbidity peak in the Mangaotama (689 NTU) was greater, than the Whakakai catchment (571 NTU) (Figure 5.21). The Mangaotama catchment showed an early peak in turbidity before Q, while the Whakakai showed the opposite, with turbidity peaking behind Q (Figure 5.22). A weak clockwise hysteresis was exhibited in the Mangotama catchment, while the Whakakai catchment had a moderate anti-clockwise hysteresis (Figure 5.23).

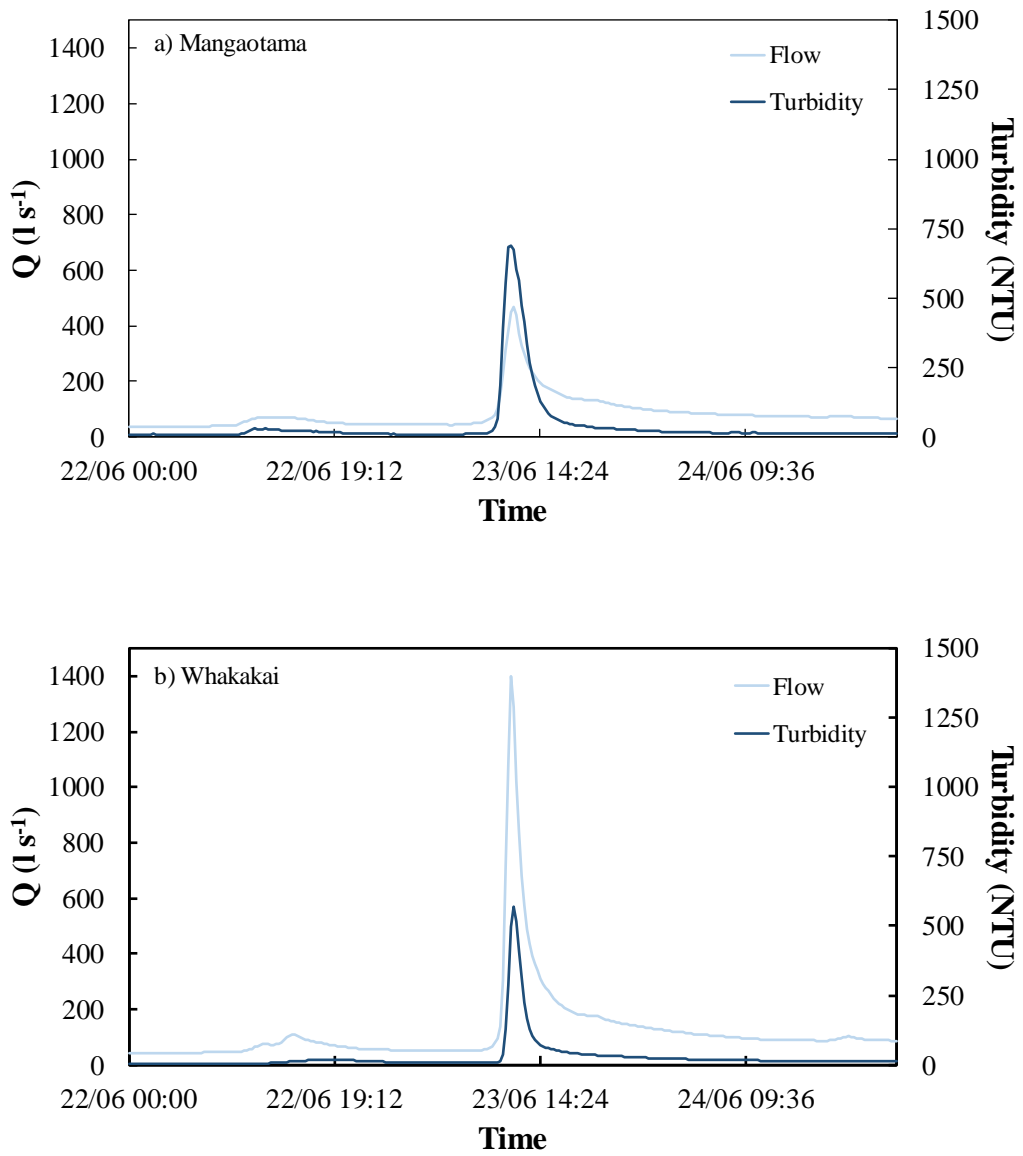


Figure 5.21. Flow (Q) and turbidity data from the storm event on 23 June 2017 in the Mangaotama (a) and Whakakai (b) catchments.

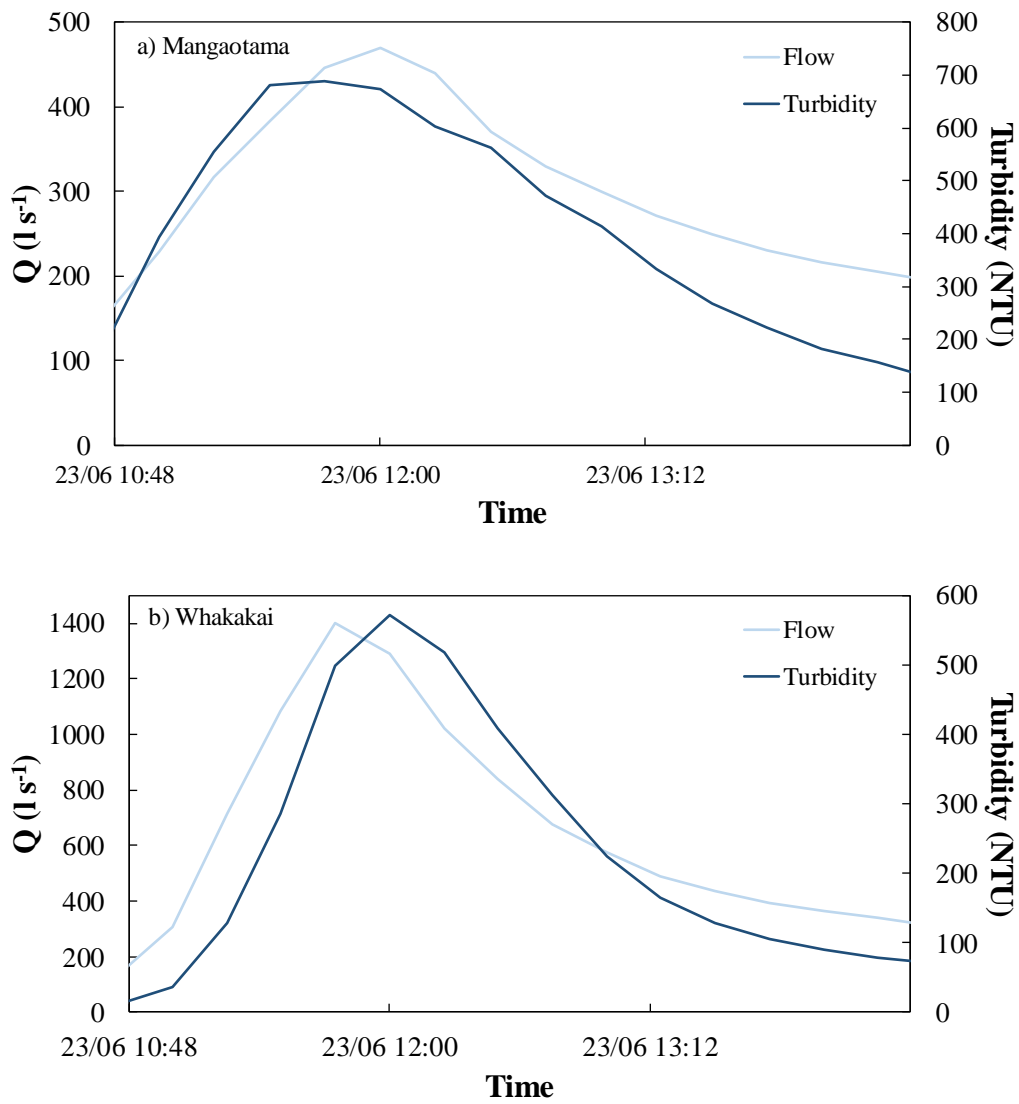


Figure 5.22. Close-up view of the storm event on 23 June 2017 in Mangaotama (a) and Whakakai (b). N.B. The graphs are not plotted on the same y-axis scale (Q and turbidity) and have instead been exaggerated to showcase the Q and turbidity peaks in both catchments.

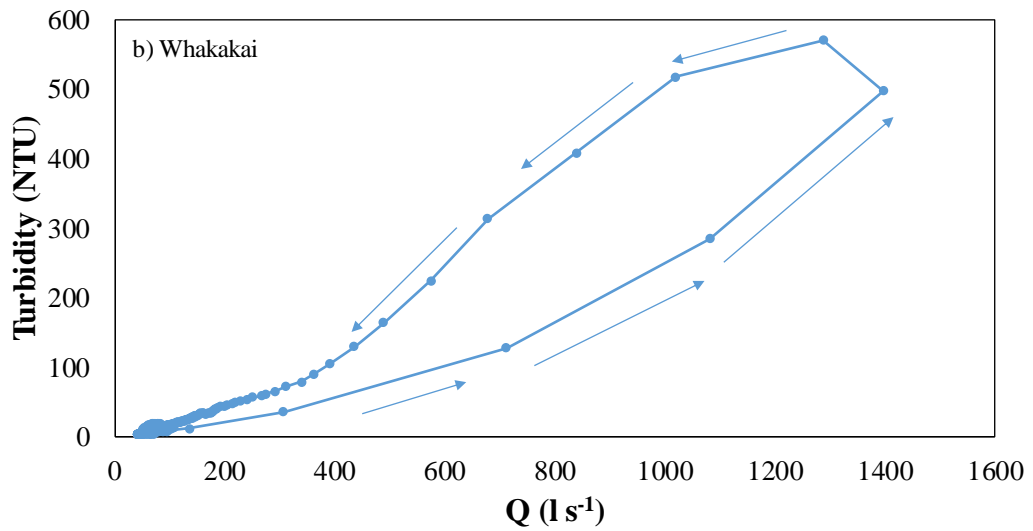
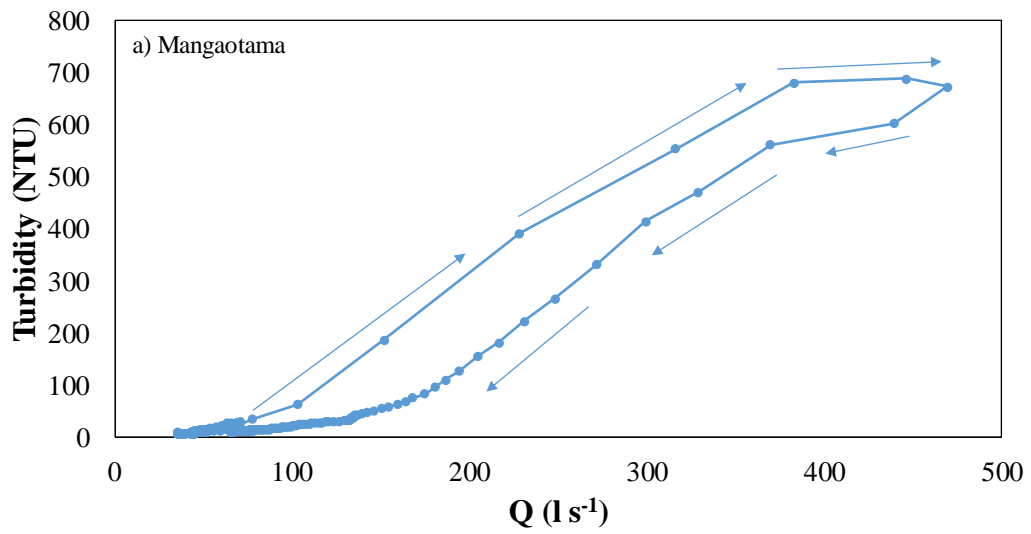


Figure 5.23. Hysteresis graphs for the storm event on 23 June 2017 in the Mangaotama (a) and Whakakai (b) catchments. N.B. The hysteresis graph scales are not equal and have instead been exaggerated to showcase the hysteresis in each catchment.

5.4 Discussion

5.4.1 Discharge

Discharge in the Whakakai catchment was greater in all flow events than the Mangaotama catchment. Hughes *et al.* (2012) also found the Whakakai catchment to have a consistently higher discharge over the course of their 10-year study. Greater amounts of rainfall could be entering the Whakakai as compared to Mangaotama, due to the proximity of the Whakakai catchment to the Hakarimata ranges, and therefore more influenced by the prevailing rainfall coming from the west. Steeper slopes and higher elevations in the Whakakai catchment could also be a factor (Griffiths & McSaveney, 1983). Discharge differences between both catchments were attributed by Hughes *et al.*, 2012 to physiographic factors such as elevation, slope and catchment shape. (Whakakai: mean slope = 23.8°; mean elevation = 169 m; Mangaotama: mean slope = 22.5°; mean elevation = 150m) (Hughes *et al.*, 2012).

The differences in catchment shape could also be a factor in discharge differences, where the Whakakai catchment is more circular in shape as opposed to the more elongated shape of the Mangaotama catchment. To assess how circular a catchment is a calculation is performed called the circularity ratio (catchment area/area of a circle with the same perimeter), where a perfect circle has a circularity ratio of 1 (Miller, 1953). The Whakakai catchment was found to be rounder (circularity ratio: 0.57), than Mangaotama catchment (circularity ratio: 0.41). The elongated shape of the Mangaotama catchment could mean that the Q peaks within the catchment would be longer due to inputs from tributaries and that Q would have to travel further to the outlet (Hughes *et al.*, 2012).

In comparing the turbidity and Q peaks between the Mangaotama catchment and Whakakai catchment, it was clear that Mangaotama catchment showed early peaking of turbidity before Q while the Whakakai catchment mostly shows a lag in turbidity peak behind Q. The early peaking of turbidity before Q indicates that sediment is eroding from sources near the stream and that source has depleted rapidly (Seeger *et al.*, 2004), while turbidity lag behind Q is indicative of sources of erosion further away from the stream (Lefrançois *et al.*, 2007).

Some events in this study showed both early and late peaking of turbidity, during double peak events. For example, the first event on April 5, showing early turbidity peaking in the Mangaotama catchment and then lagging turbidity peaking in the second peak flow. These changes in turbidity peaks indicate that during the first event channel sources of erosion were contributed most to the sediment in the stream. Streamflow may have eroded all the soil from the near channel sources (depleting sediment sources), therefore sediment sources needed to enter from further away from the channel, hence the lag (Hughes *et al.*, 2012).

5.4.2 Hysteresis

Clockwise hysteresis seemed to be exhibited mostly in the Mangaotama catchment while anti-clockwise hysteresis was observed mostly in the Whakakai catchment in this study. Hughes *et al.* (2012) also found that over their 10-year study period analysing 17 flood events, 100% of those events showed clockwise hysteresis in the Mangaotama catchment, and 67% of those events showed anti-clockwise hysteresis in the Whakakai. Hysteresis relationships can be complex, however in general clockwise hysteresis has been attributed to near channel source erosion (Williams, 1989), anti-clockwise hysteresis has been attributed to sources further away from the channel (Klein, 1984) and double peak events (exhibiting figure eight loop) have been attributed to a switch in sources of sediment (Williams, 1989). Seasonal changes can also affect dominant hysteresis patterns, for example, Oeurng *et al.* (2010) found that clockwise hysteresis was dominant in late winter and mid-autumn, while anti-clockwise hysteresis was dominant in late autumn and spring.

Despite anti-clockwise hysteresis being attributed to sources further away from the channel in the literature (Klein, 1984), it is possible that in the case of this study, anti-clockwise hysteresis could be attributed to sources of sediment near the channel (stream bank erosion), in the steeper upper part of the Whakakai catchment. The rounder shape of the Whakakai catchment (circularity ratio = 0.57), as compared to the Mangaotama catchment (circularity ratio = 0.41) would mean there would be a transit time between the erosion of the stream banks to entering the channel, and sediment being recorded at the catchment outlet.

The time lag for anti-clockwise hysteresis events, was only 15 minutes (three events) and 45 minutes for (one event) between peak Q and peak turbidity, further supporting the hypothesis that stream bank erosion in the upper part of the catchment could be responsible for the anti-clockwise hysteresis.

5.4.3 Turbidity

Measured turbidity values were greater in the Mangaotama catchment (flow events ranged from 237 NTU, 779 NTU, 689 NTU and 3,402 NTU) for four events and greater in the Whakakai catchment (flow events 1,293 NTU and 1,493 NTU) for two events (two of the largest flood events analysed). Turbidity differences between the two catchments were attributed to seasonal differences and the possible times between the previous events. For example, stream bank soils that were saturated from previous flood events would be more easily erodible than stream banks that were dry. Hughes *et al.* (2012) found that the annual specific yield in the Mangaotama catchment (55 to 157 t km⁻²) was always greater than the specific annual yield in the Whakakai catchment (32 to 100 t km⁻²) between the years 1999 to 2010. The higher specific annual yield in the Mangaotama catchment would align with generally higher turbidity found in the Mangaotama catchment in this study. The higher turbidity in the Whakakai catchment could be attributed to large stream bank collapse events, hillslope events or mass movement events quickly contributing large amounts of sediment to the stream.

5.5 Summary and conclusions

- Simultaneously continuously recorded (NIWA) streamflow (Q) and turbidity data were recorded in the Mangaotama and Whakakai catchments, were analysed for the year 2017.
- The base flow was around 20 l s⁻¹ in the Mangaotama catchment and around 30 l s⁻¹ in the Whakakai catchment.
- Six flood events from the 2017 data were selected in both catchments, three larger events and three smaller events (Mangaotama: Q between 127 l s⁻¹ to 606 l s⁻¹, Whakakai: Q between 219 l s⁻¹ and 1398 l s⁻¹), where Q and turbidity data relationships were analysed.

- Peak flow was greater in the Whakakai catchment (flow events ranged from 219 l s^{-1} to $5,982 \text{ l s}^{-1}$) than the Mangaotama catchment (flow events ranged from 126 l s^{-1} to $2,689 \text{ l s}^{-1}$) for all six events. The greater peak flow in the Whakakai catchment was potentially due to the catchments proximity to the Hakarimata ranges, and therefore more influenced by the prevailing rainfall from the west. Other explanations could relate to physiographic differences, such as elevation and catchment shape. For example, rainfall would reach the Whakakai stream faster due to its more circular shape (circularity ratio = 0.57), compared to the more elongated Mangaotama catchment (circularity ratio = 0.41) (Hughes *et al.*, 2012).
- Measured turbidity values were greater in the Mangaotama catchment (flow events ranged from 237 NTU, 779 NTU, 689 NTU and 3,402 NTU) for four events and greater in the Whakakai catchment (flow events 1,293 NTU and 1,435 NTU) for two events (two of the largest flood events analysed). The generally higher turbidity in the Mangaotama was also found by Hughes *et al.* (2012). The two events that had higher turbidity in the Whakakai catchment could have been from a bank collapse events (chapter three) contributing sediment to the stream.
- Clockwise hysteresis in the turbidity-Q relationship dominates the Mangaotama catchment, indicating sources of erosion in this catchment are derived from near the stream. Anti-clockwise hysteresis dominates the Whakakai catchment indicating sources of erosion further away from the stream. This study suggests that the anti-clockwise hysteresis is indicative of sediment derived stream bank erosion in the upper reaches of the catchment.
- Data analysis of 2017 flood events from this study were consistent with the findings of Hughes *et al.* (2012) who carried out a similar analysis on data from the same sites between 1999 and 2010.

Chapter 6

Summary, Discussion and Conclusions

6.1 Introduction

The overall aim of this thesis was to identify the contribution of various sources of sediment in the Mangaotama (pastoral and pine catchment) and Whakakai (indigenous forest) catchments. The hypothesis for this research was that stream bank erosion would be the dominant source of sediment in the pastoral catchment and hillslope erosion would be the dominant source of erosion in the native forest catchment. Three research objectives were investigated and the main findings are summarised below.

6.2 Summary of the research and main findings

6.2.1 Objective 1: Catchment surveys (Chapter 3)

Objective one was to identify the similarities and differences between the Mangaotama and Whakakai catchments by conducting catchment surveys. The Riparian Management Classification (RMC) (Quinn, 2009a, 2009b), survey method was used to describe and characterise stream and riparian margins. The RMC had criteria such as stream bank stability (erosion processes), land use (general and riparian) and stream widths (channel, water bank full) (Quinn, 2009a, 2009b).

- The RMC was carried out in the Mangaotama and Whakakai catchments in September and October 2018 and January 2019.
- The total survey length in the Mangaotama catchment was 1.3 km (starting 200m upstream of the NIWA hydrometric site), which was divided into 26 reaches (14 under pastoral land use; 12 under pine land use) with an average length of 48m.
- The total survey length in the Whakakai catchment was 0.9km (starting from the NIWA hydrometric site), which was divided into 16 reaches, with an average length of 58m.

- Reaches were determined by changes in stream characteristics such as water width, bank heights (e.g. high to low), bank erosion processes and vegetation.
- One RMC field form was completed for each reach, and where applicable measurements (e.g. bank heights, stream widths) and stream shade (abundance of light over the stream) were estimated by the author.

Key findings

- Stream banks over the total survey length were predominantly stable in the pastoral section of the Mangaotama catchment (left: 64%, right: 65%) and stock damage was most dominant erosion source (left: 23%, right: 19%).
- Stream banks over the total survey length were predominantly stable in the pine section of the Mangaotama catchment (left: 91%, right: 85%), with undercut being the main source of erosion (left: 9%, right 13%).
- Stream banks over the total survey length were predominantly stable in the Whakakai catchment (left: 84%, right: 86%), with undercut being the main erosion source (left: 15% and right: 13%). Stream bank undercutting eventually led to occasional bank collapse events resulting in quite large trees falling into the observed stream.
- Catchment management practices such as planted poplars, strong pasture cover and bridges for stock crossings, contributed to stream bank stability within the pastoral section. The stability of the pine section was attributed to the lack of cattle access in that area, and the Whakakai stream banks were stable due to most of the stream banks being bedrock and the lack of stock access.
- Mean channel widths were narrower in the pastoral (mean: 2m, std: 0.5m) and pine sections (mean: 2m, std: 0.4m) of the Mangaotama catchment, than the Whakakai catchment (mean 4m, std: 1m). Narrower stream widths in the pastoral catchment were attributed to infall from past mass movement in the catchment and other sources of transported (deposited sediment). While wider channel widths in the Whakakai catchment could be due to the shading from trees inhibiting the growth of protective continuous vegetation such as long grass.

- There was little evidence of current mass movement events in either catchment. The pastoral section of the Mangaotama showed buried fencing materials exposed on the bank and cutting through the past in-fill material.
- Future research could re-survey the Mangaotama and Whakakai catchments to compare stream bank erosion over time.

6.2.2 Objective 2: Terrestrial photogrammetry (Chapter 3)

Objective two was to investigate the potential of using terrestrial photogrammetry to monitor stream bank erosion over time. To meet objective two, a photo-based 3D model baseline was established for actively eroding stream banks in the Mangaotama and Whakakai catchments.

- Two bank erosion sites were selected in the Whakakai catchment, and four bank erosion sites (three in pine plantation and one in pasture) were selected in the Mangaotama catchment.
- Between 24 and 126 photographs (using a digital camera) were taken of eroding stream banks in the Whakakai catchment on September 20 2018, and in the Mangaotama catchment on September 29 2018.
- The photographs were then imported into the photogrammetry software Pix4D (Pix4D, 2017) and the 3D models of the stream banks were created.

Key findings

- The five successful models (one in the Whakakai catchment, and four in the Mangaotama catchment) show that terrestrial photogrammetry is potentially an effective, simple, and cost effective tool to monitor stream bank erosion over time. A baseline was established which could be re-surveyed though its recommended that further baseline sites be established to provide improved rigour.
- One attempt in the Whakakai catchment failed to have sufficient overlap in the photographs. It is crucial to take the photographs in a way where common landmarks are noticeable for the photogrammetry software to be successful at creating a 3D model (Pix4D, 2017).
- Future research could test the accuracy of the 3D modelling technique by comparing results with a more traditional method of determining stream bank erosion rates (e.g. erosion pins).

6.3 Objective 3: Sources of sediment (Chapter 3, 4 & 5)

Objective three was to identify the dominant source of sediment within the Mangaotama and Whakakai catchments. Two methods, following the characterisation survey (chapter three) were used:

- Sediment fingerprinting using radionuclides (chapter four)
- The analysis of long-term turbidity and discharge relationships (chapter five)

The two methods and key findings are discussed below.

6.3.1 Sediment fingerprinting (Chapter 4)

Sediment fingerprinting using the concentrations radionuclides (^{137}Cs , $^{210}\text{Pb}_{\text{ex}}$, ^{228}Ra and ^{226}Ra) were used to determine the relative contribution of erosion sources to stream sediment in the Mangaotama and Whakakakai catchments.

- Five stream bank and five hillslope sites were sampled were in the Mangaotama and Whakakai catchments on May and June 2018.
- At each stream bank site, soil samples were collected from five equal intervals on the exposed banks, mixed in a bucket to create a composite sample and a sub-sample was taken back to the laboratory.
- At each hillslope site, at least seven soil samples were collected using a soil auger, in a straight or semi-straight transect from the bottom to the top, and more soil samples were taken at the top of the hill. Soil samples from each hillslope site were mixed in a bucket to create a composite sample, and a sub-sample was taken back to the laboratory.
- Suspended sediment samples were collected from both catchment outlets using a “Phillips sampler” (Phillips *et al.*, 2000). Samplers were in operation in the Mangaotama catchment from April 12 2018 to September 20 2018, and the samplers in the Whakakai catchment were in operation from July 13 2018 to September 20 2018.
- Stream bank/hillslope soil samples and the suspended sediment samples were wet sieved to $<63\mu\text{m}$, dried at 60°C for 5 to 7 days, then further sieved to $<500\mu\text{m}$ and sent to the Institute of Environmental Science and Research for gamma spectrometry analysis.

- A numerical mixing model was used to determine the relative contribution of stream banks and hillslopes to suspended sediment, and student t-tests and Man-Whitney tests were used for statistical analysis.

Key findings

- The concentrations of all radionuclides were higher in the hillslopes ($P < 0.001$) ((mean ^{137}Cs : 5.8 Bq kg⁻¹, std: 2.4 Bq kg⁻¹); (mean $^{210}\text{Pb}_{\text{ex}}$: 32.5 Bq kg⁻¹, std: 16.0 Bq kg⁻¹); (mean ^{226}Ra : 24.9 Bq kg⁻¹, std: 2.1 Bq kg⁻¹); (mean ^{228}Ra : 35.3 Bq kg⁻¹, std: 4.0 Bq kg⁻¹)) of both the Mangaotama and Whakakai catchments than in the streambanks ((mean ^{137}Cs : 0.9 Bq kg⁻¹, std: 0.3 Bq kg⁻¹); (mean $^{210}\text{Pb}_{\text{ex}}$: 8.4 Bq kg⁻¹, std: 4.6 Bq kg⁻¹); (mean ^{226}Ra : 28.8 Bq kg⁻¹, std: 1.7 Bq kg⁻¹)), clearly distinguishing both sources of sediment.
- A numerical mixing model identified that the suspended sediment from both the Mangaotama and Whakakai catchments were predominantly derived from stream bank erosion (90%) with a smaller portion of sediment derived from hillslope erosion (10%).
- Recommendations for future work are to take more suspended sediment samples, ideally after every major storm event; sort and analyse the suspended sediment samples by particle size, and to possibly disaggregate the suspended sediment samples before sieving.

6.3.2 Turbidity and discharge data (Chapter 5)

Past studies have used discharge (Q) and turbidity (as a proxy for suspended sediment concentration) data to determine sources of sediment with a catchment (Hughes *et al.*, 2012). Long-term NIWA water quality monitoring sites are located in the lower end of both the Mangaotama (NIWA site PW5) and Whakakai (NIWA site NW5) catchments. Discharge (from stage height data) has been recorded in the Whakakai catchment since 1994 and in the Mangaotama catchment since 1992. Continuous turbidity data has been recorded in both catchments since 1998. Discharge and turbidity data have both been recording at 15-min intervals. Calculations have also been made by NIWA to convert turbidity to suspended sediment concentration. Hughes *et al.* (2012) analysed Q and suspended sediment

data (converted from turbidity data) from seventeen flood events between 1999 and 2010.

- NIWA Q and turbidity data recorded in the Mangaotama and Whakakai catchments, were analysed for the year 2017. In the Mangaotama catchment, Q and turbidity data spanned from 1 January to 31 December 2017 with no major gaps. In the Whakakai catchment, Q data ranged from 1 January to 14 November 2017 and turbidity data ranged from 1 January to 4 September 2017 with 16 days of missing data in July 2017.
- The base flow was around 20 l s^{-1} in the Mangaotama catchment and around 30 l s^{-1} in the Whakakai catchment.
- During 2017, there were five flood events with $Q > 500 \text{ l s}^{-1}$ in the Mangaotama catchment and eighteen flood events with $Q > 500 \text{ l s}^{-1}$ in the Whakakai catchment. Additionally, there were two flood events with $Q > 1,000 \text{ l s}^{-1}$ in the Mangaotama catchment and eleven flood events with $Q > 1,000 \text{ l s}^{-1}$ in the Whakakai catchment.
- Six flood events from the 2017 data were selected in both catchments, three larger events and three smaller events (Mangaotama: Q between 127 l s^{-1} to 606 l s^{-1} , Whakakai: Q between 219 l s^{-1} and 1398 l s^{-1}), where Q and turbidity data relationships were analysed.

Key findings

- Peak flow was greater in the Whakakai catchment (flow events ranged from 219 l s^{-1} to $5,982 \text{ l s}^{-1}$) than the Mangaotama catchment (flow events ranged from 126 l s^{-1} to $2,689 \text{ l s}^{-1}$) for all six events. The greater peak flow in the Whakakai catchment was potentially due to the catchments proximity to the Hakarimata ranges, and therefore more influenced by the prevailing rainfall from the west. Other explanations could relate to physiographic differences, such as elevation and catchment shape. For example, rainfall would reach the Whakakai stream faster due to its more circular shape (circularity ratio = 0.57), compared to the more elongated Mangaotama catchment (circularity ratio = 0.41) (Hughes *et al.*, 2012).
- Measured turbidity values were greater in the Mangaotama catchment for four events (ranging from 237 NTU to 3,402 NTU) and greater in the Whakakai catchment for two events (1,293 NTU and 1,435 NTU) (two of the largest flood events analysed). Turbidity variations within the two

catchments were attributed to seasonal differences, and the possible time between the previous events. For example, stream bank soils that were saturated from previous flood events may be more easily erodable than stream banks that were dry. Hughes *et al.* (2012) found that the annual specific yield in the Mangaotama catchment (55 to 157 t/km²) was always greater than the specific annual yield in the Whakakai catchment (32 to 100 t/km²) between the years 1999 to 2010. The higher specific annual yield in the Mangaotama catchment would align with the more frequent higher turbidity found in the Mangaotama catchment in this study. The two larger events where turbidity was higher in the Whakakai catchment could be due to stream bank collapse events contributing large amounts of sediment to the stream.

- The flood events in the Mangaotama catchment showed predominantly clockwise hysteresis (5 out of 6 events), where the time between the turbidity peak and the Q peak ranged from 30 minutes to 2 hours 45 minutes.
- The flood events in the Whakakai catchment showed predominantly anti-clockwise hysteresis (5 out of 6 events), where the time between the Q peak and the turbidity peak was mainly 15 minutes (four events), there was one event with 45 minute time lag between peak Q and peak turbidity.
- There were also double peak flood events in the Mangaotama catchment (3 out of 6 events) and in the Whakakai catchment (2 out of 6 events).
- Clockwise hysteresis in the Q-turbidity relationship has been attributed to sediment sources near the channel (Williams, 1989) while anti-clockwise hysteresis in the Q-turbidity relationship has been attributed to further away from the channel (Klein, 1984). Hughes *et al.* (2012) found similar results to this study, where the Mangaotama catchment primarily showed clockwise hysteresis (100% of events) and the Whakakai catchment was mostly showed anti-clockwise hysteresis (67% of events). Hughes *et al.* (2012) theorised that the Mangaotama catchment was dominated by stream bank erosion while the Whakakai catchment was dominated by hillslope erosion.
- The conclusions from this study are similar to Hughes *et al.* (2012), in that the dominance of clockwise hysteresis in the Mangaotama catchment is indicative of the importance of stream bank erosion. Anti-clockwise hysteresis dominates the events within the Whakakai catchment, indicating

more distant sediment sources. This study suggests that the anti-clockwise hysteresis is indicative of sediment derived stream bank erosion in the upper reaches of the catchment. Stream bank erosion in the upper catchment (and upper tributaries) would take longer to reach the monitoring station due to the rounder catchment shape and would be a reasonable explanation for the anti-clockwise hysteresis, as the time lag between peak Q and turbidity was only 15 minutes for most events (4 out of 6 events).

- Future research could calculate suspended sediment concentrations from each event, and possibly analyse hysteresis relationships for every flood event.

6.4 Discussion

6.4.1 Main findings

The evidence attained from the catchment surveys, sediment fingerprinting and turbidity-Q data, all suggest that the main sources of sediment in both the Mangaotama and Whakakai catchments, was stream bank erosion. The sediment fingerprinting results identified that the suspended sediment from both catchments was predominantly from stream bank erosion (90%), with a smaller portion from hillslope erosion (10%). The catchment surveys further supported the sediment fingerprinting, as stream bank erosion was observed in the Mangaotama pasture (stock damage: left: 23%, right: 19%) and pine (stream bank undercut: left: 9%, right 13%) and Whakakai catchment (stream bank undercut: left: 15% and right: 13%). There was no hillslope erosion observed during the surveys that was directly contributing sediment to the stream. However, there was a small mass movement event observed before the surveys in the Whakakai catchment. One small hillslope erosion event was observed in the Mangaotama catchment surveys, but that event was not contributing sediment directly to the stream.

The turbidity-Q data revealed that the Mangaotama catchment generally showed clockwise hysteresis (5 out of 6 events), further supporting the evidence that stream bank erosion was the dominant source of sediment in the Mangaotama catchment. The turbidity-Q data for the Whakakai catchment, generally showed anti-clockwise hysteresis (4 out 6 events), indicating sources of sediment further way from the catchment, inferred as hillslope erosion in the previous literature (Klein, 1984).

However, the generally short time frame (15 minutes) between peak Q and peak turbidity during the flood events suggest, that sediment could be eroding from stream banks in the steep tributaries of the upper headwaters of the Whakakai catchment (beyond the survey reach).

6.4.2 Hypothesis

Thus, the original hypothesis for this research, that stream bank erosion would dominate the Mangaotama (pasture) catchment, and hillslope erosion would dominate the Whakakai (native) catchment, is rejected in part.

Stream banks were identified as the dominant source of erosion in the Mangaotama catchment both in this study and in Hughes *et al.* (2012) where the erosion was attributed to stream bank damage from cattle trampling. However, unlike previous studies (Hughes *et al.*, 2012) this study concluded that stream bank erosion was the dominant source of sediment in the Whakakai catchment. While the common perception is that stream banks are more stable in the native areas this was not what was observed in this study.

At the time of this study, the most recent large rainfall event that resulted in widespread mass wasting was in 2007 (Quinn & Basher, 2007). Therefore it is unlikely that there are any significant unstable mass wasted areas delivering sediment to the Mangaotama and Whakakai streams. Older landslides are visible in the Mangaotama catchment but are vegetated and stable, and do not appear to be a major source of sediment to the streams. However, past landslides in the Mangaotama catchment, have been the largest contributors of sediment to the Mangaotama stream (De Rose, 1998). It is highly likely that large past mass movement and hillslope erosion events occurred in the Whakakai catchment as well. Forested catchments in New Zealand are generally found on steep slopes with higher elevations (Davies-Colley, 1997; Basher, 2013) and are therefore more prone to landslides (Basher, 2013). The minimal evidence observed in this study for current hillslope erosion or mass movement events in the Whakakai catchment may suggest a divergence from a mass movement dominated catchment, towards a stream bank erosion dominated catchment, and therefore a new equilibrium within the Whakakai catchment.

6.4.3 Implications of this study

In this study, both the native catchment (Whakakai) and the pasture catchment (Mangaotama) were both dominant in stream bank erosion. There were also two large flood events, where turbidity was higher (1,293 NTU and 1,435 NTU) in the native catchment compared to the pasture catchment (1,274 NTU and 991 NTU). The dominance of stream bank erosion in the native catchment and its higher turbidity in two events, compared to the pasture catchment, highlighted the already natural baseline of erosion from stream banks, and associated natural generation of sediment.

Stream banks are a naturally dynamic geomorphic process (Florsheim *et al.*, 2008) and water tends to erode stream banks particularly on bends, and deposit sediment on the inside of bends, striving towards reaching an equilibrium (Davies-Colley *et al.*, 2018). The generation of sediment is a natural process (Florsheim *et al.*, 2008), and some rivers have a naturally high turbidity (Davies-Colley & Bellantine, 2010). The generation of sediment through stream bank erosion can also benefit aspects of fluvial systems and their associated ecology (Florsheim *et al.*, 2008). However, current catchment management practices tend to view stream bank erosion as problem from a human value perspective (e.g. properties) and at times attempt to control stream bank erosion with hard structures (e.g. rip rap and concrete lined channel). Hard structures to control bank erosion can be detrimental to stream ecology (Florsheim *et al.*, 2008).

Thus, catchment management should not be expected to prevent all stream bank erosion, but merely focus on mitigating accelerated erosion, particularly in pastoral catchments. In this study and in Trimble and Mendel (1995), stock damage to stream banks has been identified as a major driver of sediment in pastoral catchments. Therefore, stock damage should be limited where possible in pasture catchment, to reduce accelerated erosion. Hughes (2016) also found that the removal of livestock from riparian areas was the most commonly reported reason for reduced stream bank erosion, in catchments where riparian management has taken place.

This study supports findings in Florsheim *et al.* (2008), where catchment management should differentiate between the natural dynamics of stream banks and accelerated stream bank erosion from human activities and land use, and plan catchment management accordingly. Together the combination of mitigating accelerated erosion and allowing some natural stream bank erosion to support stream ecology is the most sustainable method for catchments.

6.5 Limitations of this study

- Only one suspended sediment sample was used for sediment fingerprinting.
- Lack of opportunity to repeat photographs for a pilot study. The terrestrial photogrammetry method would have been improved with better markers and more photographs from different locations.
- The length of the stream covered in the catchment surveys lacked headwater and lowland flood plains.

6.6 Recommendations for future work

- Further baseline sites of actively eroding streams in the Mangaotama and Whakakai catchments could be established for future 3D monitoring.
- Further suspended sediment samples could be collected from both catchments to determine whether results are representative of the long-term picture and whether sources change through time (e.g. by season, event size etc).

6.7 Conclusions

- Overall stream bank erosion was the greatest contributor (90%) to sediment in both the Mangaotama and Whakakai catchment, with the remaining 10% of the stream sediment in both catchments being derived from hillslope erosion.
- The hypothesis for this research, that stream bank erosion would be the dominant source of sediment in a pastoral catchment (Mangaotama) and hillslope erosion would be the dominant source of erosion in a native forest catchment (Whakakai) was **rejected** in part, as both catchments were

dominated by stream bank erosion. Stream bank erosion dominating the Whakakai catchment was attributed to the lack of major flood rainfall events to induce hillslope erosion. The minimal evidence observed in this study for current hillslope erosion or mass movement events in the Whakakai catchment may suggest a divergence from a mass movement dominated catchment, towards a stream bank erosion dominated catchment, and therefore a new equilibrium within the native catchment.

- Sediment fingerprinting using ^{137}Cs , $^{210}\text{Pb}_{\text{ex}}$, ^{226}Ra and ^{228}Ra radionuclides (chapter four), was able to clearly distinguish between hillslope and stream bank erosion sources of sediment. Radionuclides were higher ($P < 0.001$) in the hillslopes ((mean ^{137}Cs : 5.8 Bq kg^{-1} , std: 2.4 Bq kg^{-1}); (mean $^{210}\text{Pb}_{\text{ex}}$: 32.5 Bq kg^{-1} , std: 16.0 Bq kg^{-1}); (mean ^{226}Ra : 24.9 Bq kg^{-1} , std: 2.1 Bq kg^{-1}); (mean ^{228}Ra : 35.3 Bq kg^{-1} , std: 4.0 Bq kg^{-1})) of both the Mangaotama and Whakakai catchments than in the streambanks ((mean ^{137}Cs : 0.9 Bq kg^{-1} , std: 0.3 Bq kg^{-1}); (mean $^{210}\text{Pb}_{\text{ex}}$: 8.4 Bq kg^{-1} , std: 4.6 Bq kg^{-1}); (mean ^{226}Ra : 28.8 Bq kg^{-1} , std: 1.7 Bq kg^{-1}); (mean ^{228}Ra : 47.2 Bq kg^{-1} , std: 2.2 Bq kg^{-1})). The numerical mixing model identified that stream bank erosion was the dominant source of sediment (90%) within both the Mangaotama and Whakakai catchments, while hillslopes contributed 10% to the sediment in both catchments.
- Catchment surveys (chapter three) showed that the stream banks in the Mangaotama catchment were primarily stable (pasture section (left: 64%, right: 65%); pine section (left: 91%, right: 85%)) and the Whakakai catchment was generally stable (left: 84%, right: 86%). Stock damage dominated the pastoral section of the Mangaotama catchment (left: 23%, right: 19%), and that stream bank undercutting dominated the pine section of the Mangaotama (left: 9%, right: 13%) and the Whakakai catchment (left: 15% and right: 13%). Catchment management practices (e.g. conservation planting, stock exclusion) contributed to the stability in the pastoral section of the Mangaotama, while in the pine section stability was attributed to lack of stock access. In the Whakakai catchment stability was also attributed to lack of stock access, as well as the dominance of bedrock stream banks.
- Simultaneous recorded continuous streamflow (Q) and turbidity data from 2017 (chapter five), showed that during flood events the Mangaotama catchment was dominated by clockwise hysteresis in the turbidity-Q

relationship (5 out of 6 events analysed), indicating that stream bank erosion was the dominant source of sediment. During flood events in the Whakakai catchment, the turbidity-Q relationship was dominated by anti-clockwise hysteresis (4 out of 6 events analysed). In this study, it is suggested that this is indicative of sediment derived from stream bank erosion in the upper headwater reaches of the Whakakai catchment.

- Terrestrial photogrammetry was tested in this study and is potentially an effective, simple and cost effective tool to monitor stream bank erosion over time. Further, a baseline was established which could be later re-surveyed, though it is recommended that further baseline sites be established to provide improved rigour.
- This study demonstrates that stream bank erosion is a natural process and can dominate the supply of sediment to river systems even in relatively unimpacted catchments. Catchment managers need to take this into account when considering catchment rehabilitation projects aimed at reducing the delivery of sediment to streams.

References

- Agisoft LLC. (2018). *Agisoft photoscan user manual: Professional edition, version 1.4*. Agisoft LLC.
- Anzecc, A. J. A., Environment, N. Z., Council, C., Agriculture, Australia, R. M. C. o., & New Zealand, C. (2000). Australian and New Zealand guidelines for fresh and marine water quality. 1-103.
- Barker, R., Dixon, L., & Hooke, J. (1997). Use of terrestrial photogrammetry for monitoring and measuring bank erosion. *Earth Surface Processes and Landforms*, 22(13), 1217-1227.
- Basher, L., & Matthews, K. (1993). Relationship between ¹³⁷Cs in some undisturbed New Zealand soils and rainfall. *Soil Research*, 31(5), 655-663.
- Basher, L. R. (2013). Erosion processes and their control in New Zealand. *Ecosystem services in New Zealand—conditions and trends, 2013*, 363-374.
- Basher, L. R., Hicks, D. M., Clapp, B., & Hewitt, T. (2011). Sediment yield response to large storm events and forest harvesting, Motueka River, New Zealand. *New Zealand Journal of Marine and Freshwater Research*, 45(3), 333-356.
- Best, E. (1922). *Some aspects of Maori myth and religion*. Wellington, New Zealand: Dominion museum.
- Bilotta, G., & Brazier, R. (2008). Understanding the influence of suspended solids on water quality and aquatic biota. *Water research*, 42(12), 2849-2861.
- Brierley, G. J., & Fryirs, K. A. (2013). *Geomorphology and river management: applications of the river styles framework*. John Wiley & Sons.
- Brown, A. J. E. S. P., & Landforms. (1985). The potential use of pollen in the identification of suspended sediment sources. *10*(1), 27-32.
- Caitcheon, G. G., Olley, J. M., Pantus, F., Hancock, G., & Leslie, C. (2012). The dominant erosion processes supplying fine sediment to three major rivers in tropical Australia, the Daly (NT), Mitchell (Qld) and Flinders (Qld) Rivers. *Geomorphology*, 151, 188-195.
- Campbell, B., Loughran, R., & Elliott, G. (1988). A method for determining sediment budgets using caesium-137. *Sediment Budgets. IAHS Publication*(174).
- Cawse, P. A., & Horrill, A. D. (1986). *A survey of caesium-137 and plutonium in British soils in 1977*. United Kingdom. 77p. http://inis.iaea.org/search/search.aspx?orig_q=RN:17064765; H.M. Stationery Office, London, price Pound 7.00.

- Charman, P. E. V., & Murphy, B. W. (2007). *Soils: Their properties and management*. (Third ed.). Melbourne, Australia: Oxford University Press.
- Collier, K., Cooper, A., Davies-Colley, R., Rutherford, J., Smith, C., & Williamson, R. (1995). Managing riparian zones. *A contribution to protecting New Zealand's rivers and streams*, 2.
- Collier, K. J. (1992). *Assessing river stability: use of the Pfankuch method*. Head Office, Department of Conservation.
- Collins, A., Naden, P., Sear, D., Jones, J., Foster, I. D., & Morrow, K. J. H. P. (2011). Sediment targets for informing river catchment management: international experience and prospects. *25*(13), 2112-2129.
- Costley, K. (2018). Phillip samplers in the Whakakai catchment washed downstream with a fallen tree fern.
- Davies-Colley, R., & Bellantini, D. (2010). *Suitability of New Zealand rivers for contact recreation: A pilot of application of water quality index to the national rivers water quality network (NRWQN)*. Hamilton, New Zealand: National Institute of Water & Atmospheric Research Ltd.
- Davies-Colley, R., Hicks, M., Hughes, A., Clapcott, J., Kelly, D., & Wagenhoff, A. (2015). *Fine sediment effects on freshwaters, and the relationship of environmental state to sediment load: A literature review*. Hamilton: National Institute of Water and Atmospheric Research Ltd.
- Davies-Colley, R. J. (1997). Stream channels are narrower in pasture than in forest. *New Zealand journal of marine and freshwater research*, *31*(5), 599-608.
- Davies-Colley, R. J., Ballantine, D. J., Elliott, S. H., Swales, A., Hughes, A. O., Gall, M. P. J. W. S., & Technology. (2014). Light attenuation—a more effective basis for the management of fine suspended sediment than mass concentration? , *69*(9), 1867-1874.
- Davies-Colley, R. J., Hughes, A. O., & Oviden, R. O. (2018). Channel widening of small streams following riparian planting- when will it happen? *Ka mua, ka muri, Looking back, looking forward. New Zealand Freshwater Sciences Conference, Nelson. 10-14 December 2018*.
- Davies - Colley, R. J., Nagels, J. W., Smith, R. A., Young, R. G., & Phillips, C. J. (2004). Water quality impact of a dairy cow herd crossing a stream. *New Zealand Journal of Marine and Freshwater Research*, *38*(4), 569-576.
- De Rose, R. C. (1998). Assessment of sediment storage and transfer rates along a 3rd order channel using ¹³⁷Cs. *Contract report to AgResearch Ltd, Hamilton*.
- Dodd, M. B., Thorrold, B. S., Quinn, J. M., Parminter, T. G., & Wedderburn, M. E. (2008). Improving the economic and environmental performance of a New Zealand hill country farm catchment: 1. Goal development and assessment of current performance. *New Zealand Journal of Agricultural Research*, *51*(2), 127-141.

- Douglas, G., Gray, C., Hart, B., & Beckett, R. J. G. e. C. A. (1995). A strontium isotopic investigation of the origin of suspended particulate matter (SPM) in the Murray-Darling River system, Australia. *59*(18), 3799-3815.
- Florsheim, J. L., Mount, J. F., & Chin, A. (2008). Bank erosion as a desirable attribute of rivers. *AIBS Bulletin*, *58*(6), 519-529.
- Gibbs, M. M. J. E., & Coasts. (2008). Identifying Source Soils in Contemporary Estuarine Sediments: A New Compound-Specific Isotope Method. *31*(2), 344-359.
- Glade, T. J. C. (2003). Landslide occurrence as a response to land use change: a review of evidence from New Zealand. *51*(3-4), 297-314.
- GNS Science. (2014). *1:250 000 Geological map of New Zealand (QMAP)*. from <http://data.gns.cri.nz/geology/>.
- Griffiths, G. A., & McSaveney, M. (1983). Distribution of mean annual precipitation across some stepland regions of New Zealand. *New Zealand journal of science*.
- Grimshaw, D. L., & Lewin, J. (1980). Source identification for suspended sediments. *Journal of Hydrology*, *47*(1-2), 151-162.
- Haddadchi, A., Olley, J., & Laceby, P. (2014). Accuracy of mixing models in predicting sediment source contributions. *Science of the Total Environment*, *497*, 139-152.
- Haddadchi, A., Ryder, D. S., Evrard, O., & Olley, J. (2013). Sediment fingerprinting in fluvial systems: review of tracers, sediment sources and mixing models. *International Journal of Sediment Research*, *28*(4), 560-578.
- Hamshaw, S. D., Bryce, T., Rizzo, D. M., O'Neil - Dunne, J., Frolik, J., & Dewoolkar, M. M. (2017). Quantifying streambank movement and topography using unmanned aircraft system photogrammetry with comparison to terrestrial laser scanning. *River Research and Applications*, *33*(8), 1354-1367.
- Harding, J., Clapcott, J., Quinn, J., Hayes, J., Joy, M., Storey, R., Greig, H., Hay, J., James, T., Beech, M., Ozane, R., Meredith, A., & Boothroyd, I. (2009). *Stream habitat assessment protocols for wadeable rivers and streams of New Zealand*. Christchurch, New Zealand: University of Canterbury.
- Haygarth, P. M., Bilotta, G. S., Bol, R., Brazier, R. E., Butler, P. J., Freer, J., Gimbert, L. J., Granger, S. J., Krueger, T., Macleod, C. J. A., Naden, P., Old, G., Quinton, J. N., Smith, B., & Worsfold, P. (2006). Processes affecting transfer of sediment and colloids, with associated phosphorus, from intensively farmed grasslands: an overview of key issues. *20*(20), 4407-4413.
- He, Q., & Owens, P. (1995). Determination of suspended sediment provenance using caesium-137, unsupported lead-210 and radium-226: a numerical mixing model approach. *Sediment and water quality in river catchments*, 207-227.

- Hicks, D. M., Shankar, U., McKerchar, A. I., Basher, L., Lynn, I., Page, M., & Jessen, M. (2011). Suspended sediment yields from New Zealand rivers. *Journal of Hydrology (New Zealand)*, 81-142.
- Hill, A. (1973). Erosion of river banks composed of glacial till near Belfast, Northern Ireland. *Zeitschrift für Geomorphologie*, 17(4), 428-442.
- Hill, R., & Kelly, J. (2002). *Regional riparian characteristics - 2002 survey manual*. Waikato Regional Council, Hamilton, New Zealand.
- Hughes, A. (2016). Riparian management and stream bank erosion in New Zealand. *New Zealand Journal of Marine and Freshwater Research*, 50(2), 277-290.
- Hughes, A., & Hoyle, J. (2014). *The importance of bank erosion as a source of suspended sediment within the Kopurererua catchment*. NIWAA, Hamilton, New Zealand.
- Hughes, A. O., Olley, J. M., Croke, J. C., & McKergow, L. A. J. G. (2009). Sediment source changes over the last 250 years in a dry-tropical catchment, central Queensland, Australia. *104(3-4)*, 262-275.
- Hughes, A. O., Quinn, J. M., & McKergow, L. A. (2012). Land use influences on suspended sediment yields and event sediment dynamics within two headwater catchments, Waikato, New Zealand. *New Zealand Journal of Marine and Freshwater Research*, 46(3), 315-333.
- Jackson, S. (2006). Compartmentalising Culture: the articulation and consideration of Indigenous values in water resource management. *Australian Geographer*, 37(1), 19-31.
- James, M., & Robson, S. J. J. o. G. R. E. S. (2012). Straightforward reconstruction of 3D surfaces and topography with a camera: Accuracy and geoscience application. *117(F3)*.
- Jones, H., Kimberley, M., Hill, R., & Borman, D. (2015). *Riparian characteristics of pastoral waterways in the Waikato region, 2002-2012*. Waikato Regional Council, Hamilton, New Zealand.
- Kemp, H. A. (1949). Soil Pollution in the Potomac River Basin. *Journal (American Water Works Association)*, 41(9), 792-796.
- Klaminder, J., Bindler, R., Emteryd, O., Appleby, P., & Grip, H. J. B. (2006). Estimating the Mean Residence Time of Lead in the Organic Horizon of Boreal Forest Soils using 210-lead, Stable Lead and a Soil Chronosequence. *78(1)*, 31-49.
- Klein, M. (1984). Anti clockwise hysteresis in suspended sediment concentration during individual storms: Holbeck Catchment; Yorkshire, England. *Catena*, 11(2-3), 251-257.
- Knighton, A. (1973). Riverbank erosion in relation to streamflow conditions, River Bollin-Dean, Cheshire. *East Midland Geographer*, 5(8), 416-426.
- Knighton, D. (2014). *Fluvial forms and processes: a new perspective*. Routledge.

- Lawler, D. (1995). The impact of scale on the processes of channel-side sediment supply: a conceptual model. *IAHS Publications-Series of Proceedings and Reports-Intern Assoc Hydrological Sciences*, 226, 175-186.
- Lawler, D., Couperthwaite, J., Bull, L., & Harris, N. (1997). Bank erosion events and processes in the Upper Severn basin. *Hydrology and Earth System Sciences Discussions*, 1(3), 523-534.
- Lawler, D. M. (1993). The measurement of river bank erosion and lateral channel change: a review. *Earth surface processes and landforms*, 18(9), 777-821.
- Lefrançois, J., Grimaldi, C., Gascuel - Odoux, C., & Gilliet, N. (2007). Suspended sediment and discharge relationships to identify bank degradation as a main sediment source on small agricultural catchments. *Hydrological Processes: An International Journal*, 21(21), 2923-2933.
- Livens, F. R., & Baxter, M. S. (1988). Chemical associations of artificial radionuclides in Cumbrian soils. *Journal of Environmental Radioactivity*, 7(1), 75-86.
- Livens, F. R., & Loveland, P. J. (1988). The influence of soil properties on the environmental mobility of caesium in Cumbria. 4(3), 69-75.
- Lomenick, T. F., & Tamura, T. (1965). Naturally Occurring Fixation of Cesium-137 on Sediments of Lacustrine Origin. 29(4), 383-387.
- Longmore, M. (1982). The caesium-137 dating technique and associated applications in Australia-a review. In *Archaeometry: an Australasian perspective*.
- Mabit, L., Benmansour, M., Abril, J., Walling, D., Meusbürger, K., Iurian, A., Bernard, C., Tarján, S., Owens, P., & Blake, W. (2014). Fallout ²¹⁰Pb as a soil and sediment tracer in catchment sediment budget investigations: a review. *Earth-science reviews*, 138, 335-351.
- Matthews, K. M. (1989). *Radioactive fallout in the South Pacific: a history Part 1: deposition in New Zealand*. New Zealand. 52p. http://inis.iaea.org/search/search.aspx?orig_q=RN:27031048; National Radiation Laboratory, P.O. Box 25-099, Christchurch, New Zealand. (ISSN 0111-753X).
- McKergow, L. A., Weaver, D. M., Prosser, I. P., Grayson, R. B., & Reed, A. E. (2003). Before and after riparian management: sediment and nutrient exports from a small agricultural catchment, Western Australia. *Journal of Hydrology*, 270(3), 253-272.
- McLaren, R. G., & Cameron, K. C. (1996). *Soil science sustainable production and environmental protection*. Auckland: Oxford Univ. Press.
- Miller, V. C. (1953). Quantitative geomorphic study of drainage basin characteristics in the Clinch Mountain area, Virginia and Tennessee. *Technical report (Columbia University. Department of Geology); no. 3*.

- Minella, J. P. G., Walling, D. E., & Merten, G. H. (2008). Combining sediment source tracing techniques with traditional monitoring to assess the impact of improved land management on catchment sediment yields. *Journal of Hydrology*, 348(3-4), 546-563.
- Montgomery, D. R. (1997). River management: What's best on the banks? *Nature*, 388(6640), 328.
- Mukundan, R., Walling, D. E., Gellis, A. C., Slattery, M. C., & Radcliffe, D. E. (2012). Sediment Source Fingerprinting: Transforming From a Research Tool to a Management Tool 1. *JAWRA - Journal of the American Water Resources Association*, 48(6), 1241-1257.
- Munsell, A. (1975). *Munsell soil colour charts*. Baltimore, Maryland (Vol. 21218).
- Nakamura, N. (2008). An 'Effective' Involvement of Indigenous People in Environmental Impact Assessment: the cultural impact assessment of the Saru River Region, Japan. *Australian Geographer*, 39(4), 427-444.
- Neale, M., W, Barnes, G., E, & McArdle, B. (2009). *A survey of the riparian characteristics of the Auckland region*. Auckland Regional Council, Auckland, New Zealand.
- Oeurng, C., Sauvage, S., & Sanchez-Perez, J. M. (2010). Dynamics of suspended sediment transport and yield in a large agricultural catchment, southwest France. *Earth Surface Processes and Landforms*, 35(11), 1289-1301.
- Olley, J., Brooks, A., Spencer, J., Pietsch, T., & Borombovits, D. (2013). Subsoil erosion dominates the supply of fine sediment to rivers draining into Princess Charlotte Bay, Australia. *Journal of environmental radioactivity*, 124, 121-129.
- Olley, J., & Caitcheon, G. (2000). Major element chemistry of sediments from the Darling-Barwon river and its tributaries: implications for sediment and phosphorus sources. *Hydrological Processes*, 14(7), 1159-1175.
- Olley, J., Caitcheon, G., Hancock, G. J., & Wallbrink, P. J. (2001). *Tracing and dating techniques for sediment and associated substances*. Canberra.
- Ongley, E. D. (1996). *Control of water pollution from agriculture*. Food & Agriculture Org.
- Parkyn, S. M., Davies - Colley, R. J., Halliday, N. J., Costley, K. J., & Croker, G. F. (2003). Planted riparian buffer zones in New Zealand: do they live up to expectations? *Restoration ecology*, 11(4), 436-447.
- Parsons, A. J., Cooper, J., & Wainwright, J. (2015). What is suspended sediment? *Earth Surface Processes and Landforms*, 40(10), 1417-1420.
- Pfankuch, D. J. (1975). Stream reach inventory and channel stability evaluation. *US Department of Agriculture Forest Service, Region, 1*.

- Phillips, J. M., Russell, M. A., & Walling, D. E. (2000). Time - integrated sampling of fluvial suspended sediment: A simple methodology for small catchments. *Hydrological Processes*, 14(14), 2589-2602.
- Pix4D. (2017). *Pix4D mapper 4.1: User manual*. from <https://support.pix4d.com/hc/en-us/articles/204272989-Offline-Getting-Started-and-Manual-pdf->.
- Prosdocimi, M., Calligaro, S., Sofia, G., Dalla Fontana, G., Tarolli, P. J. E. S. P., & Landforms. (2015). Bank erosion in agricultural drainage networks: new challenges from structure - from - motion photogrammetry for post - event analysis. *40*(14), 1891-1906.
- Prosser, I. P., Hughes, A. O., & Rutherford, I. D. (2000). Bank erosion of an incised upland channel by subaerial processes: Tasmania, Australia. *Earth Surface Processes and Landforms*, 25(10), 1085-1101.
- Quinn, J., & Basher, L. (2007). Testing times at Whatawhata. *Water & Atmosphere*, 15(2), 5.
- Quinn, J., Stroud, M., Thorrold, B., McGowan, A., & Collier, K. (1998). *Hill-farming effects on stream water quality and possible solutions*. NIWA 32-33p.
- Quinn, J. M. (2009a). *Field manual for riparian management classification*. National Institute for Water and Atmospheric Research Ltd, Hamilton, New Zealand.
- Quinn, J. M. (2009b). *Riparian management classification reference manual*. Hamilton, New Zealand: National Institute of Water & Atmospheric Research Ltd.
- Ritchie, J. C., & McHenry, J. R. (1990). Application of radioactive fallout cesium-137 for measuring soil erosion and sediment accumulation rates and patterns: a review. *Journal of environmental quality*, 19(2), 215-233.
- Roche, M. M. (1994). *Land and Water: Water and Soil Conservation and Central Government in New Zealand, 1941-1988*. Historical Branch Department of Internal Affairs.
- Seeger, M., Errea, M.-P., Begueria, S., Arnáez, J., Martí, C., & Garcia-Ruiz, J. (2004). Catchment soil moisture and rainfall characteristics as determinant factors for discharge/suspended sediment hysteretic loops in a small headwater catchment in the Spanish Pyrenees. *Journal of Hydrology*, 288(3-4), 299-311.
- Smith, H. G., & Blake, W. H. (2014). Sediment fingerprinting in agricultural catchments: A critical re-examination of source discrimination and data corrections. *Geomorphology*, 204, 177-191.
- Smith, H. G., Spiekermann, R., Dymond, J., & Basher, L. (2018). Predicting spatial patterns in riverbank erosion for catchment sediment budgets. *New Zealand Journal of Marine & Freshwater Research*, 1-25.

- Stewart, G. J., Caldwell, J. M., & Cloutier, A. R. (2003). *Water resources data Maine water year 2002: Water-data report ME-02-01*. U.S. Geological Survey, Augusta, ME.
- Storey, R. (2010). *Riparian characteristics of pastoral streams in the Waikato region, 2002 and 2007*. Waikato Regional Council, Hamilton, New Zealand.
- Stott, T. (1997). A comparison of stream bank erosion processes on forested and moorland streams in the Balquhiddier catchments, central Scotland. *Earth Surface Processes and Landforms: The Journal of the British Geomorphological Group*, 22(4), 383-399.
- Syvitski, J. P., Vörösmarty, C. J., Kettner, A. J., & Green, P. J. s. (2005). Impact of humans on the flux of terrestrial sediment to the global coastal ocean. *308(5720)*, 376-380.
- Te Aho, L. (2010). Indigenous challenges to enhance freshwater governance and management in Aotearoa New Zealand—the Waikato river settlement.
- Thorne, C., & Lewin, J. (Compiler) (1979). *Bank processes, bed material movements and planform development in meandering river*. Rhodes DD, Williams GP ed., *Adjustments of the fluvial system*: London: Allen & Unwin.
- Thorne, C. R., & Tovey, N. K. (1981). Stability of composite river banks. *Earth Surface Processes and Landforms*, 6(5), 469-484.
- Trimble, S. W. (1997). Contribution of stream channel erosion to sediment yield from an urbanizing watershed. *Science*, 278(5342), 1442-1444.
- Trimble, S. W., & Mendel, A. C. (1995). The cow as a geomorphic agent—a critical review. *Geomorphology*, 13(1-4), 233-253.
- Waikato-Tainui Te Kauhanganui Incorporated. (2013). *Waikato-Tainui environmental plan: Tai tumu tai pari tai ao*. Hamilton, New Zealand: Waikato-Tainui Te Kauhanganui Incorporated.
- Wallbrink, P., Murray, A., Olley, J., & Olive, L. (1998). Determining sources and transit times of suspended sediment in the Murrumbidgee River, New South Wales, Australia, using fallout ¹³⁷Cs and ²¹⁰Pb. *Water Resources Research*, 34(4), 879-887.
- Walling, D. (2006). Tracing versus monitoring: New challenges and opportunities in erosion and sediment delivery research. *Soil erosion and sediment redistribution in river catchments*, 13-27.
- Walling, D., & Quine, T. (1992). The use of caesium-137 measurements in soil erosion surveys. *Erosion and sediment transport monitoring programmes in river basins*, 210, 143-152.
- Walling, D. E. (1999). Linking land use, erosion and sediment yields in river basins. In *Man and River Systems* (pp. 223-240). Springer.

- Walling, D. E. (2013). The evolution of sediment source fingerprinting investigations in fluvial systems. *Journal of Soils and Sediments*, 13(10), 1658-1675.
- Wasson, R., Caitcheon, G., Murray, A. S., McCulloch, M., & Quade, J. (2002). Sourcing sediment using multiple tracers in the catchment of Lake Argyle, Northwestern Australia. *Environmental Management*, 29(5), 634-646.
- Wasson, R., Furlonger, L., Parry, D., Pietsch, T., Valentine, E., & Williams, D. (2010). Sediment sources and channel dynamics, Daly River, northern Australia. *Geomorphology*, 114(3), 161-174.
- Watson, A., & Basher, L. (2006). Stream bank erosion: a review of processes of bank failure, measurement and assessment techniques, and modelling approaches. *A report prepared for stakeholders of the Motueka Integrated Catchment Management Programme and the Raglan Fine Sediment Study. Landcare Research, Hamilton, New Zealand.*
- Watson, A. J., & Mardern, M. (2004). Live root-wood tensile strengths of some common New Zealand indigenous and plantation tree species. *New Zealand journal of forestry science*, 34(3), 344.
- Westoby, M. J., Brasington, J., Glasser, N. F., Hambrey, M. J., & Reynolds, J. J. G. (2012). 'Structure-from-Motion' photogrammetry: A low-cost, effective tool for geoscience applications. *179*, 300-314.
- Whitehead, K., Moorman, B., & Hugenholtz, C. J. T. C. (2013). Brief Communication: Low-cost, on-demand aerial photogrammetry for glaciological measurement. *7(6)*, 1879-1884.
- Williams, G. P. (1989). Sediment concentration versus water discharge during single hydrologic events in rivers. *Journal of Hydrology*, 111(1-4), 89-106.
- Wolman, M. G. (1959). Factors influencing erosion of a cohesive river bank. *American Journal of Science*, 257(3), 204-216.

Appendices



Site state assessment											
Site				Site Code				Date		Length (m) =	
GPS Top: E				Bottom: E				N		N	
Gen. land use left side			native forest	planted forest	sheep	beef	deer	dairy	horticulture	peri-urban	urban
Gen. land use right side			native forest	planted forest	sheep	beef	deer	dairy	horticulture	peri-urban	urban
Riparian land use (mark R for right & L for left bank)					conservation	filter strip	woodlot	urban	stopbank	whitebaiting	
cattle	sheep	deer	crop	hort	esplanade	reserve	waterfowl	shooting	engineered floodway Other=		
Widths (m)		Water=		Channel=		Bankfull=		valley bottom=			
Channel plan shape		channelised	straight	meandering	sinuous		Valley form		V	U	plain
Flow		ephemeral	intermittent	perennial	regulated	wetland		Stream shade (%) =			

Sketch stream plan, cross-section & comments: (including where planting zones occur, position of current fencing)

	Photo numbers and descriptions
--	--------------------------------

Streambed	clay	mud	silt	sand	gravel	cobble	boulder	bedrock	% riffle/run/pool	/	/
Bank left	Height (m) lower=		upper=		Stability		%stable=	%undercut=	%slumping=	%earthflow=	
Bank right	Height (m) lower=		upper=		Stability		%stable=	%undercut=	%slumping=	%earthflow=	
Stabilised by	Left	grasses	shrubs	sedge/rushes	trees	bedrock	riprap/artificial				
	Right	grasses	shrubs	sedge/rushes	trees	bedrock	riprap/artificial				
Macrophytes	% cover =		Type =								
Periphyton	none	slippery	obvious	abundant	excessive, Fil Alg>30%		Wood	absent	sparse	common	abundant

Live-stock access to stream & bank damage	Left	Y / N	Left damage		none	minor	moderate	extensive	Other		
	Right	Y / N	Right damage		none	minor	moderate	extensive	damage		
Riparian veg: mark left (L) & right (R)			rock	bare soil	annuals	grass	toetoe	flax			
		treeferns	low shrubs	high shrubs	native trees	coniferous	deciduous	exotic	other=		
Dominant riparian plant species				Left =				Right =			
Local runoff potential	Left slope length (m)		Left land slope class				<2°	2-5°	5-10°	10-15°	15-25°
	Right slope length (m)		Right land slope class				<2°	2-5°	5-10°	10-15°	15-25°
Riparian wetlands	Left	absent	sparse	common	extensive	Right	absent	sparse	common	extensive	

Riparian Function Assessment Field Sheet

John Quinn, NIWA

13/11/2009

Figure A.1. Riparian Management Classification (RMC) form used to characterise stream and riparian health (Quinn, 2009a).

Table A.1: Raw gamma spectrometry results from the Institute of Environmental Science and Research used for sediment fingerprinting.

Sample ID	Type	Catchment	Landuse	Cs-137 (Bq/kg)	Cs-137 error (Bq/kg)	Pb-210 (Bq/kg)	Pb-210 error (Bq/kg)	Pb-210ex (Bq/kg)	Ra-226 (Bq/kg)	Ra-226 error (Bq/kg)	Ra-228 (Bq/kg)	Ra-228 error (Bq/kg)	Ra-228 - Ra- 226 ratio	Pb210ex - Cs137 ratio	Pb210ex error bars
WBank 1	Stream bank	Whakakai	Native	< 0.82	-	33.10	6.40	4.80	28.30	3.70	47.80	7.60	1.69	5.85	2.70
WBank 2	Stream bank	Whakakai	Native	0.38	0.29	24.90	5.50	-3.10	28.00	3.60	50.20	7.90	1.79	-8.16	1.90
WBank 3	Stream bank	Whakakai	Native	0.78	0.25	41.70	6.90	14.50	27.20	3.40	43.60	6.60	1.60	18.59	3.50
WBank 4	Stream bank	Whakakai	Native	0.55	0.28	30.70	6.50	8.10	22.60	2.90	42.40	6.50	1.88	14.73	3.60
WBank 5	Stream bank	Whakakai	Native	< 0.8	-	31.80	6.10	5.10	26.70	3.50	46.60	7.30	1.75	6.38	2.60
Bank 2M	Stream bank	Mangaotama	Pasture	0.82	0.34	44.40	7.70	12.20	32.20	4.20	49.4	7.80	1.53	14.88	3.50
Bank 3M	Stream bank	Mangaotama	Pasture	< 0.8	-	37.60	6.80	8.20	29.40	3.80	48.4	7.50	1.65	10.25	3.00
Bank 6M	Stream bank	Mangaotama	Pine	0.96	0.33	44.70	7.80	13.90	30.80	3.90	45.3	7.10	1.47	14.48	3.90
Bank 7M	Stream bank	Mangaotama	Pine	0.97	0.37	47.50	8.40	14.40	33.10	4.20	48.8	7.60	1.47	14.85	4.20
Bank 11M	Stream bank	Mangaotama	Pasture	1.93	0.46	35.40	6.70	5.40	30.00	3.80	49.9	7.80	1.66	2.80	2.90
WHill 1	Hillslope	Whakakai	Native	9.8	1.40	107	17.00	86.60	20.4	2.80	36.2	6.10	1.77	8.84	14.20
WHill 2	Hillslope	Whakakai	Native	7.6	1.10	57.1	9.70	30.20	26.9	3.50	41.3	6.60	1.54	3.97	6.20
WHill 3	Hillslope	Whakakai	Native	5.53	0.77	53	8.50	27.40	25.6	3.20	39.5	6.00	1.54	4.95	5.30
WHill 4	Hillslope	Whakakai	Native	3.28	0.62	35.6	6.70	10.90	24.7	3.20	39.9	6.40	1.62	3.32	3.50
WHill 5	Hillslope	Whakakai	Native	4.07	0.55	35.7	6.00	13.40	22.3	2.80	33.3	4.90	1.49	3.29	3.20
Hill 1M	Hillslope	Mangaotama	Pasture	9.1	1.50	60	12.00	33.80	26.2	3.80	30.7	5.60	1.17	3.71	8.20
Hill 5M	Hillslope	Mangaotama	Pasture	7.4	1.30	58	12.00	31.40	26.6	3.90	30.6	5.70	1.15	4.24	8.10
Hill 6M	Hillslope	Mangaotama	Pine	4.26	0.86	59	12.00	36.90	22.1	3.30	25.1	4.80	1.14	8.66	8.70
Hill7M	Hillslope	Mangaotama	Pine	3.11	0.75	50	11.00	23.20	26.8	3.80	36.3	6.40	1.35	7.46	7.20
Hill 8M	Hillslope	Mangaotama	Pasture	3.61	0.67	59	11.00	31.40	27.6	3.70	40	6.50	1.45	8.70	7.30
SSW	Suspended Sediment	Whakakai	-	0.91	-	48.7	-	-	23.3	-	45.8	-	-	25.4	-
SSM	Suspended Sediment	Mangaotama	-	0.86	-	53.3	-	-	30.1	-	45.9	-	-	23.2	-